7. SITE 628: LITTLE BAHAMA BANK[1]

Shipboard Scientific Party[2]

HOLE 628A

Date occupied: 17 February 1985, 2355 EST

Date departed: 19 February 1985, 1600 EST

Time on hole: 1 day, 16 hr

Position: 27°31.85′N, 78°18.95′W

Water depth (sea level; corrected m, echo-sounding): 966

Water depth (rig floor; corrected m, echo-sounding): 976

Bottom felt (m, drill pipe): 974

Total depth (m): 1274.7

Penetration (m): 298.4

Number of cores: 32

Total length of cored section (m): 298.4

Total core recovered (m): 216.9

Core recovery (%): 72.7

Oldest sediment cored:
Depth sub-bottom (m): 298.4
Nature: silicified limestone and chert
Age: late Paleocene (NP8)
Measured velocity (km/s): 1.85, Hamilton Frame (at 280 m sub-bottom); 1.75/2.26, multichannel seismic-reflection profile LBB-18

Principal results: Site 628 on the northern slope of Little Bahama Bank was occupied from 17 to 19 February 1985. Hole 628A is located at 27°31.65′N, 78°18.95′W, in 959 m water depth. Drilling penetrated 298 m of sediment using the hydraulic-piston-core/extended-core-barrel (HPC/XCB) techniques. Overall recovery was 73%. The hole terminated in nannofossil ooze of late Paleocene age.

From top to bottom, the following sequence was recovered: (1) 0–137 m sub-bottom; carbonate ooze having turbidites, slumps, and debris flows; (2) 137–272 m sub-bottom; carbonate ooze and chalk having slumps and turbidites, latest Eocene to late Oligocene in age; and (3) 272–298 m sub-bottom; siliceous chalk and limestone, some carbonate ooze, late Paleocene to middle Eocene in age.

This sequence records the upward transition from a marginal plateau with purely pelagic sedimentation in the Paleocene–early Oligocene to the toe-of-slope of a carbonate platform in the late Oligocene–Holocene. Increases in sedimentation rates and in amount of bank-derived material during the Neogene reflect the gradual progradation of the platform slope. Cores and seismic profiles suggest that creep and slumping along curved (listric?) and bedding-parallel shear planes are dominant processes in the toe-of-slope environment between Site 628 and Site 627.

OPERATIONS SUMMARY

The *JOIDES Resolution* left Site 627 for Site 628 at 2030 hr, 17 February 1985. The ship ran slightly west of south along the trend of site survey line LBB-18 for BAH-8-A approximately 6 n. mi away (Fig. 1). Speed was maintained at about 4 kt with thrusters extended. Positioning was successfully achieved by using the programs SATNAV and LORAN C, and a beacon on the taut wire was deployed slightly before midnight, which allowed adjustments of the ship's final position without deploying an additional beacon. The final position of Site 628 was as follows (based on continuous monitoring of SATNAV during operations at this location): 27°31.828–873′N, 78°18.901–19.029′W. This compares closely to the originally designated BAH-8-A position: 27°32′N, 78°19′W.

The water depth at Site 628 was 956 m (uncorr.), 966 m (corr.), and a successful mud-line core was achieved at 0708 hr, 18 February, after several attempts. During the next 14.5 hr, 21 hydraulic-piston cores (HPC) were recovered (Cores 628A-1H through 628A-22H) to a sub-bottom depth of 192.7 m for a recovery of 89%. Eleven extended-core-barrel (XCB) cores were then taken to a total depth of 298.4 m sub-bottom. Recovery using the XCB was 43%. In summary, 32 cores were acquired in only 30.5 hr from Hole 628A.

Immediately after retrieving Core 628A-32X, pipe was pulled out of the hole (POOH) in preparation for the transit (approximately 10 n. mi) to BAH-7-A. The ship left Site 628 at approximately 1600 hr on 19 February.

The coring summary for Site 628 appears in Table 1.

SEDIMENTOLOGY

Introduction

Sediments at Site 628 are mainly unlithified packstones and grainstones in the top 50 m, downward fining into unlithified oozes containing thin packstone beds and rare floatstones. Grains within the packstones and grainstones are dominantly planktonic foraminifers having varying proportions of benthic foramini-

[1] Austin, J. A., Jr., Schlager, W., Palmer, A. A., et al., 1986. *Proc., Init. Repts. (Pt. A), ODP*, 101.

[2] James A. Austin Jr. (Co-Chief Scientist), Institute for Geophysics, University of Texas at Austin, Austin, TX 78751; Wolfgang Schlager (Co-Chief Scientist), Rosenstiel School of Marine and Atmospheric Sciences, Miami, FL 33149 (current address: Vrije Universiteit, Instituut v. Aardwetenschappen, Postbus 7161, 1007 MC Amsterdam, Netherlands); Amanda A. Palmer, Staff Scientist, Ocean Drilling Program, Texas A&M University, College Station, TX 77843; Paul A. Comet, The University, Newcastle-Upon-Tyne, Newcastle, United Kingdom (current address: Core Labs Singapore, 24A-Lim Teck Boo Rd., Singapore 1953); André Droxler, Rosenstiel School of Marine and Atmospheric Sciences, Miami, FL 33149 (current address: Department of Geology, University of South Carolina, Columbia, SC 29208); Gregor Eberli, Geologisches Institut, ETH-Zentrum, Zürich, Switzerland (current address: Fisher Island Station, University of Miami, Miami, FL 33139); Eric Fourcade, Laboratoire de Stratigraphie, Université Pierre et Marie Curie, 4 Place Jussieu 75230, Paris Cedex 05, France; Raymond Freeman-Lynde, Department of Geology, University of Georgia, Athens, GA 30602; Craig S. Fulthorpe, Department of Geological Sciences, Northwestern University, Evanston, IL 60201; Gill Harwood, Department of Geology, The University, Newcastle-Upon-Tyne, NE1 7RU United Kingdom; Gerhard Kuhn, Geologisches Institut Göttingen, Federal Republic of Germany (current address: Alfred Wegener Institut für Polarforschung, Columbus Center, D-2850 Bremerhaven, West Germany); Dawn Lavoie, NORDA Code 363, Seafloor Geosciences Division, NSTL, MS 39529; Mark Leckie, Woods Hole Oceanographic Institution, Woods Hole, MA 02543 (current address: Department of Geology and Geography, University of Massachusetts, Amherst, MA 01003); Allan J. Melillo, Department of Geological Sciences, Rutgers University, New Brunswick, NJ 08903 (current address: Chevron U.S.A., New Orleans, LA 70114); Arthur Moore, Marathon Oil Company, P.O. Box 269, Littleton, CO 80160; Henry T. Mullins, Department of Geology, Syracuse University, Syracuse, NY 13210; Christian Ravenne, Institut Français du Pétrole, B.P. 311, 92506 Rueil Malmaison Cedex, France; William W. Sager, Department of Oceanography, Texas A&M University, College Station, TX 77843; Peter Swart, Fisher Island Station, University of Miami, Miami, FL 33139 (current address: Marine Geology and Geophysics, Rosenstiel School of Marine and Atmospheric Sciences, Miami, FL 33149); Joost W. Verbeek, Dutch Geological Survey, P.O. Box 157, 2000 A.D. Haarlem, Netherlands; David K. Watkins, Department of Geology, University of Nebraska, Lincoln, NE 68588; Colin Williams, Borehole Research Group, Lamont-Doherty Geological Observatory, Palisades, NY 10964.

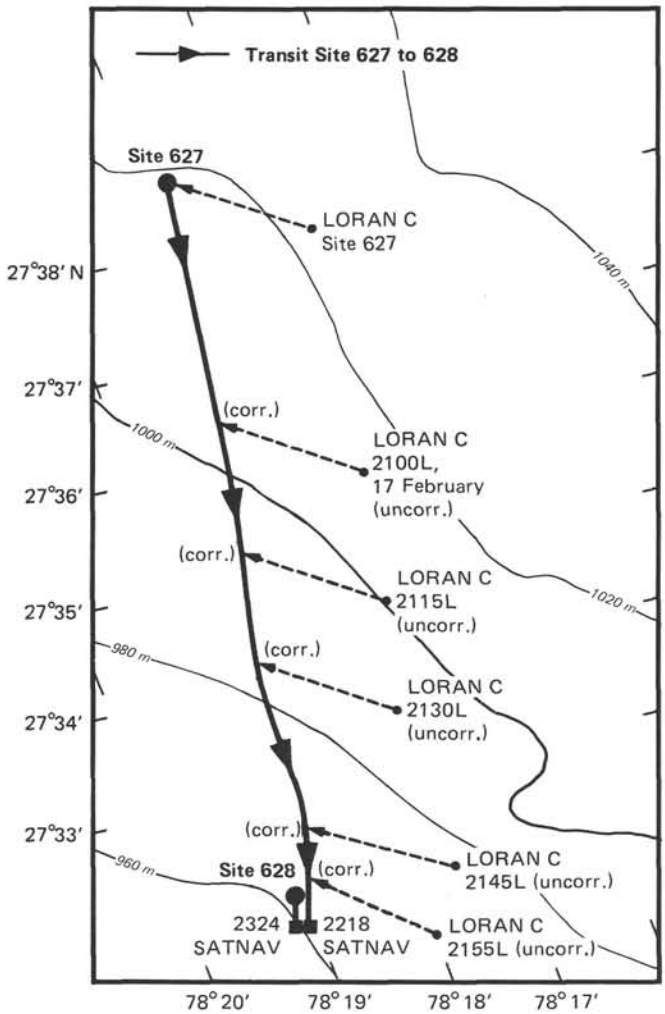

Figure 1. Transit from Site 627 to Site 628. Only 12 kHz was run during this 6-n.-mi run. *L* refers to local time.

fers and skeletal debris. In the oozes, foraminifers and nannofossils are present; some parts of the section have more than 80% nannofossils. Below 136.8 m sub-bottom, oozes and chalks predominate, lithified siliceous green carbonates being in the last three cores (628A-30X to 628A-32X). The top 40–50 cm of many cores consists of unlithified floatstones, most probably the result of drilling deformation.

Sediments cored from Hole 628A are divided into three major lithologic units: Unit I from 0 to 136.8 m sub-bottom (Cores 628A-1H to 628A-16H), Unit II from 136.8 to 271.7 m sub-bottom (Cores 628A-16H to 628A-30X), and Unit III from 271.7 to 298.4 m sub-bottom (Cores 628A-30X to 628A-32X).

Unit I (0–136.8 m sub-bottom; Cores 628A-1H to 628A-16H)

Unit I contains packstones and oozes (mudstones/wackestones) containing minor amounts of grainstones and floatstones. Lithification is partial throughout, except for clasts within the floatstones, and decreases downward within the unit, varying from 80% to zero. Most of the packstones and grainstones are unlithified; they exhibit upward-fining, graded bedding cycles and/or show an upward increase of mud content within an individual cycle, which may range from a few centimeters to tens of centimeters in thickness. Floatstones have unlithified packstone matrices and lithified clasts, which are dominantly foraminiferal packstones. Within the oozes, the foraminifer and nannofossil contents vary (Fig. 2). A higher percentage of siliceous sponge spicules and skeletal fragments occurs in the lower part of Unit I. The oozes are completely bioturbated; recognition of individual burrows is obscured by drilling deformation (and by cutting) in some core sections.

Unit I was dated as middle Miocene to Pleistocene in age (see "Biostratigraphy" section, this chapter). It is here subdivided into four subunits based on lithologic differences and supportive data from smear slide analysis and color changes (Fig. 2):

Subunit IA (0–5 m sub-bottom; Cores 628A-1H and 628A-2H); unlithified floatstone.
Subunit IB (5–48.10 m sub-bottom; Cores 628A-2H to 628A-6H); packstones, grainstones with minor amounts of ooze, chalk, and floatstones.
Subunit IC (48.10–110.8 m sub-bottom; Cores 628A-6H to 628A-13H); bioturbated oozes and chalks.
Subunit ID (110.8–136.8 m sub-bottom; Cores 628A-13H to 628A-16H); oozes, packstones, and minor amounts of floatstones.

Subunit IA comprises a white (10YR 8/1) unlithified floatstone 5 m thick, containing subrounded to rounded clasts (as much as 10 cm in diameter) of skeletal–foraminiferal packstone in a matrix of soupy, unlithified packstone–wackestone containing nannofossils and small skeletal clasts with planktonic foraminifers and rare pteropods. This unit is interpreted as being a debris flow. Because it is considerably coarser than the underlying remainder of Unit I, Subunit IA is defined as a subunit, which is consistent with the biostratigraphic evidence ("Biostratigraphy" section, this chapter) that dates Subunit IA as Pleistocene.

Subunit IB comprises a series of white (10YR 8/1), unlithified to partly lithified packstones and grainstones (Fig. 2). The grainstones and packstones contain multiple upward-fining cycles of graded beds over a scale of centimeters to tens of centimeters; coarse to very coarse grains occur in the base of a cycle, upward-fining through to medium and fine grains. Either packstones or grainstones may form the base of a cycle. Dominant grains are foraminifers with varying percentages of skeletal fragments, aggregate clasts, and pteropods (Fig. 2); pteropods are more common in the grainstones. Unlithified and semilithified grainstones and packstones contain up to 71% aragonite on x-ray-diffraction (XRD) analysis (see Table 2 and "Inorganic Geochemistry" section, this chapter). These graded beds are interpreted as being turbidites. Floatstones and rudstones, probably debris flows, are minor within Subunit IB. Chalks and oozes are present but reach only a few cm in thickness. Terrigenous clays occur in the oozes in some zones (e.g., Section 628A-2H-5, Fig. 3), which contain higher than average percentages of dolomite (see Table 2 and "Inorganic Geochemistry" section, this chapter). Probable pyrite occurs as dark specks throughout this subunit. The bases of the upward-fining cycles remain unlithified, although the upper few cm of finer packstones are partly lithified. Grainstones are unlithified. Burrows are evident in the lower part of this section.

Smear slide analysis indicates that as much as 60% of grains within the turbidites are derived from shallow-water or neritic environments. Subunit IB was dated as late Pliocene to early Pliocene in age ("Biostratigraphy" section, this chapter).

Subunit IC contains oozes and minor amounts of chalk, interbedded with thin packstones (Fig. 2). Oozes contain both nannofossils and planktonic foraminifers; some contribution of terrigenous clays changes color within the sediments (e.g., Cores 628A-7H, 52.9–53.5 m sub-bottom, and 628A-8H, 65.9–70.0 m sub-bottom). Gradual upward darkening of color within thin sequences may reflect a change from carbonate to carbonate plus

Table 1. Coring summary, Site 628.

Core no.	Core type[a]	Date (Feb. 1985)	Time	Sub-bottom depths (m)	Length cored (m)	Length recovered (m)	Percentage recovered
Hole 628A							
1	H	18	0715	0–3.6	3.6	3.58	99
2	H	18	0805	3.6–13.2	9.6	9.37	97
3	H	18	0930	13.2–22.9	9.7	9.45	97
4	H	18	1025	22.9–32.6	9.7	9.73	100
5	H	18	1115	32.6–41.9	9.3	8.84	95
6	H	18	1205	41.9–51.5	9.6	9.64	100
7	H	18	1245	51.5–60.9	9.4	9.63	102
8	H	18	1345	60.9–70.6	9.7	9.91	102
9	H	18	1430	70.6–79.7	9.1	10.11	111
10	H	18	1500	79.7–89.1	9.4	9.71	103
11	H	18	1545	89.1–98.5	9.4	9.41	100
12	H	18	1605	98.5–107.9	9.4	9.83	104
13	H	18	1635	107.9–117.4	9.5	9.59	100
14	H	18	1700	117.4–127.0	9.6	9.49	98
15	H	18	1745	127.0–136.6	9.6	5.13	53
16	H	18	1815	136.6–146.1	9.5	9.64	100
17	H	18	1900	146.1–155.7	9.6	9.56	99
18	H	18	1945	155.7–165.2	9.5	8.67	91
19	H	18	2015	165.2–174.2	9.0	5.43	60
20	H	18	2110	174.2–183.2	9.0	0	0
21	H	18	2145	183.2–192.7	9.5	4.85	51
22	X	18	2315	192.7–202.3	9.6	9.79	101
23	X	19	0045	202.3–211.9	9.6	8.32	86
24	X	19	0215	211.9–221.5	9.6	3.77	39
25	X	19	0335	221.5–231.4	9.9	3.71	37
26	X	19	0510	231.4–241.0	9.6	4.00	41
27	X	19	0635	241.0–250.6	9.6	3.39	35
28	X	19	0745	250.6–260.2	9.6	3.79	39
29	X	19	0900	260.2–269.9	9.7	2.54	26
30	X	19	1015	269.9–279.2	9.3	5.24	56
31	X	19	1210	279.2–288.8	9.6	0.36	3
32	X	19	1330	288.8–298.4	9.6	0.47	4

[a] H = hydraulic piston; X = extended core barrel.

clay, especially where interbedded with thin (1–2-cm) packstones. These clay-rich layers are similar to ones occurring in Section 627B-15H-4 (see Site 627 chapter, Fig. 10, this volume; Table 2). The increase in nannofossil content relative to Subunit IB (Fig. 2) is coincident with the appearance of slight to moderate (as much as 60% of surface area) visible burrowing within the oozes. Minor lithification of the oozes (as much as 20%) is present in Core 628A-8H, but otherwise oozes are unlithified. Deformed bedding laminae are present between 75 and 87 m sub-bottom (Cores 628A-9H and 628A-10H), immediately underlying a thin floatstone.

Packstones and grainstones exist throughout Subunit IC. Packstones are thin (a few centimeters) near the top of the subunit but reach several meters in thickness near the base (89–107 m sub-bottom) (Fig. 2). The packstones contain graded, upward-fining cycles having coarse to very coarse grains at their bases to medium to coarse grains near their tops. Packstones are mostly unlithified and do not contain evidence of bioturbation. Two colors of unlithified packstones appear, white (2.5Y 8/2) and light gray (2.5Y 7/0). The former have marginally higher percentages of skeletal fragments plus micrite, whereas the light gray packstones contain foraminifers and specks of pyrite within their tests. Thin grainstones within the packstones have sharp upper and lower boundaries and do not grade into packstones. The lowest packstone package (108.3–110.8 m sub-bottom) contains deformed bedding laminations.

The oozes within Subunit IC are interpreted as being deep-water sediments having some input from the adjacent platform; as such they are periplatform oozes. The puzzling higher clay contents of some layers may indicate proximity to an exposed source. A further possibility is that these clays resulted from pulses of turbidity carried in the Gulf Stream and originating in the Gulf of Mexico from the Mississippi River. The oozes, which show deformation (Cores 628A-9H and 628A-10H), are interpreted as a major downslope slump. Thin packstones, present within the oozes, contain upward-fining cycles and are taken to represent periodic incursions of distal turbidites. The whiter packstones may indicate some reworking of platform-derived material, whereas grayer grains may be the result of rapid deposition of undecomposed foraminifers; these packstones will be analyzed in shore-based studies. Although drilling may have homogenized the sediments, unlithified packstones and grainstones without graded bedding may be turbidites. Subunit IC has been dated as early Pliocene to late Miocene in age.

Subunit ID is defined by the abrupt change in components present, in conjunction with a slight lithologic and color change (Fig. 2). The top of the subunit corresponds to a faunal break between the late Miocene and middle Miocene. The top of this subunit is difficult to delineate precisely. It is taken at a thin limestone in Section 628A-13H-3. Below this limestone are clasts belonging to the underlying slumped sequence; no clasts occur above the limestone. At the base of Subunit ID is a faunal break between the middle Miocene and the late Oligocene ("Biostratigraphy" section, this chapter). Subunit ID contains oozes, thin packstones, and few floatstones. The oozes between 120 and 124 m sub-bottom (Core 628A-14H) show deformed bedding. Bioturbation is rare throughout the oozes within this subunit. Components of the oozes are foraminifers, dominantly planktonic, and nannofossils with skeletal debris and micrite. Thin packstones fine upward. They are of two types, defined by color and constituent grains, and are similar to those described in Subunit IC. Grain size within these packstones rarely exceeds

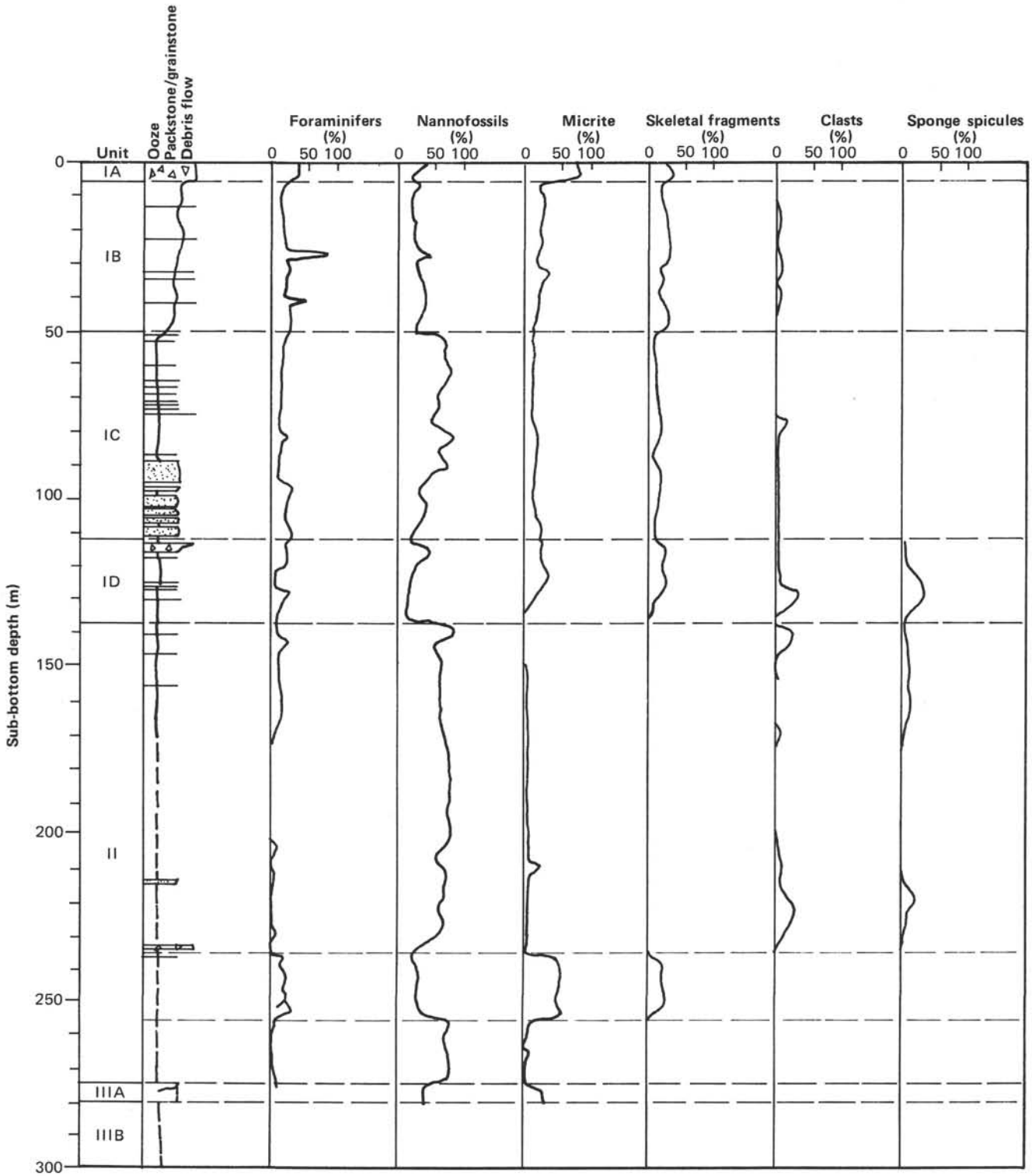

Figure 2. Relationship between lithologic units, sediment type, and smear slide data, Site 628.

coarse-sand grade and, more commonly, is medium to fine. One floatstone (111.4–115 m sub-bottom; Core 628A-13H) is present near the top of this subunit.

Oozes within this subunit show an increased percentage of platform-derived fauna and are thus interpreted to be periplatform oozes. Thin packstones are taken to represent distal turbidites. The floatstone is interpreted as being a debris flow. Subunit ID contains a high aragonite content relative to the units above and below ("Inorganic Geochemistry" section, this chapter). This may in part result from the higher content of platform-derived sediments within this unit as well as from downslope slumping.

Table 2. Composition of sediments from x-ray analyses, Site 628.[a]

	Lithologic unit	Calcite (%)	Aragonite (%)	Dolomite (%)	Other minerals present
IB:	Packstone with lithification; top of turbidite, 8.9 m (Core 628A-3H-4, 76 cm)	36	62	2	
	Unlithified grainstone from base of turbidite, 9.0 m (Core 628A-2H-4, 93 cm)	27	69	3	
	Clay from near top of turbidite, 9.8 m (Core 628A-2H-5, 15–16 cm)	33	41	15	Illite and quartz
	Unlithified packstone; base of turbidite, 10.0 m (Core 628A-2H-5, 43 cm)	26	71	3	
IC:	Clay-rich layers in ooze, 57.6 m (Core 628A-7H-5, 15 cm)	82	13	4	Clays and quartz

[a] See also Table 4.

Unit II (136.8–271.7 m sub-bottom; Cores 628-16H to 628-30X)

Unit II was deposited during the latest Eocene and Oligocene. The top of Unit II is taken as a hardground present near the top of Section 628A-16H-1 (Fig. 4). Unit II is dominated by bioturbated oozes and chalks. Pyrite is present in small amounts throughout the unit and is commonly found within both horizontal and vertical burrows. A single pyrite concretion was found at 260.2 m sub-bottom (base of Core 628A-28X). Lithification is lacking in the upper part (136.8–190 m sub-bottom) of this unit, but below 190 m sub-bottom chalks predominate. Below 165.2 m sub-bottom, recovery was reduced; drilling rate slowed during recovery of Core 628A-21H, necessitating a change to XCB coring and indicating an increase in lithification below this depth. Here, chalk and ooze with some limestones replace unlithified ooze. Chalk and ooze occur in varying proportions below this depth; much of the ooze content appears to be the result of drilling deformation, producing artificial chalk/ooze couplets similar to those present in the Campanian chalks (Unit III) of Hole 627B (Fig. 5).

Nannofossils are the major component of oozes within the upper 94 m of the unit (136.8–230.2 m sub-bottom, Cores 628A-16H to 628A-21H) and again between 250.0 and 271.7 m sub-bottom (Cores 628A-28X to 628A-30X). Between 230.2 and 250.0 m (Cores 628A-26X to 628A-28X), skeletal debris, planktonic foraminifers, and micrite increase, whereas nannofossil content decreases. Quartz, siliceous limestone, and chert are also present (Fig. 2). Echinoid fragments were recognized in this interval, along with some benthic foraminifers. Radiolarians are present throughout much of Unit II (Fig. 2) but become rare below 250 m sub-bottom. Although this unit is dominated by chalks and oozes, a thin unlithified floatstone and thin packstone were recovered from Core 628A-26X.

The nannofossil-rich oozes and chalks within this unit were deposited away from the influence of either carbonate-platform or terrigenous input, probably on a submarine plateau. The decrease in nannofossils and the increase of skeletal debris, micrite, and foraminifers between 230.2 and 250.0 m sub-bottom indicate some input of platform-derived fine sediment into the area; this interval is therefore interpreted as being periplatform ooze.

Unit III (271.7–298.4 m sub-bottom; Cores 628A-30X to 628A-32X)

The top of Unit III is defined by an abrupt change from an ooze having minor chalk content to a lithified packstone (Section 628A-30X-2, Fig. 6). This part of the unit is dated as late Paleocene–early Eocene ("Biostratigraphy" section, this chapter) and is coincident with a faunal break with the overlying upper Eocene chalks and oozes. Recovery in Unit III was poor but allowed division into two subunits: (1) Subunit IIIA (2.4 m recovered, Cores 628A-30X and 628A-31X); lithified, burrowed foraminiferal packstone with fine- to medium-sized grains; and (2) Subunit IIIB (0.70 m recovered, Cores 628A-31X and 628A-32X); green (10GY 7/2) hard, burrowed siliceous limestone and chert without visible fauna (Fig. 7).

Subunit IIIA was recovered as fragmented core surrounded by drilling slurry (Fig. 8); Subunit IIIB was present only as fragments in drilling breccias. Lack of recovery prevents interpretation on lithologic evidence alone of the depositional environments of these two subunits.

Discussion

Seismic interpretation indicates channeling into the top of sequence E at Site 628 ("Seismic Stratigraphy" section, this chapter). The sediments within Unit III are poorly recovered and indicate a distinct increase in lithification compared with the overlying chalks and oozes. They probably represent the top of seismic unit E, and the packstone (Subunit IIIA) may well be a channel fill.

Unit II is dominantly oceanic-plateau ooze containing a high percentage of nannofossils compared with other fauna (Fig. 2). The interval between 230.2 and 250.0 m sub-bottom (Cores 628A-26X to 628A-28X) does, however, contain a higher proportion of platform-derived fauna and thus is interpreted as being periplatform ooze. This interval may represent an episodic northward incursion of the ancestral Little Bahama Bank in the Oligocene and subsequent restoration of an oceanic-plateau regime in this area, resulting from a major early Oligocene fall in sea level (Vail et al., 1977) during this time (nannofossil Zone NP23, "Biostratigraphy" section, this chapter). Some dispute exists, however, as to the exact timing of this sea-level fall. Noticeably, the only coarse sediments within Unit II directly overlie the periplatform-ooze interval and may be part of this short-lived northward progradation.

Unit I contains a much higher component of slope- and platform-derived sediments. The middle Miocene (Subunit ID) contains an upward-coarsening sequence of plateau and periplatform ooze through turbidites and debris flows; possible slump zones also occur. This subunit is equivalent to Unit II at Site 626 and to Subunit IC at Site 627 and is coeval with the Abaco Member of the Blake Ridge Formation. In the late Miocene section (Subunit IC), turbidites predominate, although oozes with

Figure 3. Terrigenous clays within oozes, Sample 628A-2H-5, 6-50 cm. Base of clays (darker color) is fractured by drilling disturbance. Clay content decreases upsection.

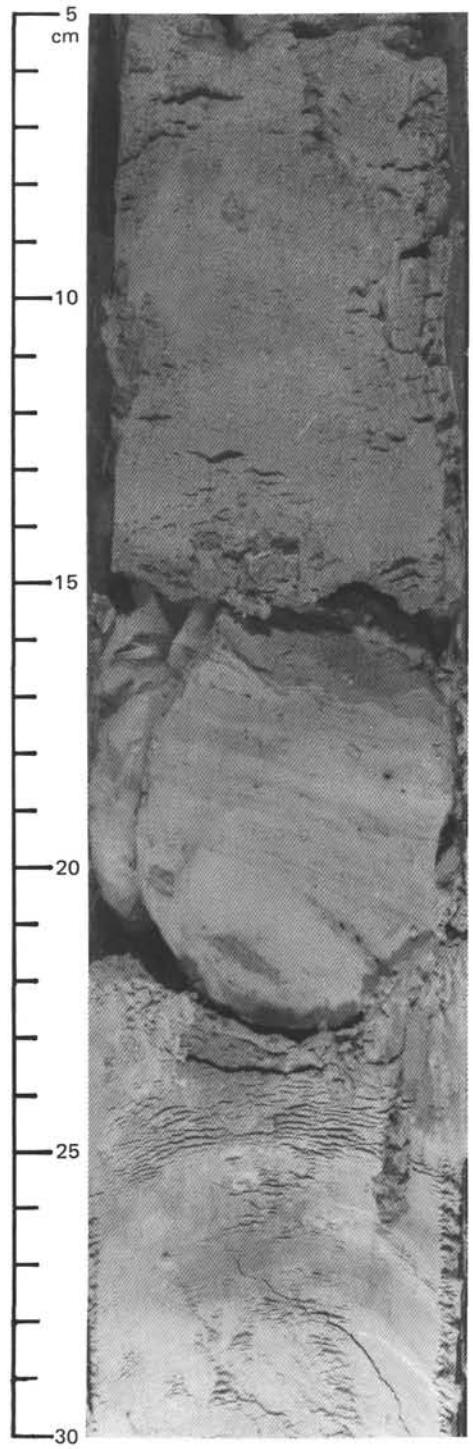

Figure 4. Hard limestone (possible hardground) taken as the top of Unit II, Sample 628A-16H-1, 9–30 cm. Subhorizontal, dark laminations contain some pyrite–marcasite.

thin, distal turbidites recur higher in the subunit at both upper Miocene and Pliocene sequences. At Subunit IB, the slope sediments migrate once more into the area, producing a succession of graded turbidites and grain flows. Subunit IA represents further northward progradation of the slope and deposition of late Pleistocene debris flows.

Seismic stratigraphic sections through this site (see "Seismic Stratigraphy" section, this chapter) indicate the presence of a

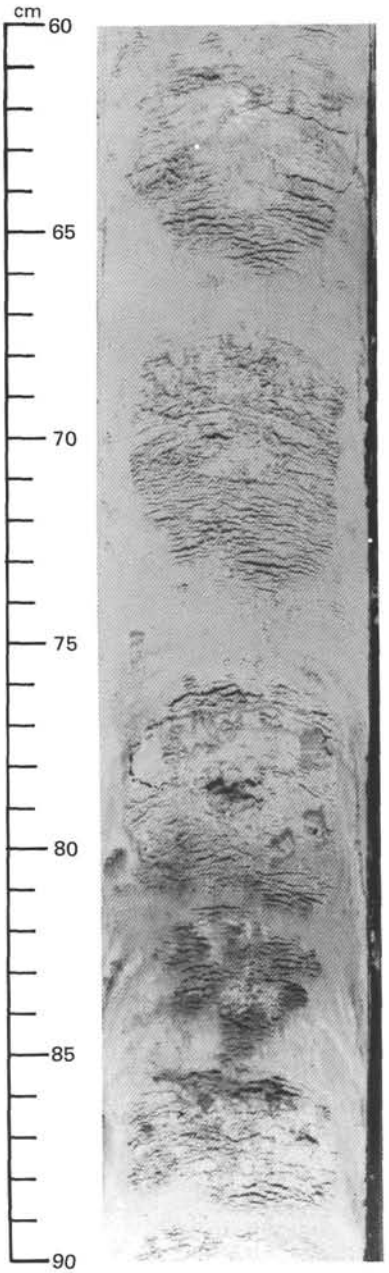

Figure 5. Artificial chalk/ooze couplets produced by drilling deformation, Sample 628A-28X-1, 60–90 cm. Burrows are shown by darker colors.

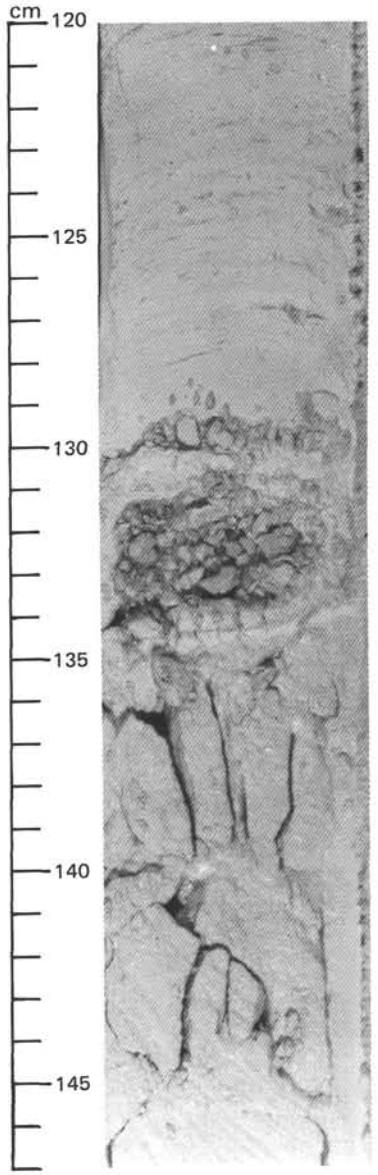

Figure 6. Top of Unit III, with soft ooze overlying fractured, lithified packstone, Sample 628A-30X-2, 120–147 cm.

basal slide plane and associated imbricate thrusts within the Neogene sediments both northeast and southwest of Site 628. The sediments in this interval are largely unlithified. Any imbricate propagation through the sediments is likely to disturb sedimentary structures within an interval; such disturbance may be similar in appearance to surficial slumping. Therefore, some of the folded and disturbed sediments within these cores are possibly involved in the imbricate thrust zones. Because the sediments were unlithified when imbrication took place, and this was a shallow, gravity-induced process, we consider them to be part of the synsedimentary gravity movement down a carbonate slope.

Correlation with Site 627

Unit I at Site 628 represents the same age range as that of Unit I described from Site 627; sediments are of similar lithologies, although those from Site 627, being farther from the sediment source, are finer grained throughout the upper parts of the section (Fig. 9). Subunit ID, lying between the same two faunal breaks, also correlates with Subunit IC from Site 627. Unit I is noticeably thicker at Site 627 than at Site 628 (182 vs. 137 m). This may be the result of sediment bypass or of imbrication.

No correlation exists below Unit I. Although Unit II at Site 628 contains a chalk lithology (Oligocene) similar to Unit III (Campanian) at Site 627, there is a major discrepancy in age. The considerable thickness of Oligocene sediments at this site may be either a depression fill or an imbricate thrust slice.

Summary

The section drilled at Site 628 contains three major units: (1) Unit I, 0–136.8 m sub-bottom; foraminiferal packstones and grainstones with oozes and some floatstones; these sediments are largely unlithified, although lithification does increase upward; (2) Unit II, 136.8–271.7 m sub-bottom; oozes and chalks,

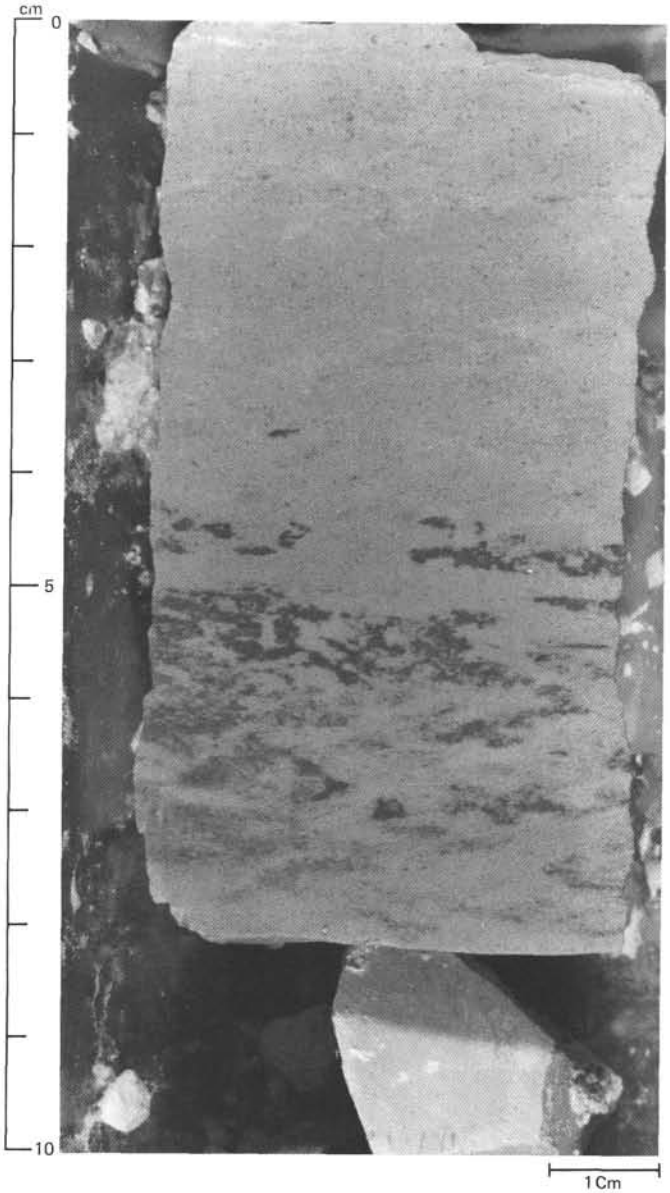

Figure 7. Burrowed green siliceous limestone of Unit IIIB, Sample 628A-32X, CC, 0–8 cm.

with partial lithification below 190 m sub-bottom; and (3) Unit III, 271.7–298.4 m sub-bottom; lithified packstones and siliceous limestones.

BIOSTRATIGRAPHY

Introduction

Hole 628A was drilled using the HPC to a sub-bottom depth of 192.7 m. Drilling then continued using the XCB to a sub-bottom depth of 298.4 m. Samples were examined from the core catcher of each core and are so referred to herein unless otherwise specified.

Dr. J. Butterlin helped identify the larger foraminifers.

Calcareous Nannofossils

Core 628A-1H contains *Emiliania huxleyi, Gephyrocapsa oceanica, G. caribbeanica*, and small gephyrocapsids, indicating the presence of Zone NN21 of late Pleistocene age. In Cores 628A-2H and 628A-3H, no gephyrocapsids and no discoasters were observed. The only age-diagnostic species observed were *Pseudoemiliania lacunosa* and *Reticulofenestra pseudoumbilica*. The nannofloras were tentatively assigned to Zones NN15/NN16 of early–late Pliocene age. In Core 628A-4H, these two species occur with *Discoaster brouweri, Discoaster pentaradiatus*, and *Discoaster surculus*, indicating the latest early Pliocene Zone NN15. Cores 628A-5H and 628A-6H contain the same

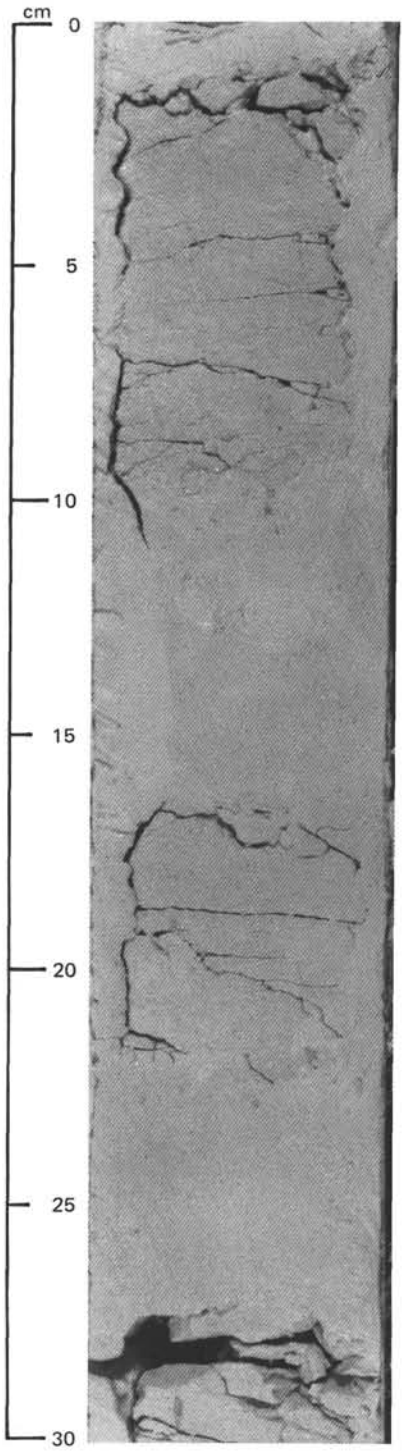

Figure 8. Fragmented pieces of fractured, lithified packstone of Unit IIIA, surrounded by drilling paste, Sample 628A-30X-4, 0–30 cm.

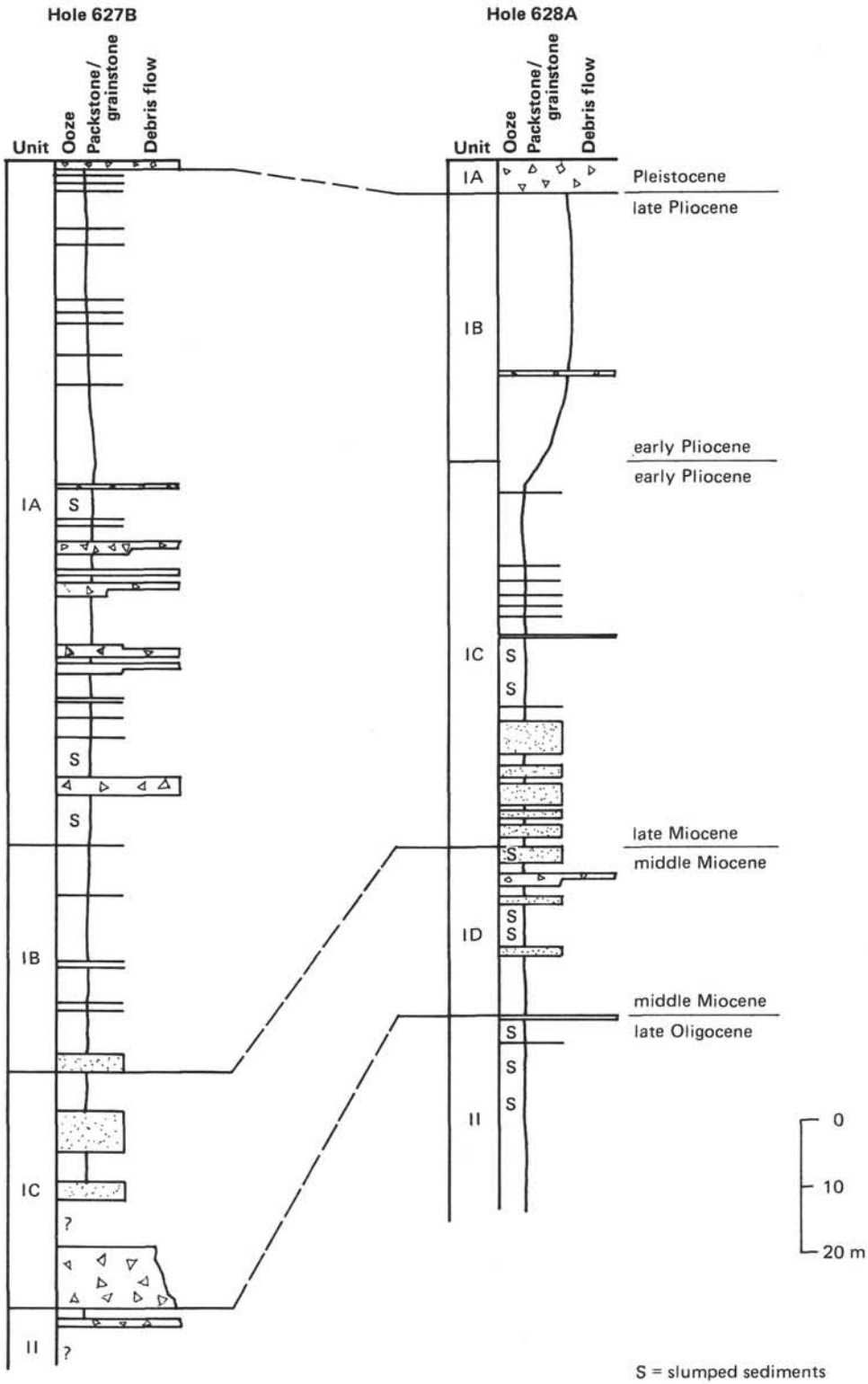

Figure 9. Correlation between Site 628 and Site 627, showing sediment type, lithologic units, and age ranges.

species as well as *Sphenolithus abies* and *Amaurolithus* sp. cf. *A. tricorniculatus* (Core 628A-6H only). Thus, this assemblage is assigned to Zones NN14/15 of early Pliocene age. In Core 628A-7H, *A. tricorniculatus* and *Ceratolithus rugosus* are present, indicating an early Pliocene age (NN14).

In Core 628A-8H, *C. rugosus* occurs with *Discoaster* sp. cf. *D. asymmetricus*, indicating the presence of Zones NN13/15 of early to late Pliocene age. *Discoaster* sp. cf. *D. asymmetricus* is not present in Core 628A-9H, suggesting Zone NN13 of early Pliocene age. The poorly preserved flora of Core 628A-10 con-

tains *D. brouweri, D. variabilis*, and *D. pentaradiatus*, tentatively assigned to Zone NN12 of late Miocene–early Pliocene age.

The sediment in Core 628A-11H is coarse and contains no age-diagnostic nannofossils. Nannofossil preservation in Core 628A-12H is rather poor. The presence of *Discoaster* sp. cf. *D. quinqueramus* tentatively suggests an age of late Miocene–earliest Pliocene (N11/12). Nannofossils are common in Cores 628A-13H to 628A-15H, but preservation is too poor to assign a reliable zone.

Core 628A-16H contains a nannofossil assemblage with *Sphenolithus ciperoensis, Helicopontosphaera recta, Zygrhabdolithus bijugatus*, and abundant *Reticulofenestra bisecta*, indicating a late Oligocene (NP25) age. The sequence from Core 628A-17H through 628A-24X contains similar assemblages but also contains *Sphenolithus distentus* and forms transitional between *S. distentus* and *S. ciperoensis*. The presence of these transitional forms complicates the separation of NP25 from NP24, as was seen at sites drilled in the southeastern Gulf of Mexico during Leg 77 (Lang and Watkins, 1984). Further shore-based studies are planned to obtain a better understanding of this lineage. For the present, this interval is assigned to NP24 (latest early Oligocene–late Oligocene). The Oligocene nannofossil assemblages in the interval from Core 628A-16H through 628A-20H contain numerous specimens of *Braarudosphaera* and *Pemma*, which may indicate a relatively shallow-water paleoenvironment. In Cores 628A-25X and 628A-26X, *S. ciperoensis* is absent and *Sphenolithus predistentus* is few to common in abundance, indicating the presence of Zone NP23, which is generally correlated with the early Oligocene. The occurrence of *Helicopontosphaera reticulata, Reticulofenestra umbilica*, and *Reticulofenestra hillae* in Core 628A-27X indicates Zone NP22, which is correlated with the early Oligocene. The addition of *Cyclococcolithina formosa* to the assemblage in Cores 628A-28X and 628A-29X indicates Zone NP21 of latest Eocene–early Oligocene age. The presence of more than 15% braarudosphaerid debris and holococcoliths in the sediment from Core 628A-28X suggests the general environmental deterioration that is commonly associated with the Eocene/Oligocene boundary.

Core 628A-30X contains *Discoaster lodoensis, Discoaster sublodoensis, Discoaster saipanensis*, and *Chiasmolithus grandis*, indicating Zone NP14 of latest early Eocene–earliest middle Eocene age. The nannofossil assemblage in Core 628A-31X is poorly preserved and contains significant downhole contamination. It is tentatively assigned to Zone NP13 of early Eocene age.

The flora in the Core 628A-32X is confusing because many Eocene species have been recognized as well as the characteristic middle late Paleocene (NP8) species *Discoaster mohleri, Cruciplacolitus tenuis, Ericsonia subpertusa, E. robusta, Heliolitus riedelii*, and *Prinsius* sp. This may be explained by the seismic record, which indicates a channel structure of possible Eocene age containing Paleocene debris.

Planktonic Foraminifers

Pleistocene sediments (*Globorotalia truncatulinoides* Zone, N22/N23) are present in Core 628A-1H, as indicated by the presence of *Globorotalia truncatulinoides*. The benthic-foraminiferal assemblage includes deep-water forms (*Planulina wuellerstorfi* and *Orisodorsalis tener umbonatus*) as well as shallow-water forms (*Elphidium, Nonionella*, and miliolids).

Core 628A-2H appears to have recovered the upper Pliocene *Globorotalia miocenica* Zone (N19 part), as indicated by the presence of *Globorotalia* sp. cf. *G. miocenica* and *G.* sp. cf. *G. praehirsuta* and the absence of *G. margaritae, G. truncatulinoides*, and *G. tosaensis*. Redeposited material is abundant and includes many shallow-water benthic foraminifers (*Elphidium, Nonionella*, and miliolids) and juvenile planktonic foraminifers. Deep-water benthic foraminifers include *Globocassidulina subglobosa* and *Cibicidoides mundulus*.

A similar assemblage occurs in Core 628A-3H, except that well-developed specimens of *Globorotalia miocenica* are present. Thus, these sediments are contained within the upper Pliocene *Globorotalia miocenica* Zone (N19 part). The benthic-foraminiferal assemblage contains a mixture of deep-water forms (*Cibicidoides mundulus, Gyroidinoides neosoldanii*, and *Planulina wuellerstorfi*) and shallow-water forms (*Elphidium, Nonionella*, and *Guttulina*).

Cores 628A-4H through 628A-8H are contained within the lower Pliocene *Globorotalia margaritae* Zone (N18/19 part). Diagnostic species include *Globorotalia margaritae, G. plesiotumida, Globoquadrina altispira altispira, Sphaeroidinellopsis paenedehiscens, Globigerinoides congoblatus*, and *Neogloboquadrina humerosa*. Most samples contain mixed deep-water (*Laticarinina pauperata, Planulina wuellerstorfi*, and very large *Sphaeroidina bulloides*) and shallow-water assemblages (*Nonionella, Elphidium*, and *Fursenkoina*).

Uppermost Miocene (Messinian) to lowermost Pliocene sediments occur in Core 628A-9H. The older age is indicated by the presence of *Neogloboquadrina humerosa*, a species that first occurs in the Messinian. Rare specimens of primitive forms of *Globorotalia margaritae* are also present, which may indicate an earliest Pliocene age. Thus, these sediments are contained within the upper part of the *Neogloboquadrina acostaensis* Zone (N17) to the lower part of the *Globorotalia margaritae* Zone (N18). Other species present include *Neogloboquadrina acostaensis*, abundant *Globorotalia juanai, Globigerinoides extremus*, and *Globigerinoides* sp. cf. *G. seigliei*. The benthic-foraminiferal assemblage is composed mainly of deep-water forms including *Planulina wuellerstorfi, Cibicidoides mundulus, Gyroidinoides neosoldanii, Siphonina bradyana*, and *Pleurostomella* sp.

Cores 628A-10H through 628A-12H are contained within the lower part of the late Miocene *Neogloboquadrina acostaensis* Zone (N16). Diagnostic species include *Neogloboquadrina acostaensis, Globorotalia juanai, G. plesiotumida, Globoquadrina baroemoenensis*, and *Candeina nitida*. *Neogloboquadrina humerosa* is absent. A mixed shallow- and deep-water benthic-foraminiferal assemblage is present in Core 628A-10H, which includes *Elphidium*, large *Sphaeroidina bulloides*, and *Osangularia*. Few benthic foraminifers occur in Core 628A-11H. A deep-water benthic-foraminiferal assemblage is present in Core 628A-12H, which includes *Gyroidinoides neosoldanii, Planulina wuellerstorfi*, and *Cibicidoides mundulus*.

An apparent hiatus exists between Cores 628A-12H and 628A-13H in which the late middle Miocene *Globorotalia menardii* Zone (N15) and the *Globorotalia mayeri* Zone (N13 part/14) are missing. The presence of *Globorotalia mayeri* and *G. fohsi lobata* in Cores 628A-13H through 628A-15H indicates that these sediments are contained within the middle Miocene *Globorotalia fohsi lobata/robusta* Zone (N11 part/13 part). The benthic-foraminiferal assemblage includes platform (*Amphistegina*), shallow-water (*Lenticulina*), and deep-water (*Gyroidinoides neosoldanii, Cibicidoides mundulus*, and *Vulvulina spinosa*) forms.

Paleogene strata are first encountered in Core 628A-16H. A hiatus spanning the early Miocene to early middle Miocene separates the Neogene and Paleogene at Site 628. Planktonic foraminifers of the upper Oligocene *Globigerina ciperoensis* Zone (P22) are recorded in samples from Cores 628A-16H through 628A-23X. Diagnostic taxa include *Globigerina ciperoensis, G. angulisuturalis, G. sellii*, and *Globorotalia opima nana*. *Globorotalia kugleri* and *Globorotalia opima opima* are absent, whereas *Globigerinoides primordius* occurs in all samples but Core 628A-23X. Berggren et al. (1985) report a 25.8 Ma first-appear-

ance datum for *G. primordius*. This would imply that Cores 628A-16H through 628A-22X occur in the upper half of the *Globigerina ciperoensis* Zone (i.e., latest Oligocene). The nannofloras yield an early late Oligocene age for Cores 628A-17H through 628A-24X. Further shore-based study should clarify this age discrepancy.

The co-occurrence of *Chiloguembelina* sp. and *Globigerina angulisuturalis* in Core 628A-24X indicates a latest early Oligocene age (*Globorotalia opima opima* Zone, P21a). Cores 628A-25X and 628A-26X are assigned to the lower Oligocene *Globigerina ampliapertura* Zone (P19/P20) on the basis of the occurrence of *G. ampliapertura* and *G. angiporoides*. An earliest Oligocene age (*Cassigerinella chipolensis–Pseudohastigerina micra* Zone, P17 part/18) is assigned to Cores 628A-27X and 628A-28X, as indicated by the presence of the nominate taxa. Core 628A-29X is latest Eocene in age. Taxa indicative of the *Globorotalia cerroazulensis* Zone (P16/17 part) include *G. cerroazulensis, G. cocoaensis*, and *Hantkenina alabamensis*.

Early Eocene–early middle Eocene sediments occur in Cores 628A-30X through 628A-32X. *Morozorella aragonensis, Acarinina* sp. cf. *A. bullbrooki*, and ?*Truncorotaloides* sp. cf. *T. rohri* suggest an early middle Eocene age (P10/11) for Cores 628A-30X and 628A-31X, whereas *Morozorella aragonensis, M. formosa formosa, Acarinina querta*, and *A. wilcoxensis* suggest an early Eocene age (P7/8) for Core 628A-32X.

Larger Foraminifers

At Site 628, larger foraminifers are absent from most cores. Rare *Amphistegina* sp. are present, however, in Cores 628A-1X (3.6 m sub-bottom), 628A-12H (107 m sub-bottom), and 628A-13H (117.4 m sub-bottom). Sample 628A-7H-01, 50–52 cm, yields *Lepidocyclina yurnagunensis*. This foraminifer, which disappeared in the early Miocene, seems to be reworked in this core of early latest Miocene age. No larger foraminifers are present in Cores 628A-15H (136.6 m sub-bottom) and 628A-16H (146.1 m sub-bottom), which bracket an upper middle Miocene/upper Oligocene unconformity identified with planktonic foraminifers and nannofossils. Sample 628A-24X-02, 50–52 cm, contains *Heterostegina antillea, Heterostegian* cf. *panamensis, Lepidocyclina (L.) yurnagunensis, Lepidocyclina (L.) canellei*, and *Lepidocyclina (L.) giraudi*, an assemblage that indicates an Oligocene–early Miocene age. Samples 628A-26X-1, 70–72 cm, 628A-26X-2, 40–42 cm, and 628A-26X-2, 86–88 cm, yield *Lepidocyclina (L.) yurnagunensis, Lepidocyclina (L.) waylanvaughani, Lepidocyclina (L.) miraflorensis, Lepidocyclina (L.) undosa*, and *Nummulites* sp., which indicate an age of Oligocene–early Miocene. Planktonic foraminifers and nannofossils indicate that the age of this core is early Oligocene (P19/20, NP23). Thus, these larger foraminifers of shallow-water origin are interpreted as being penecontemporaneously redeposited. Sample 628A-26X-2, 40–42 cm, contains *Dictyoconus floridanus*, known only in middle–upper Eocene sediment. This member of the Orbitolinidae is clearly a reworked older fossil and has been transported from the Little Bahama Platform.

Radiolarians

Samples from fine-grained calcareous ooze and clay-rich intervals of Cores 628A-14H through 628A-29X were processed for radiolarian study. Only Cores 628A-14H through 628A-19H ultimately proved to contain radiolarians. Siliceous sponge spicules were the predominant siliceous component in these samples.

Neogene radiolarians occur in Cores 628A-14H and 629A-15H. The presence of *Didymocyrtis mammifer* and *Calocycletta costata* suggests the upper part of the *Calocycletta costata* Zone or the lower part of the *Dorcadospyris alata* Zone. Additional species that support this dating are *Cyrtocapsella cornuta* and *Solenosphaera tritubus*; tholoniids, a family that occurs strictly in the Neogene, are also present.

Samples from Cores 628A-16H though 628A-19H contain an unusual radiolarian assemblage. The predominant radiolarian group is the orosphareids, which occur as distinctive fragments and spines in samples from Hole 628A. According to Friend and Riedel (1967), this group of radiolarians is particularly solution-resistant, and their robust skeletons persist even in red clays. However, silica preservation is good in this interval, delicate radiolarians and diatoms being well preserved. Another unusual aspect of the radiolarian assemblage is that approximately 90% of the non-orosphaerid radiolarian assemblage consists of *Dorcadospyris* spp.

The occurrence of *Dorcadospyris ateuchus* and *Lithocyclia angusta* in Cores 628A-16H through 628A-19H indicates the lower part of the *Dorcadospyris ateuchus* Zone of late Oligocene age. This age assignment is supported by the occurrence of *Didymocyrtis prismatica, Lychnocanium trifolium, Tristylospyris triceros, Dorcadospyris simplex*, and *Dorcadospyris circularis*. Orosphaerid species identified on the basis of characteristic features observed in shell fragments and spines include *Oradapis spongiosa, Orescena carolae, Orescena gegenbauri, Orodapis spongiosa*, and *Oropagis doliolum*. These species are all typical of the late Oligocene, which conforms to Friend and Riedel's (1967) general observation that orosphaerids are more abundant in sediments of late Oligocene and early Miocene age than in other deposits.

SEDIMENT-ACCUMULATION RATES

An abbreviated Pleistocene section unconformably(?) overlies a continuous sequence of upper Miocene–upper Pliocene nannofossil–foraminifer ooze in Cores 628A-12H to 628A-2H. The average accumulation rate (Fig. 10) through this interval is 33 m/m.y. A debris flow in Core 628A-13H marks a stratigraphic break of as much as 5 m.y. separating ?uppermost Miocene from middle Miocene sediments in Cores 628A-15H through 628A-13H. This latter section accumulated at a rate of more than 10 m/m.y. A sharp lithologic break in Sample 628A-16-1, 15 cm, represents a hiatus of at least 10 m.y. spanning the latest Oligocene through early middle Miocene. Cores 628A-24X through 628A-16H record a sequence of uppermost lower Oligocene to upper Oligocene nannofossil–foraminifer ooze. Shipboard age determinations reveal a discrepancy between planktonic foraminifers and calcareous nannofossils through this interval, whereas radiolarian zonation overlaps the two. Accumulation-rate estimates vary between 12 and 27 m/m.y. Further shore-based study may reveal that this upper Oligocene section is incomplete, as suggested by planktonic-foraminiferal evidence in Cores 628A-22X through 628A-24X. A mid-Oligocene hiatus of no more than 2 m.y. may separate the upper Oligocene section from a continuous sequence of uppermost Eocene to lower Oligocene nannofossil ooze in Cores 628A-29X through 628A-25X. This latter section accumulated at an average rate of 9–10 m/m.y. An uppermost Paleocene–lower Eocene section unconformably underlies the uppermost Eocene in Cores 628A-32X through 628A-30X but is not well constrained by shipboard biostratigraphy. Preliminary estimates of sediment accumulation suggest an average rate of less than 5 m/m.y. for this interval.

INORGANIC GEOCHEMISTRY

Interstitial-Water Studies

Analyses of interstitial-water samples from Site 628 revealed gradients of Ca and Mg similar to those previously encountered. The Ca concentration increases from a seawater value of 10.44 to 17 mmol/L over an interval of 262 m, whereas Mg declined from 54 to 42 mmol/L (see Fig. 11 and Table 3). The pH, alka-

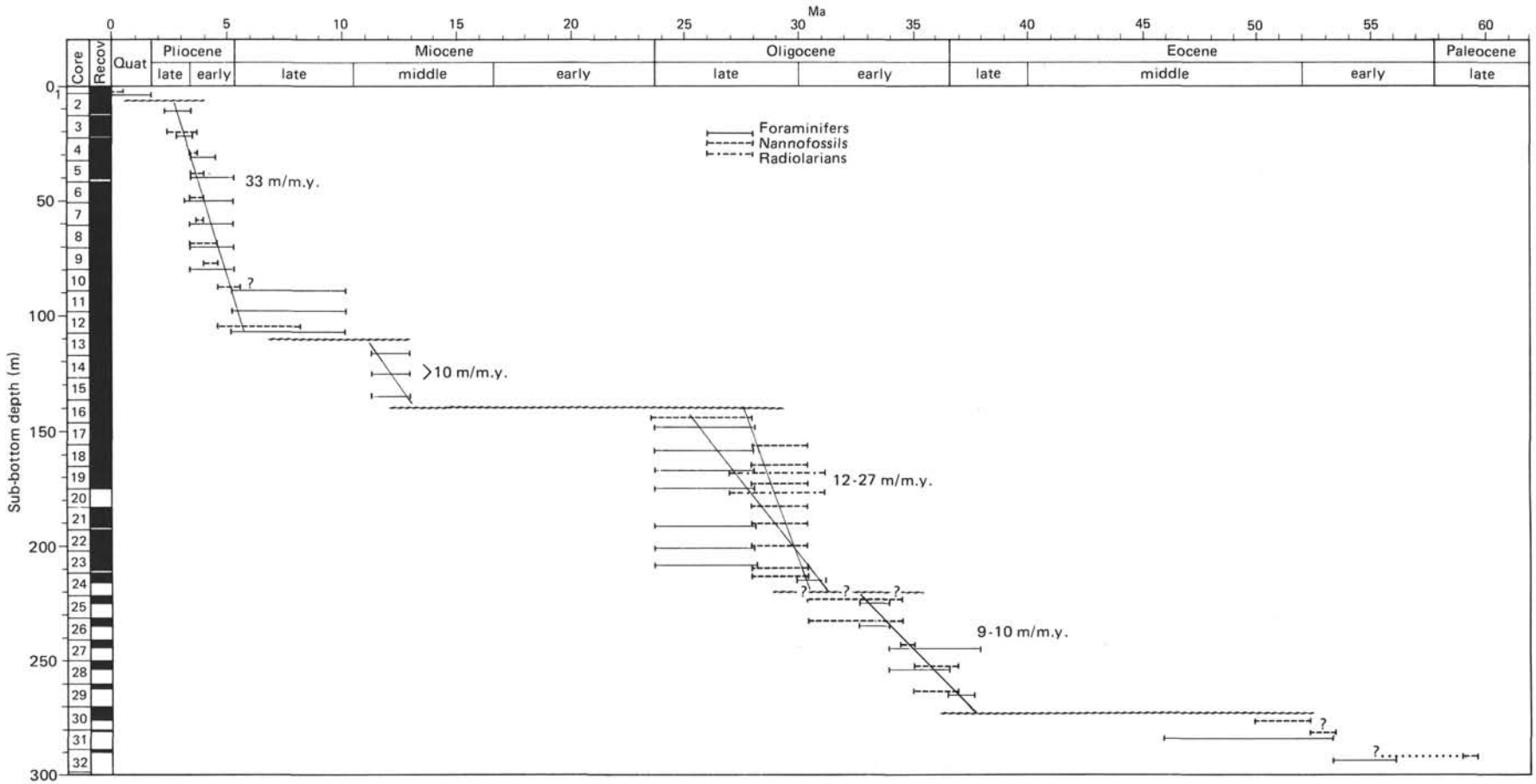

Figure 10. Sediment-accumulation rates, Site 628.

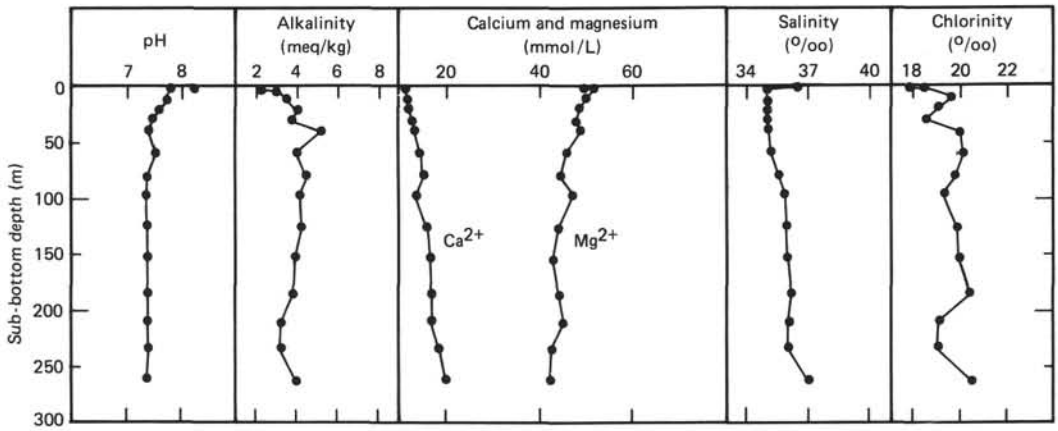

Figure 11. Summary of interstitial-water analyses, Hole 628A.

Table 3. Analyses of interstitial waters from Hole 628A.

Sub-bottom depth (m)	pH	Alkalinity (meq/kg)	Salinity (‰)	Chlorinity (‰)	Ca (mmol/L)	Mg (mmol/L)	SO_4 (mmol/L)
Surface seawater	8.23	2.34	36.1	17.73	10.70	54.50	—
1.4	7.80	3.01	35.0	18.46	10.47	52.60	27.40
11.0	7.74	3.51	35.0	19.65	11.53	52.90	25.59
20.6	7.61	4.05	35.0	19.00	11.64	51.55	25.88
30.3	7.47	3.77	35.0	18.59	12.67	50.72	25.05
40.0	7.42	5.22	35.1	20.02	12.84	51.70	26.02
58.9	7.54	4.02	35.2	20.14	14.13	48.73	26.02
79.5	7.39	4.52	35.6	19.81	14.58	47.49	27.43
96.5	7.36	4.19	35.9	19.27	12.96	50.01	26.81
124.8	7.40	4.30	35.9	19.88	15.41	47.17	26.39
153.5	7.39	3.94	36.0	19.95	16.09	45.87	27.75
184.7	7.41	3.85	36.2	20.46	16.35	47.18	24.63
209.7	7.40	3.27	36.0	19.04	16.26	48.39	23.84
232.8	7.43	3.21	36.0	18.97	17.89	45.81	22.49
261.6	7.39	4.02	37.0	20.53	19.27	45.49	23.65

linity, and sulfate concentrations all showed variations over the top 45 m, compatible with microbial sulfate reduction rates (Fig. 12). Below 45 m, alkalinity declined, as did sulfate. However, the magnitude of these changes is insignificant considering those documented by previous DSDP legs. Typically, the presence of abundant organic material causes a reduction in the interstitial-water sulfate concentration, an increase in CO_2, and a consequent rise in alkalinity. The absence of such trends in Holes 628A, 626C, and 627B would suggest a combination of the following processes: (1) the absence of sufficient initial amounts of organic materials to deplete the interstitial-water sulfate concentration, (2) sufficiently slow rates of sediment accumulation (less than 50 m/m.y.) to allow all or most of the organic material to be oxidized in the aerobic zone, and (3) an external source of sulfate ions, such as the underlying gypsum deposits at Sites 627 and 628. A further parameter needing consideration is the presence of methane in these sediments, which is thought to be bacterial in origin. If the methane is indigenous, then methanogenesis clearly is not restricted to sulfate-depleted waters, as envisaged in an ideal diagenetic sequence.

X-Ray Studies

X-ray studies of the bulk mineralogy of the sediments from Hole 628A showed the persistence of aragonite into sediments as old as late Oligocene (see Figs. 13 and 14 and Table 4). This distribution, however, can be divided into two sections. The upper 20 m, middle Pliocene to late Pleistocene in age, contains aragonite in concentrations of over 50%, together with minor amounts of dolomite (2%–3%), but no quartz. Below this, perhaps extending into the late Oligocene section (150 m), aragonite falls to an average composition of 10%. Beneath this, the sediments are dominantly low-Mg calcite and between 1% and 2% quartz.

Small quantities of clays, thought to be mixtures of illite, montmorillonite, and palygorskite, were detected throughout the sequence (see Table 4).

Carbonate-Bomb Data

Carbonate percentages varied between 80% and 95% and showed little systematic changes relative to mineralogy (see Fig. 15 and Table 5).

ORGANIC GEOCHEMISTRY

Thirty-eight samples were taken for Rock-Eval analysis. The Rock-Eval data are given in Figures 16 through 19.

The lithology at Site 628 has been subdivided into three major units (see Fig. 16; "Sedimentology" section, this chapter): Unit I, carbonate oozes (late Miocene–Pleistocene); Unit II, nannofossil oozes (late Eocene–Oligocene); Unit III, foraminifer packstones (late Paleocene–early Eocene).

The organic material in most of this sequence is detrital, oxidized, terrestrial material (see Fig. 17). However, at the base of Unit I, within the late Miocene section, the S_2 content of the kerogen increases to approximately 0.4 (see Fig. 16). The S_2/S_3 ratio of this kerogen is also higher than in the other samples (0.25/0.75) (see Fig. 17).

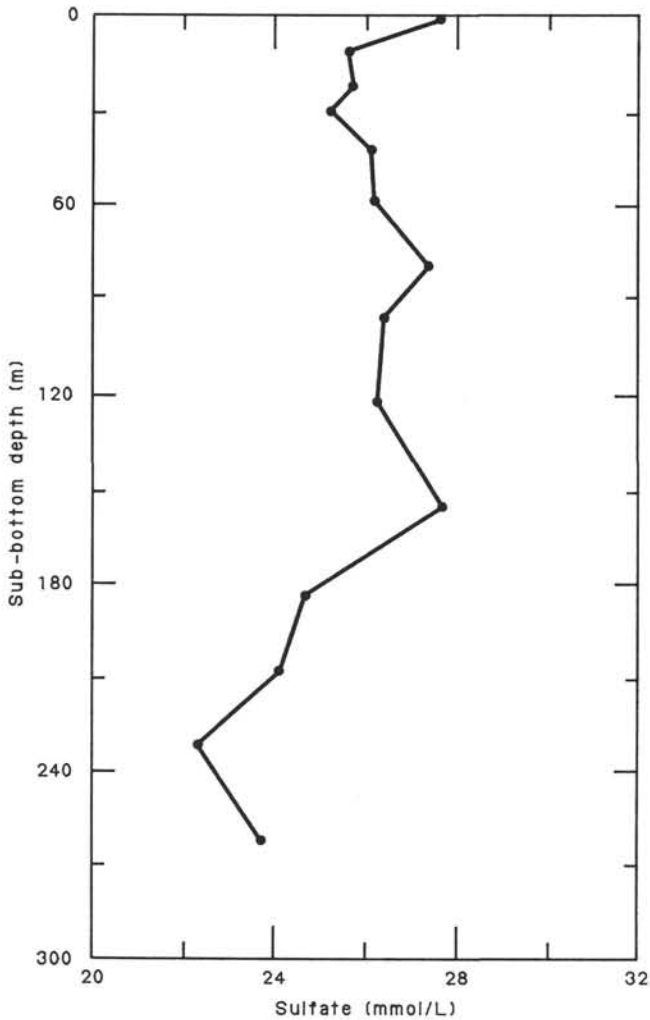

Figure 12. Interstitial-water sulfate concentrations, Hole 628A.

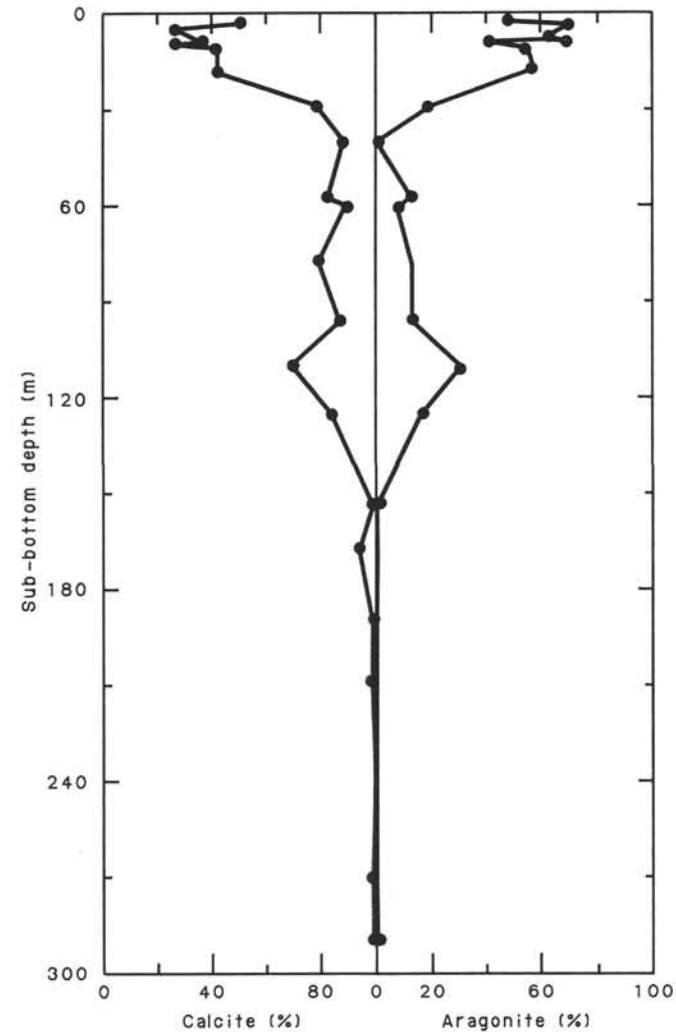

Figure 13. Percentage variations in the calcite and aragonite content of sediments from Hole 628A.

T_{max} values of Site 628 showed a random scatter, as would be expected of a mixture of detrital sources of different provenances and maturities (see Fig. 18). The S_1 content, soluble organics, was generally very low (Fig. 19).

PALEOMAGNETISM

Hole 628A could yield some of the most interesting paleomagnetic data of Leg 101. A relatively complete Oligocene sedimentary section having good microfossil control was recovered in Cores 628A-16H through 628A-29X. This section should provide valuable constraints on the correlation of the Oligocene geomagnetic time scale with the corresponding biostratigraphic time scale. From Hole 628A cores, 124 oriented 7-cm^3 paleomagnetic samples were taken, including 63 from the Oligocene section. Additionally, three oriented 12-cm^3 minicores were drilled from limestones recovered in Core 628A-30X. The magnetizations of all the samples were too small to be measured with the shipboard Molspin spinner magnetometer and await analysis on land.

Magnetic-susceptibility measurements were made as at the previous sites (see "Paleomagnetism" section, Site 626 chapter, this volume), resulting in 2158 individual readings. The results of these measurements are shown in Figure 20, where susceptibility is plotted versus depth. With the exception of large-amplitude spikes evidently due to drill-pipe rust contamination (see "Paleomagnetism," Site 627 chapter, this volume, for discussion), the susceptibility values show minor variation. Most values are about -0.4×10^{-6} G/Oe, indicating that the sediments contain little magnetic material.

PHYSICAL PROPERTIES

Seven types of physical-property measurements, grouped in four main categories, were made at Site 628 (see Fig. 21 and Table 6): (1) compressional wave velocities measured on samples both in and out of the core liner; (2) wet-bulk density, porosity, and water content; (3) thermal conductivity; and (4) shear strength.

Compressional Wave Velocity

Compressional wave velocity measurements were made on samples removed from Sections 2, 4, and 6 of each core. Measured values vary around a mean value increasing with depth from 1600 to 1800 m/s.

Compressional wave velocity measurements made on recovered sediment remaining in the core liner are clustered around a mean value of 1750 m/s and do not display a clear increase in velocity with depth. A zone of high-frequency variations is evident between 65 and 170 m sub-bottom (Fig. 21). Measurements

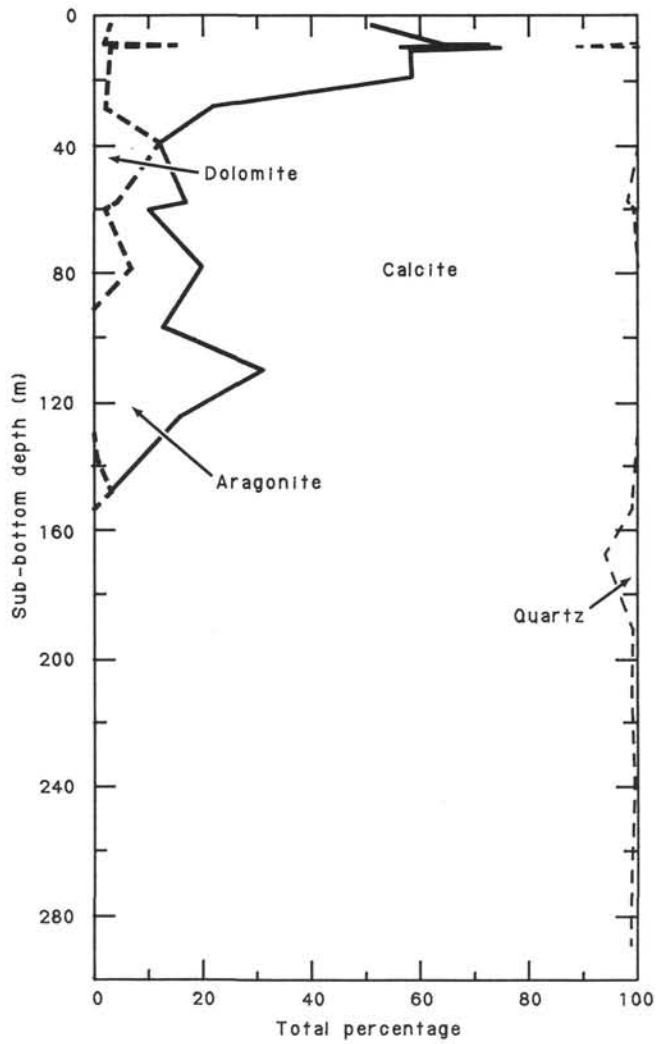

Figure 14. X-ray data, Hole 628A.

could not be made on disturbed and cracked samples; thus, sample choice may have affected the lack of overall trend in velocity.

Index Properties

Overall, wet-bulk density determined gravimetrically and volumetrically on discrete samples increases slightly with increasing depth from 1.8 g/cm^3 at the water/sediment interface to 1.9 g/cm^3 at 240 m sub-bottom. In comparison, wet-bulk density determined with the GRAPE gamma-ray counts shows a distinct peak at about 145 m sub-bottom. Otherwise, GRAPE densities remain constant with depth.

Porosity (Fig. 21), like density, shows little variation. Values decrease slowly with depth from 60% to 55%.

The water-content profile (Fig. 21) does not display a general trend with depth. Water content averages 40% throughout the hole. The profile can be separated at 145 m sub-bottom into an upper zone of values displaying high-frequency variations and a lower zone lacking much variation in values.

Thermal Conductivity

Thermal-conductivity values (Fig. 21) increase slightly with depth from 2.5×10^{-3} cal $\times$ °C^{-1} $\times$ cm^{-1} $\times$ s^{-1} at the top of the hole to 2.9×10^{-3} cal $\times$ °C^{-1} $\times$ cm^{-1} $\times$ s^{-1} at 200 m sub-bottom. Below 200 m, the conductivity profile stabilizes to an average of 3.0×10^{-3} cal $\times$ °C^{-1} $\times$ cm^{-1} $\times$ s^{-1}. The change in slope at 200 m sub-bottom divides this profile into two main parts, neither of which displays much variation in values.

Shear Strength

Shear strength is difficult to characterize, although there is a slight general increase from 2 to 15 kPa between 1.5 and 250 m sub-bottom and some extreme values of more than 50 kPa (Fig. 21).

Specifically, five main zones may be distinguished within the shear-strength profile:

Zone 1: 0–40 m, relatively flat slope, measured values less than 10 kPa.
Zone 2: 40–105 m, bell-shaped curve, average value of 25 kPa. This zone can be subdivided at 65 m by the low value of 0.2 kPa.
Zone 3: 105–200 m, bell-shaped zone, high value of 60 kPa.
Zone 4: 200–230 m, bell-shaped zone, high value of 50 kPa.
Zone 5: 230–260 m, relatively homogeneous zone, measured values increasing from about 4 to 16 kPa.

Discussion

Hole 628A was sampled to 298 m sub-bottom. Most of the physical properties except shear strength display little variation downhole. For more information, therefore, acoustic impedance was calculated. The acoustic-impedance profile shows a major excursion at 245 m sub-bottom that correlates with an increase in GRAPE density (Fig. 22). This excursion, imperceptible on the other physical-property profiles, occurs at the base of a long unit of pelagic calcareous ooze and chalks and just above a debris flow.

Another event suggested by physical-property profiles occurs at 145 m sub-bottom, where GRAPE-measured density values are markedly higher. This interval is also the point in the water-content profile that divides the upper section having high-frequency oscillations from the lower section having more uniform values. This point marks the beginning of Zone 4 on the undrained shear-strength curve. The shear-strength profile in this hole is the most sensitive indicator of change. The five zones obvious in this profile correlate well with observed lithologic changes. Slumps punctuate the lithologic section at 40 m sub-bottom (base of Zone 2), at 145 m sub-bottom (base of Zone 3), and at 170 m sub-bottom. Undrained shear strength changes markedly with minor disturbances of soil, slumps, and flows, as well as with drilling disturbance. These changes, evidenced by shear-strength measurements, may not be as readily observable in selected discrete samples analyzed for index properties.

Six main zones were distinguished on the basis of physical-property measurements:

Z1: 0–40 m sub-bottom.
Z2: 40–65 m sub-bottom.
Z3: 65–145 m sub-bottom.
Z4: 145–200 m sub-bottom.
Z5: 200–260 m sub-bottom.

These zones correlate with the following lithologic units (see Fig. 21 and "Sedimentology" section, this chapter):

Z1: turbidites and debris flows.
Z2: calcareous ooze.
Z3: calcareous ooze with abundant alternations of nannofossil–foraminifer chalk. The break observed in the shear-strength curve at 50 m sub-bottom occurs at the point of a turbidite. This feature greatly affected much of the underlying ooze, where we noticed a regular increase of shear strength after this break.
Z4: Marking a lithologic change from nannofossil ooze to nannofossil–foraminifer ooze, possibly reflecting the change in grain

Table 4. X-ray analyses of samples from Hole 628A.

Sub-bottom depth (m)	Calcite (%)	Aragonite (%)	Dolomite (%)	Quartz (%)	Comments
3.0	49	48	3	0	
8.9	36	62	2	0*	Packstone, semilithified top of turbidite
9.0	27	69	3	0	Grainstone, base of turbidite, unlithified
9.8	33	41	15	11*	Top of turbidite
10.0	26	71	3	0	Base of turbidite
11.0	42	55	3	0*	
18.6	42	58	0	0*	
28.8	78	20	2	0*	
40.0	88	0	12	0	
57.6	82	13	4	2	
59.9	89	8	2	1	
78.0	79	13	7	0*	
96.5	87	13	0	0*	
110.0	69	31	0	0*	
124.8	84	16	0	0	
148.3	96	0	3	1	
153.5	99	0	0	1*	
167.3	94	0	0	6*	
190.6	99	0	0	1	
209.7	99	0	0	1	
238.4	100	0	0	0	
267.6	99	0	0	1	
288.8	99	0	0	1*	

*Clay minerals present, thought to be an illite-montmorillonite mixture.

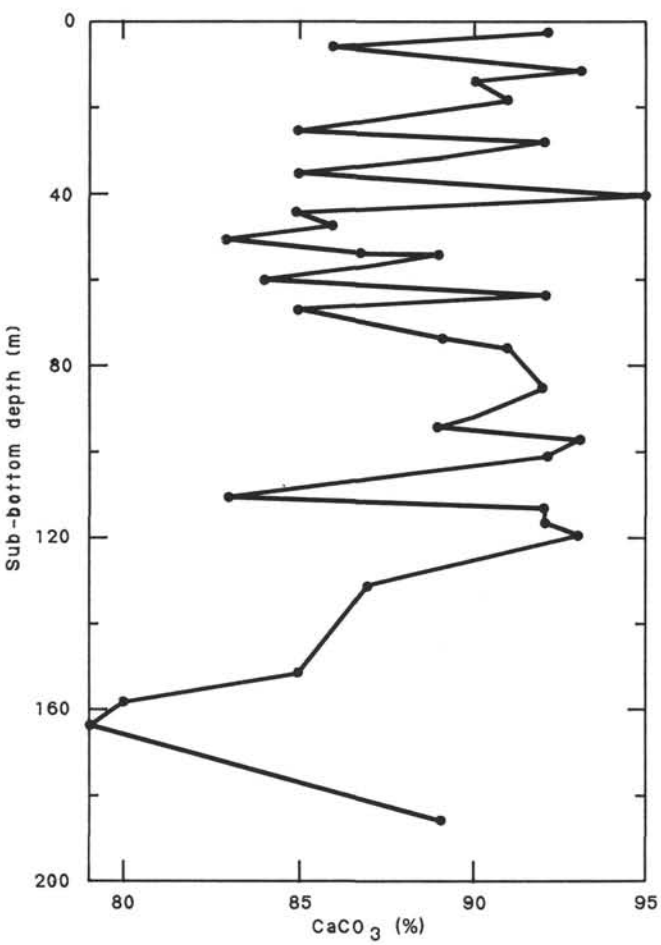

Figure 15. Carbonate-bomb data, Hole 628A.

Table 5. Carbonate-bomb data, Site 628.

Sub-bottom depth (m)	$CaCO_3$ content (%)
2.2	92
5.8	86
11.8	93
13.9	90
18.4	91
25.1	85
28.1	92
31.1	89
34.8	85
37.8	90
40.8	95
44.1	85
47.1	86
50.1	83
53.7	87
53.7	89
56.7	87
59.7	84
63.1	92
66.1	85
72.8	89
75.8	91
84.9	92
91.3	90
94.3	89
97.3	93
100.7	92
110.1	83
113.1	92
116.1	92
119.6	93
130.7	87
151.3	85
157.9	80
163.9	79
185.4	89

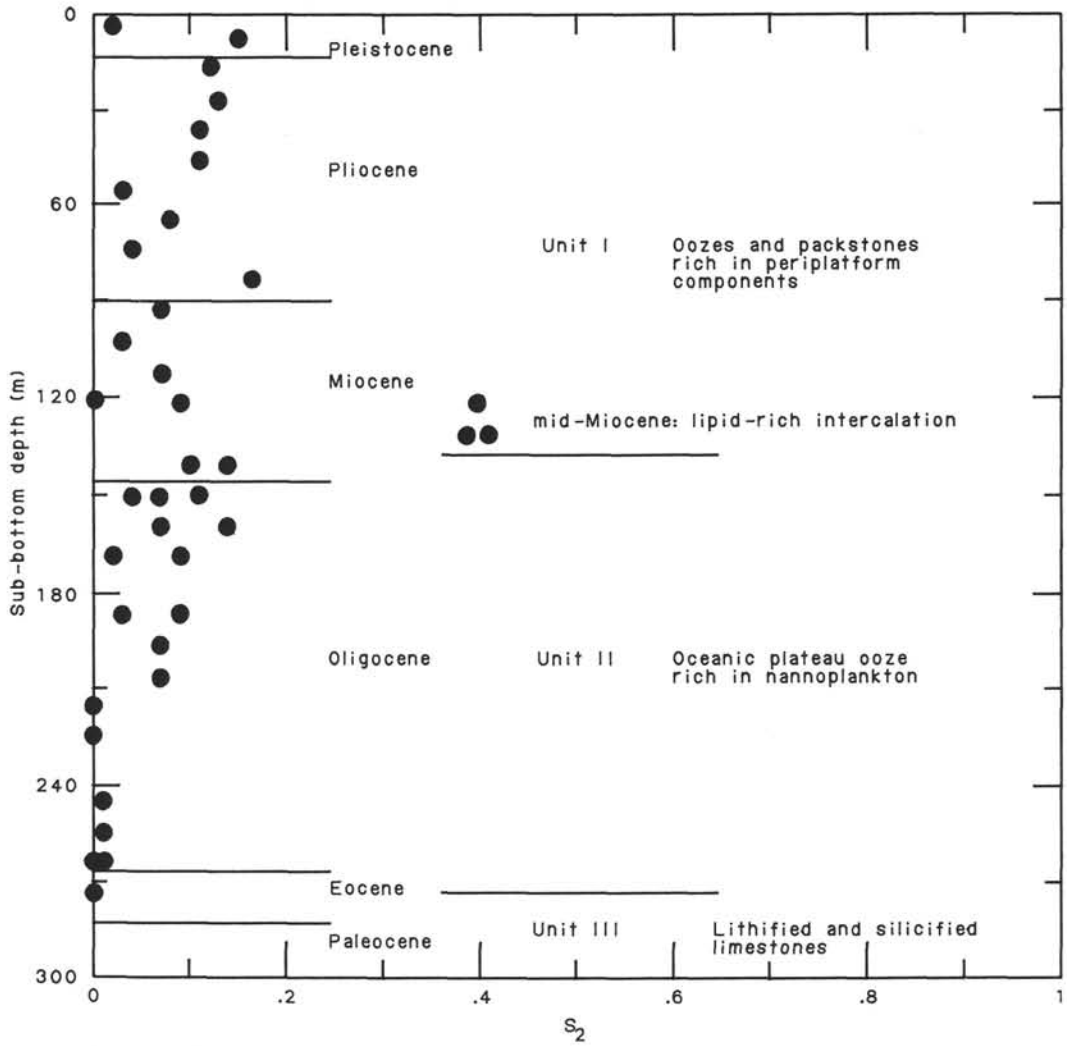

Figure 16. S_2 content of lithologies at Site 628, indicating the poor source potential of the kerogens.

size of the sediment, this break is clearly observed only on the water-content curve.

Z5: Generally attributed to drilling effects, this zone does not represent a lithologic change. However, the recognition of this zone on all the physical-property profiles clearly suggests that this zone must be distinguished even though there is currently no evident interpretation.

SEISMIC STRATIGRAPHY

Introduction

Hole 628A sampled the four uppermost sequences previously sampled at Site 627: A, B, C, and D (see Fig. 33, Site 627 chapter). At Site 628, depths to the A/B, B/C, C/D, and D/E sequence boundaries were calculated using traveltimes from LBB-18 and the same velocity-time curve from LBB-18 used in computing thicknesses at Site 627. This extrapolation seemed justified given the short distance between the two sites and the general seismic stratigraphic similarity of the two locations (see "Operations Summary," this chapter; Fig. 23 and Table 7). All these sequence boundaries correlate with either lithologic boundaries or hiatuses in Hole 628A, and a firm correlation is established below between Sites 627 and 628 along line LBB-18 (Fig. 33, Site 627 chapter).

Seismic Correlations

Sequence A/Sequence B

At a calculated depth of 52 m sub-bottom, this boundary falls within Core 628A-7H (51.5–60.9 m sub-bottom), an apparently complete lower Pliocene section of unlithified grainstones, packstones, and ooze. In Core 628A-6H, a transition occurs at 48.1 m sub-bottom from lower Pliocene graded grainstones and packstones interpreted as turbidites (Subunit IA, "Sedimentology" section, this chapter) downward to oozes and chalks with few if any turbidites (Subunit IB, "Sedimentology" section, this chapter). Given the inherent 5%–10% uncertainty of time-to-depth conversions using semblance velocities, the A/B sequence boundary is here interpreted to coincide with the lithologic change in Core 628A-6H. That the A/B boundary at Site 627 occurs at almost the same depth and is also early Pliocene in age substantiates this interpretation.

Sequence B/Sequence C

The base of sequence B occurs at 120 m sub-bottom. The B/C boundary coincides in depth with a late middle–early late Miocene hiatus between Cores 628A-12H and 628A-13H (107.9–117.4 m sub-bottom). As with the A/B boundary, the B/C

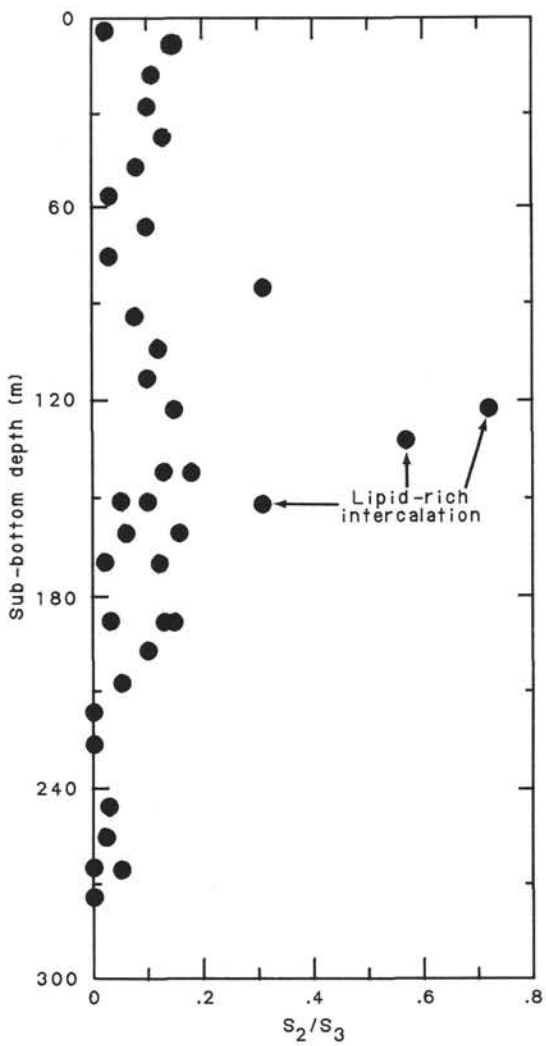

Figure 17. S_2/S_3 ratio (kerogen typing) of lithologies at Site 628, indicating the highly oxidized nature of the kerogens.

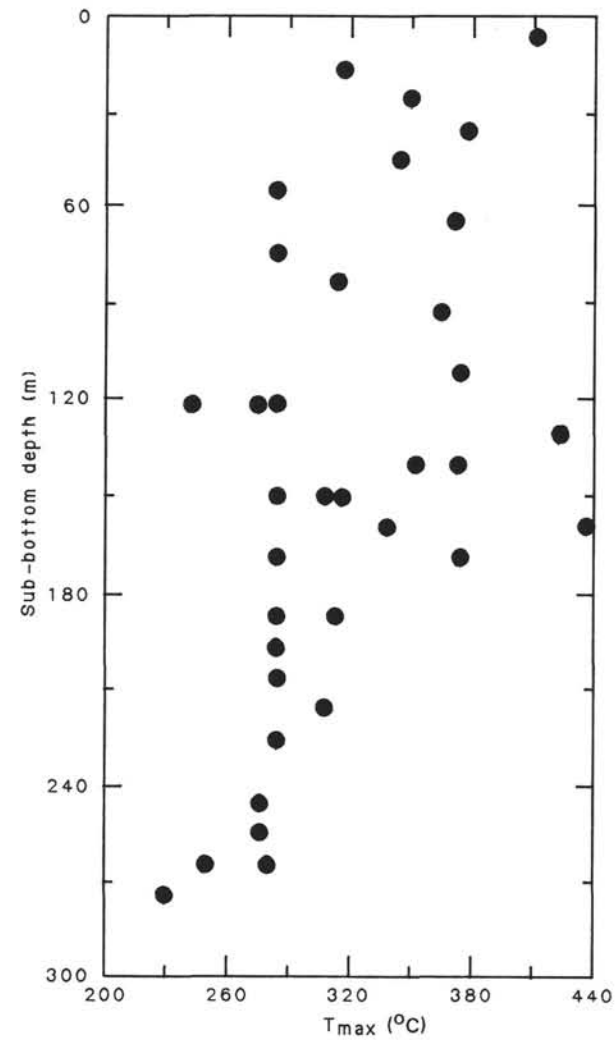

Figure 18. T_{max} (maturity estimate) at Site 628, showing a mixture of kerogens of differing maturities.

boundary at Site 628 is analogous in depth, age, and geologic significance to the B/C boundary at Site 627.

Sequence C/Sequence D

The C/D boundary falls at 138 m sub-bottom in Hole 628A, which corresponds in depth to the latest Oligocene–middle Miocene hiatus between Cores 628A-15H and 628A-16H (136.6–146.1 m sub-bottom) and to a slump at 137.9 m sub-bottom (Section 628A-16H-1). This is the most prominent unconformity, lithologic break, and sequence boundary in the section sampled by Hole 628A. Once again, the C/D boundary at Site 628 is approximately coeval with the same sequence boundary at Site 627, although they do not occur at the same sub-bottom depths.

Sequence D/Sequence E

The D/E sequence boundary, occurring at 294 m sub-bottom, was the target of Hole 628. On LBB-18, the boundary appears to be the base of a channel eroded into the top of sequence E (see "Summary and Conclusions" section, Site 627 chapter, this volume; Fig. 23). The bottom of Core 628A-32X (298.4 m sub-bottom) coincides with the base of this interpreted channel. Although recovery was poor, this core did contain chert fragments and lower Paleocene limestone. The canyon-cutting episode at Site 628 can, therefore, be tied to the late Paleocene–early Eocene hiatus in Hole 627B, which is the top of sequence E.

The top of the interpreted channel fill on LBB-18 occurs at approximately 266 m sub-bottom. This can be tied to a prominent middle-late Eocene hiatus, which occurs between Cores 628A-29X and 628A-30X (269.9–279.2 m sub-bottom). No obvious lithologic break occurs at this depth, but poor recovery in both cores suggests coarse-grained and/or friable material, further substantiated by chert fragments in Core 628A-31X (279.2–288.8 m sub-bottom), reminiscent of the coeval interval of very slow sedimentation in Hole 627B.

Conclusions

Correlations, or the lack thereof, between the seismic-sequence boundaries identified beneath the northern slope of Little Bahama Bank and global sea-level curves have been discussed (Site 627 chapter, this volume). A seismic stratigraphic tie between Sites 627 and 628 seems established, despite the presence of interpreted imbricate thrusts, which affect the intervening section (Fig. 23).

Despite this general correlation, however, complications exist. First, virtually the entire Oligocene section is missing at Site 627, whereas at Site 628, more than 100 m of relatively undisturbed Oligocene oozes and chalks (sequence D) occur. Second,

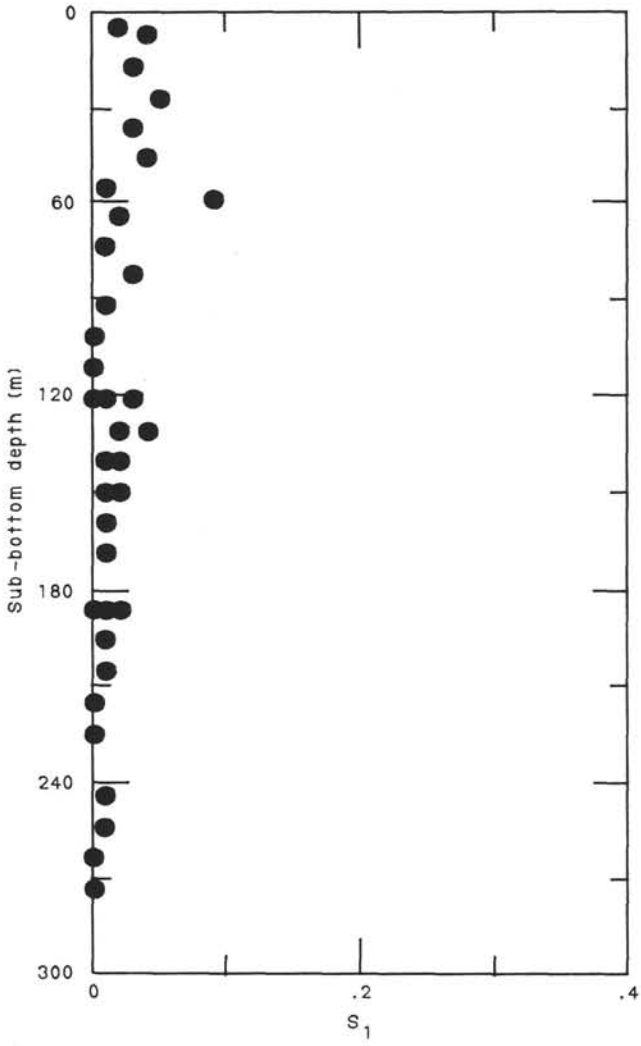

Figure 19. S_1 content (free bitumen) at Site 628, showing negligible bitumen content.

at least one seismic unconformity within sequence D (*D′*, Fig. 23) can be recognized at Site 628 (219 m sub-bottom) and must either pinch out between Site 628 and Site 627 or lie so near the top of sequence E that it cannot be resolved seismically at Site 627 (Fig. 23). In Hole 628A, *D′* may represent an early Oligocene hiatus between Cores 628A-24X and 628A-25X (221.5–231.4 m sub-bottom), but whether or not this represents a correlation with the prominent latest Eocene/latest Oligocene unconformity in Core 627B-20X (see "Summary and Conclusions" section, Site 627 chapter, this volume) remains uncertain. The possibility that *D′* is a lower Oligocene marker previously unrecognized at Site 627 would offer an explanation for the depth mismatch between the latest Eocene–latest Oligocene hiatus in Hole 627B and both the overlying C/D and underlying D/E sequence boundaries there (Site 627 chapter, this volume; Fig. 23).

SUMMARY AND CONCLUSIONS

Site 628 on the northern flank of Little Bahama Bank is the second in a three-site slope transect. Hole 628A penetrated 298 m of sediment with the HPC/XCB system. From top to bottom, the sequence consisted of the following units (Fig. 24 and "Sedimentology" and "Biostratigraphy" sections, this chapter): (1) Unit I, periplatform carbonate ooze (with bank-derived aragonite) and turbidites, slumps, and debris flows, middle Miocene

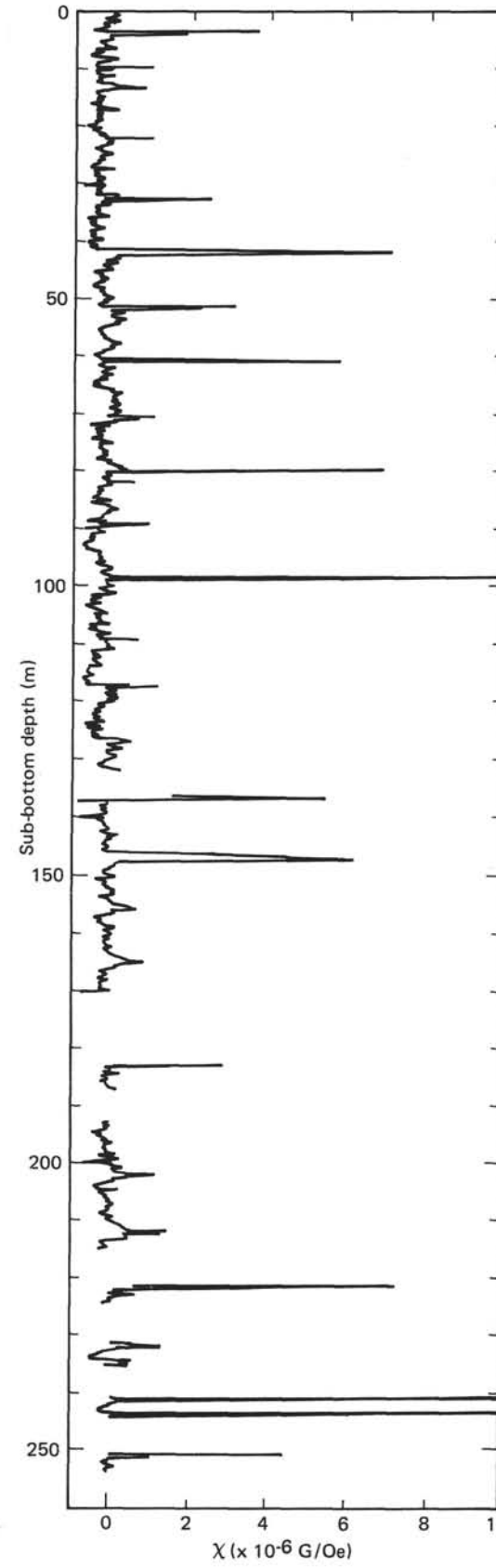

Figure 20. Magnetic-susceptibility values ($\times 10^{-6}$ G/Oe) plotted vs. sub-bottom depth in Hole 628A. Arrows indicate large-amplitude spikes evidently from rust contamination.

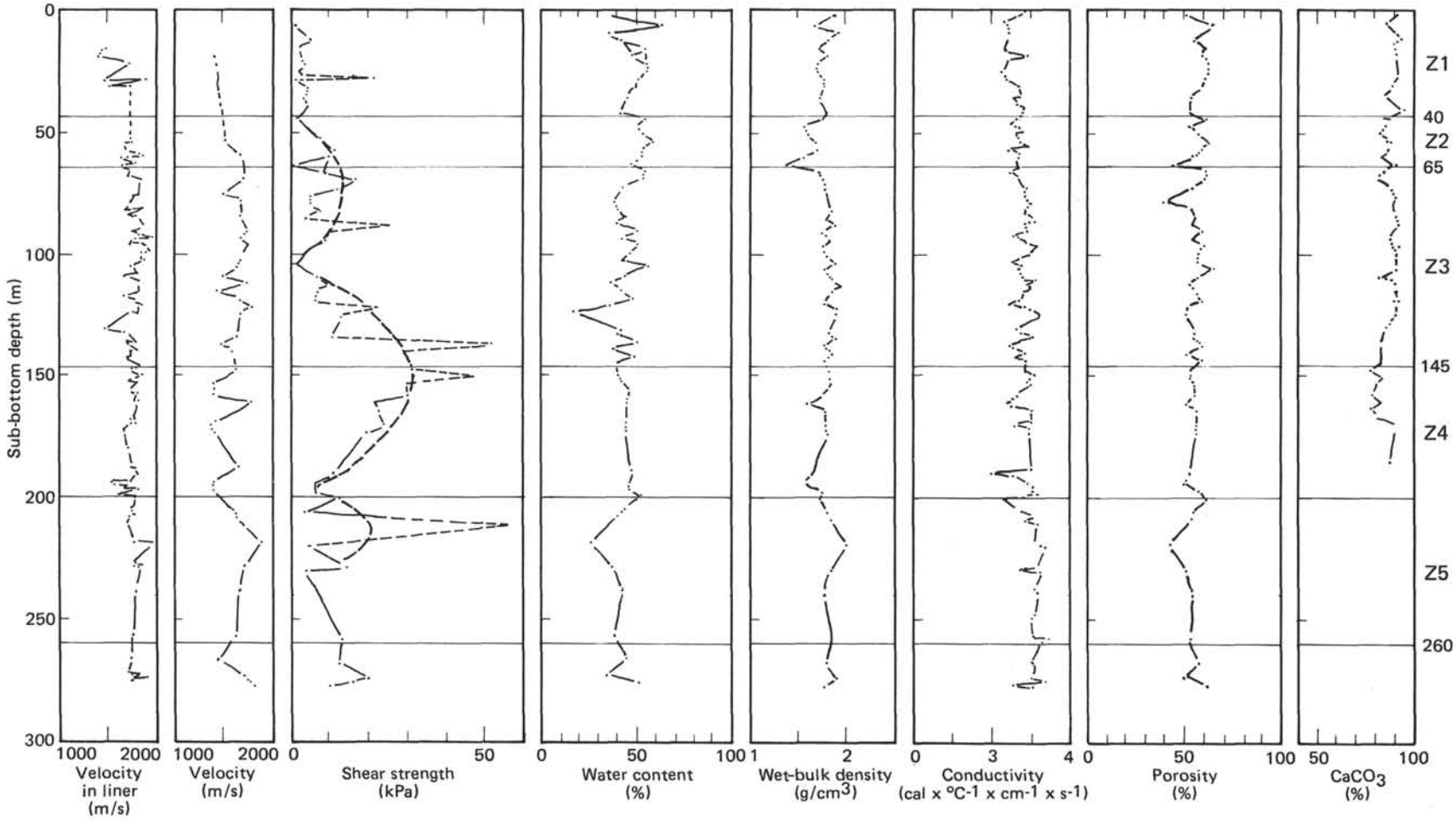

Figure 21. Graphic summary of the physical properties at Site 628. *Z1* through *Z5* indicate physical-property zonations.

Table 6. Physical properties of sediments, Site 628.

Sample (level in cm)	Sub-bottom depth (m)	Velocity (m/s)	Velocity in liner (m/s)	Wet-bulk density (g/cm^3)	Dry water content (%)	Porosity (%)	Thermal conductivity ($10^{-3} \times cal \times °C^{-1} \times cm^{-1} \times s^{-1}$)	Shear strength (kPa)
1-1, 70	0.7						2.889	
1-2, 75	2.2			1.91	38.04	52.41	2.696	
2-2, 75	6.0			1.67	64.03	65.34	2.342	1.13
2-3, 75	7.5						2.441	
2-4, 75	9.0			1.93	35.82	50.65	2.458	0.45
2-4, 75	10.5							
2-6, 75	12.0			1.84	43.28	55.53		5.55
3-2, 25	15.2		1480					
3-2, 75	15.8		1473	1.74	54.53	61.61	2.373	2.27
3-2, 110	16.2		1437					
3-4, 30	18.2		1400					
3-4, 60	18.4							
3-4, 75	18.7	1433		1.81	48.62	59.04	2.939	2.83
3-5, 75	20.2						2.450	
3-6, 30	21.3							
3-6, 75	81.7		1715	1.72	56.19	61.92		3.85
3-6, 120	22.2							
4-2, 20	24.6		1767					
4-2, 75	25.1		1460	1.72	56.33	62.17	2.306	2.49
4-2, 120	25.6		1492					
4-4, 25	27.6							
4-4, 75	28.1		1878	1.78	51.86	60.91	2.411	1.36
4-4, 120	28.6		1461					
4-6, 25	30.6		1485					
4-6, 75	31.1		1709	1.78	49.75	59.09	2.691	4.02
4-6, 120	31.6		1633					
5-2, 75	35.3			1.74	45.59	54.45	2.771	3.52
5-4, 75	38.3			1.81	41.99	53.26	2.633	4.47
5-5, 75	39.8						2.838	
5-6, 75	41.3			1.76	54.61	62.16	2.805	
6-2, 75	44.1			1.76	54.47	62.03	2.675	1.25
6-3, 75	45.6						2.519	
6-4, 75	47.1			1.57	51.58	53.38	2.698	3.96
6-5, 75	48.6						2.798	
6-6, 75	50.1			1.62	53.71	56.60	2.676	6.68
7-2, 20	53.2		1718					
7-2, 70	53.7	1547		1.70	59.12	63.32	2.765	8.49
7-2, 110	54.1		1646					
7-3, 75	55.2						2.925	
7-4, 20	56.2		1766					
7-4, 70	56.7		1664	1.70	54.10	59.62	2.384	11.33
7-5, 75	58.2						2.710	
7-6, 30	59.3		1842					
7-6, 70	59.7		1623	1.56	53.33	54.38	2.686	9.63
7-6, 100	60.1		1648					
8-2, 20	62.6		1760					
8-2, 70	63.1	1743		1.37	47.89	44.29	2.605	0.68
8-2, 100	63.4		1614					
8-3, 75	64.5						2.710	
8-4, 70	66.1		1694	1.72	54.50	60.70	2.450	8.49
8-5, 75	67.5						2.630	
8-6, 10	68.4		1669					
8-6, 70	69.1	1738		1.76	53.75	61.57	2.705	17.21
8-6, 100	69.4		1808					
9-2, 75	72.8			1.80	42.98	53.98	2.895	12.19
9-4, 30	75.4		1793					
9-4, 70	75.8	1514					2.870	5.28
9-4, 110	76.1		1733					
9-5, 75	77.3						2.890	
9-6, 20	78.3		1716					
9-6, 70	78.8	1687	1709	1.84	39.28	51.67	3.014	5.28
10-2, 20	81.4		1832					
10-2, 70	81.9	1694	1665	1.86	41.44	54.34	2.826	7.31
10-2, 100	82.2		1743					
10-3, 75	83.4						2.844	
10-4, 20	84.4		1706					
10-4, 75	84.9	1693	1754	1.80	44.99	55.80	3.041	3.68
10-4, 100	85.2		1717					
10-5, 75	86.4						3.104	
10-6, 20	87.4		1817					
10-6, 70	87.9	1740	1816	1.90	39.93	54.05	2.863	25.60
10-6, 100	88.2		1837					
11-2, 20			1728					
11-2, 70	91.3	1762		1.75	51.54	59.40	2.921	10.16
11-2, 100			1755					
11-3, 75	92.8						2.538	
11-4, 20			1762					

Table 6 (continued).

Sample (level in cm)	Sub-bottom depth (m)	Velocity (m/s)	Velocity in liner (m/s)	Wet-bulk density (g/cm^3)	Dry water content (%)	Porosity (%)	Thermal conductivity ($10^{-3} \times$ cal $\times$ °C^{-1} $\times$ cm^{-1} $\times$ s^{-1})	Shear strength (kPa)
11-4, 70	94.3	1700	1791	1.84	43.59	55.62	2.744	8.94
11-4, 100			1940					
11-5, 75	95.8						2.919	
11-6, 20			1820					
11-6, 70	97.3	1772	1707	1.78	51.37	60.32	3.135	5.28
11-6, 100			1858					
12-2, 20			1892					
12-2, 70	100.7	2264	1809	1.81	46.89	57.63	2.957	3.25
12-2, 100			1858					
12-3, 75	102.2						2.716	
12-4, 20			1811					
12-4, 70	103.7	1707		1.90	43.48	57.27	2.511	1.63
12-4, 100			1851					
12-5, 75	105.2						2.731	
12-6, 20			1738					
12-6, 70	106.7	1644	1708	1.78	57.64	65.08	2.686	3.68
12-6, 100			1728					
13-2, 20			1784					
13-2, 70	110.1	1508		1.85	44.09	56.56	2.763	6.91
13-2, 100			1632					
13-3, 75	111.6						3.180	
13-4, 20			1760					
13-4, 70	113.1	1749	1798	1.96	37.07	52.82	2.905	10.16
13-4, 100			1788					
13-5, 75	114.6						2.995	
13-6, 20			1797					
13-6, 70	116.1		1796	1.87	43.02	56.20	2.847	6.91
13-6, 100			1777					
14-2, 20	119.2		1640					
14-2, 70	119.7	1690	1744	1.79	48.77	58.57	2.692	6.91
14-2, 100			1712					
14-3, 75	121.2						2.515	
14-4, 20			1810					
14-4, 70	122.7		1780	1.92	37.34	52.04	2.848	22.35
14-5, 75	124.2						3.112	
14-6, 20			1787					
14-6, 70	125.7	1685	1715	1.91	37.07	51.33	3.257	13.82
14-6, 100			1768					
15-1, 75	131.7						2.676	
15-2, 75	133.2			1.83	43.30	55.26	2.732	
15-3, 20			1643					
15-3, 70	134.7	1654		1.90	40.81	54.96	3.051	10.97
15-3, 110			1685					
16-2, 20			1660	1.77	50.51	59.46		
16-2, 70	138.2	1486	1760				2.451	52.83
16-2, 100			1682					
16-3, 75	139.7						2.663	
16-4, 20			1747					
16-4, 70	141.2	1620	1750	1.87	38.19	51.56	2.853	29.66
16-4, 100			1701					
16-5, 75	142.7						2.622	
16-6, 20			1774					
16-6, 70	144.2	1628	1762	1.77	49.73	58.86	2.886	30.48
16-6, 100			1715					
17-2, 75	148.3			1.84	40.27	52.69	2.850	31.25
17-3, 75	149.8						3.101	
17-4, 20			1748					
17-4, 70	151.3		1822	1.84	41.14	53.51	2.947	47.14
17-4, 100			1739					
17-5, 75	152.8						2.907	
17-6, 20			1699					
17-6, 70	154.3		1680	1.84	42.72	53.00	3.019	30.47
17-2, 100			1759					
18-2, 20			1694					
18-2, 70	158.7		1768	1.74	46.84	55.32	2.661	30.47
18-2, 100			1724					
18-3, 75	160.2						2.556	
18-4, 20			1779					
18-4, 70	161.7	1799	1743	1.60	46.26	50.49	2.387	21.58
18-4, 100			1777					
18-5, 75	163.2						2.506	
18-6, 20			1707					
18-6, 70	164.7		1757	1.60	45.35	55.97	3.010	22.22
19-1, 75	169.5						2.988	
19-2, 20			1757					
19-2, 70	171.0		1743	1.80	45.10	55.85	2.581	24.75
19-1, 100			1695					

Table 6 (continued).

Sample (level in cm)	Sub-bottom depth (m)	Velocity (m/s)	Velocity in liner (m/s)	Wet-bulk density (g/cm^3)	Dry water content (%)	Porosity (%)	Thermal conductivity ($10^{-3} \times$ cal $\times$ °C^{-1} $\times$ cm^{-1} $\times$ s^{-1})	Shear strength (kPa)
19-3, 75	172.5						2.935	
19-4, 20			1632					
19-4, 30							2.983	
19-4, 40		1439		1.81	44.87	55.79		19.68
19-4, 50	173.8		1629					
21-1, 75	188.6						3.009	
21-2, 20			1670					
21-2, 70	190.1	1682	1709	1.64	47.45	52.65	1.988	11.43
21-2, 100			1738					
21-3, 75	191.6						2.560	
21-4, 20	192.6		1787					
22-2, 20			1705					
22-2, 70	194.7			1.57	47.01	50.05	2.891	6.35
22-3, 75	196.2						3.078	
22-4, 20			1657					
22-4, 70	197.7		1632	1.76	47.45	56.70	3.053	6.35
22-4, 100			1767					
22-5, 75	199.2						3.166	
22-6, 20			1582					
22-6, 70	200.7		1757	1.74	53.42	60.58	2.184	12.69
22-6, 100			1755					
23-2, 20			1746					
23-2, 70	205.81	1620		1.81	44.35	55.47	2.757	3.17
23-2, 100			1718					
23-3, 75	207.3						2.967	
23-4, 20			1725					
23-4, 70	208.8	1650	1749	1.87	41.19	54.31	3.066	26.66
23-4, 100			1691					
23-5, 75	210.3						2.846	
23-6, 10	211.2		1681					
23-6, 30	211.4						3.147	57.13
24-1, 75	218.4						3.119	
24-2, 30			1732					
24-2, 75	219.9	1904	1963	2.03	26.89	42.7	3.221	4.44
24-2, 120			1921					
24-3, 20	220.9						3.340	
25-1, 75	228.4						3.211	
25-2, 30			1833					
25-2, 80	230.0	1730	1742	1.85	37.92	50.75	2.763	14.60
25-2, 120			1785					
25-3, 30	230.9						3.279	
26-1, 75	237.7						3.108	
26-2, 30	228.8		1753					
26-2, 75	239.2	1675	1752	1.79	43.73	54.26	2.763	3.81
26-2, 110	239.6		1773					
26-3, 50	240.4						3.221	
27-1, 75	248.0						3.103	
27-2, 75	249.5						3.083	
28-1, 75	257.1						3.086	
28-2, 25	258.1		1741					
28-2, 70	258.6	1661	1757	1.87	35.82	52.93	3.485	13.33
28-2, 120	259.1		1729					
28-3, 20	259.6						3.336	
29-1, 30	267.7		1717					
29-1, 70	268.1	1475	1745	1.81	45.64	56.70	3.057	12.06
29-1, 120	268.6		1725					
29-2, 30	269.1						3.118	
30-1, 25	274.6	1728	1810	1.92	35.56	49.97		20.31
30-1, 75							3.066	
30-2, 25	275.7		1762					
30-2, 70	276.2		1898				3.417	16.50
30-2, 120	276.7		1738					
30-3, 25	277.3		1769					
30-3, 75	277.8	1832	1748	1.80	52.83	62.21	2.548	10.16
30-3, 120	278.3		1467					
30-4, 15	278.7						3.049	
32, CC	298.0	3966						

to Pleistocene, 137 m; this unit includes a basal slump complex coeval with the Abaco Member of the Blake Ridge Formation; (2) Unit II, nannofossil–foraminifer ooze and chalk with one interval of turbidites, debris flows, and redeposited neritic biota, latest Eocene to late Oligocene, 135 m; and (3) Unit III, siliceous chalk and limestone with some nannofossil ooze and chert, late Paleocene to middle Eocene, 28 m.

Much as does the upper part of Hole 627B, this sequence records the upward transition from a marginal plateau with purely pelagic sedimentation in the Paleocene to late Oligocene to the

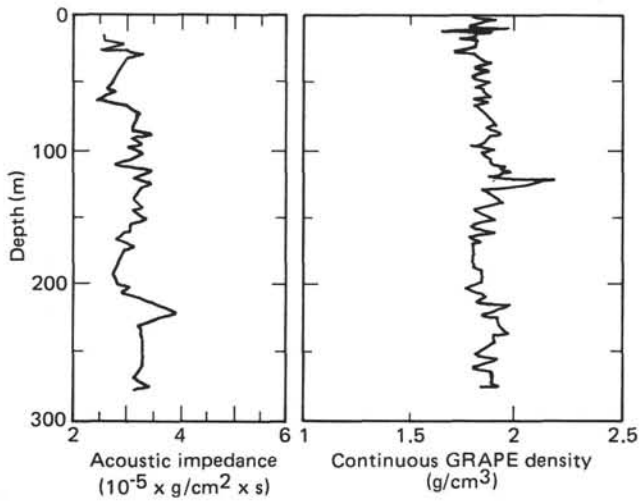

Figure 22. Calculated acoustic impedance vs. density (GRAPE) variations, Hole 628A.

toe-of-slope of a carbonate platform in the mid-Miocene to Holocene. The thickness and grain size of sediment gravity flows increase upward in Unit I, the marginal rise being at the foot of the platform over the pelagic deposits of the Blake Plateau. The slump and associated turbidites at the base of Unit I are coeval with the gravity flows of the Abaco Member (Bliefnick et al., 1983) and may be related to a regional (probably tectonic) event. However, unlike Sites 626 and 627, slumps and debris flows are scattered throughout the Neogene section, and the Abaco interval does not stand out as clearly.

The interval with neritic material from the early Oligocene may indicate an important event. This episode coincides rather precisely with a major regression on the eastern North American margin (Olsson et al., 1980; Fig. 25) and may relate to the large drop in sea level postulated for the early late Oligocene (Vail et al., 1977; Kennett, 1982). A long-lasting sea-level lowstand of minus 200–300 m would shift the active parts of the platform downslope and closer to the Blake Plateau proper or even raise parts of the plateau into the photic zone. The timing of this event of the eastern United States margin and at Site 628 predates the sea-level fall postulated by Vail et al. (1977).

As at Site 627 the pelagic sequence of the marginal-plateau stage is thin and punctuated by hiatuses. However, the intervals of deposition and nondeposition at Sites 627 and 628 do not match ("Sediment-Accumulation Rates" section, this chapter, and Site 627 chapter). Most noticeable is a thick interval of Oligocene and lower Miocene carbonate ooze that has no equivalent at Site 627. At this time, we attribute this pattern of intermittent sedimentation to a phase of general starvation in the southwestern North Atlantic combined with episodic Gulf Stream scouring. Current erosion at the two sites on the Blake Plateau was probably facilitated by a more easterly position of the western margin of Little Bahama Bank in the Paleogene, analogous to the paleogeography of Great Bahama Bank described in the Site 626 chapter (this volume). A comparison of the sediment record at Sites 627 and 628 with Site 626 in the Straits of Florida reveals a distinct difference: at Site 626, where the current is confined to a narrow seaway, we observe steady winnowing over long periods. On the Blake Plateau, erosion seems to be episodic, and intervening sediments are not winnowed. These pulses of erosion may have been caused by eddies that spun off the main current and reached through the thermocline, rather than by the main body of the current.

Borehole stratigraphy and seismic stratigraphy are well correlated at Site 628 and, for the most part, can be confidently tied to Site 627 ("Physical Properties" and "Seismic Stratigraphy" sections, this chapter). Cores and seismic profiles suggest that the rise at the foot of the platform is shaped not only by deposition from sediment gravity flows and pelagic sources but also by large-scale creep and slumping. It is possible that (listric?) normal faults related to slumping on the midslope are connected with imbricate thrust planes on the lower slope through bedding-parallel and near-bedding-parallel shear zones. This type of lower-slope gravity tectonics seems to affect the entire Neogene section. Slump folds and related structures in both boreholes may be another expression of this large-scale mass wasting.

REFERENCES

Berggren, W. A., Kent, D. V., Flynn, J. J., and Van Couvering, J. A., 1985. Cenozoic geochronology. *Geol. Soc. Am. Bull.*, 96:1407–1418.

Bliefnick, D. M., Robertson, A. H. F., and Sheridan, R. E., 1983. Deposition and provenance of Miocene intraclastic chalks, Blake-Bahama Basin, western North Atlantic. *In* Sheridan, R. E., Gradstein, F. M., et al., *Init. Repts. DSDP*, 76: Washington (U.S. Govt. Printing Office), 727–748.

Friend, J. K., and Riedel, W. R., 1967. Cenozoic orosphaerid radiolarians from tropical Pacific sediments. *Micropaleontology*, 13:217–232.

Kennett, J. P., 1982. *Marine Geology:* Englewood Cliffs, NJ (Prentice Hall).

Lang, T. H., and Watkins, D. K., 1984. Cenozoic calcareous nannofossils from Deep Sea Drilling Project Leg 77: Biostratigraphy and delineation of hiatuses. *In* Buffler, R. T., Schlager, W., et al., *Init. Repts. DSDP*, 77: Washington (U.S. Govt. Printing Office), 629–648.

Olsson, R. K., Miller, K. G., and Ungrady, T. E., 1980. Late Oligocene transgression of middle Atlantic coastal plain. *Geology*, 8:549–554.

Vail, P. R., Mitchum, R. M., Jr., Todd, R. G., Widmier, J. M., Thompson, S., III, et al., 1977. Seismic stratigraphy and global changes of sea level. *In* Payton, C. E. (Ed.), *Seismic Stratigraphy—Applications to Hydrocarbon Exploration*: AAPG Mem., 26:49–212.

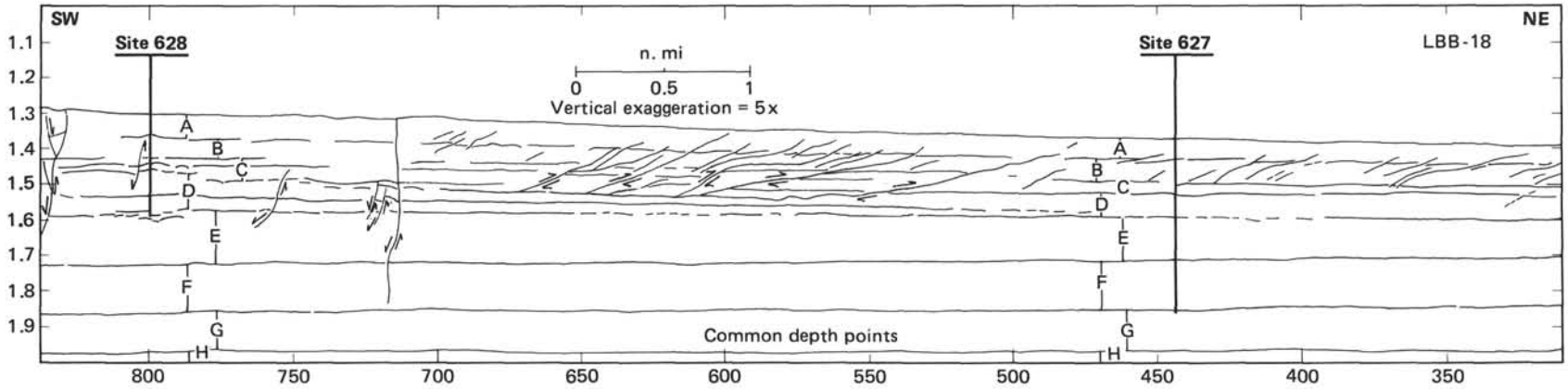

Figure 23. Interpretation of line LBB-18, showing location of Sites 627 and 628. Note both imbricate thrusts and normal faults.

Table 7. Seismic velocities, Site 628.

Seismic sequence	Thickness[a] (s/m)	Sub-bottom depth[a] (s/m)	Interval velocity (km/s)
A	0.06/52	0.06/52 (A/B)	1.75
B	0.078/68	0.138/120 (B/C)	1.75
C	0.02/18	0.158/138 (C/D)	1.75
D	0.138/156	0.296/294 (D/E)	2.26

[a] Two-way traveltime in seconds; sub-bottom depth in meters.

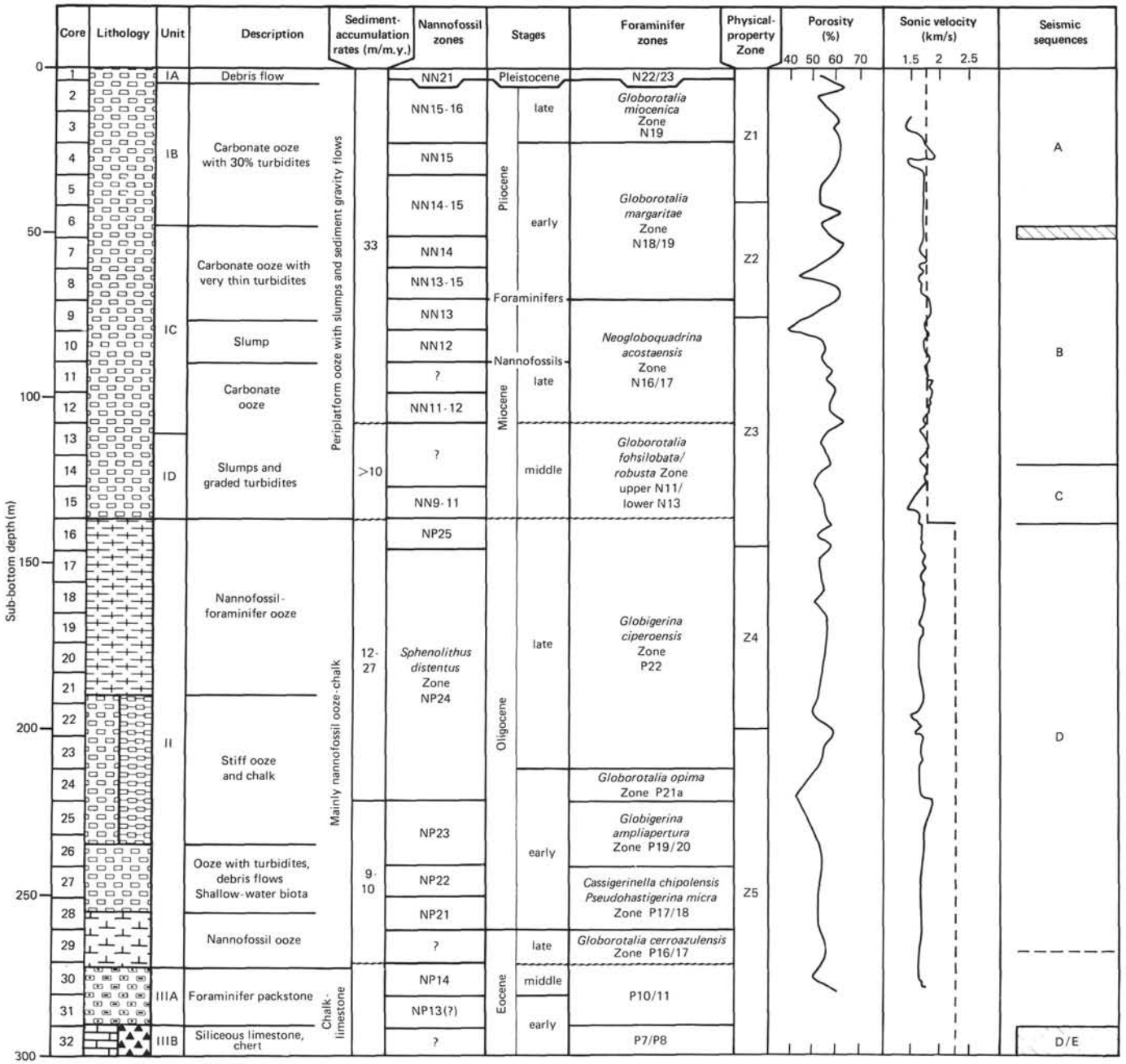

Figure 24. Summary of data for Site 628.

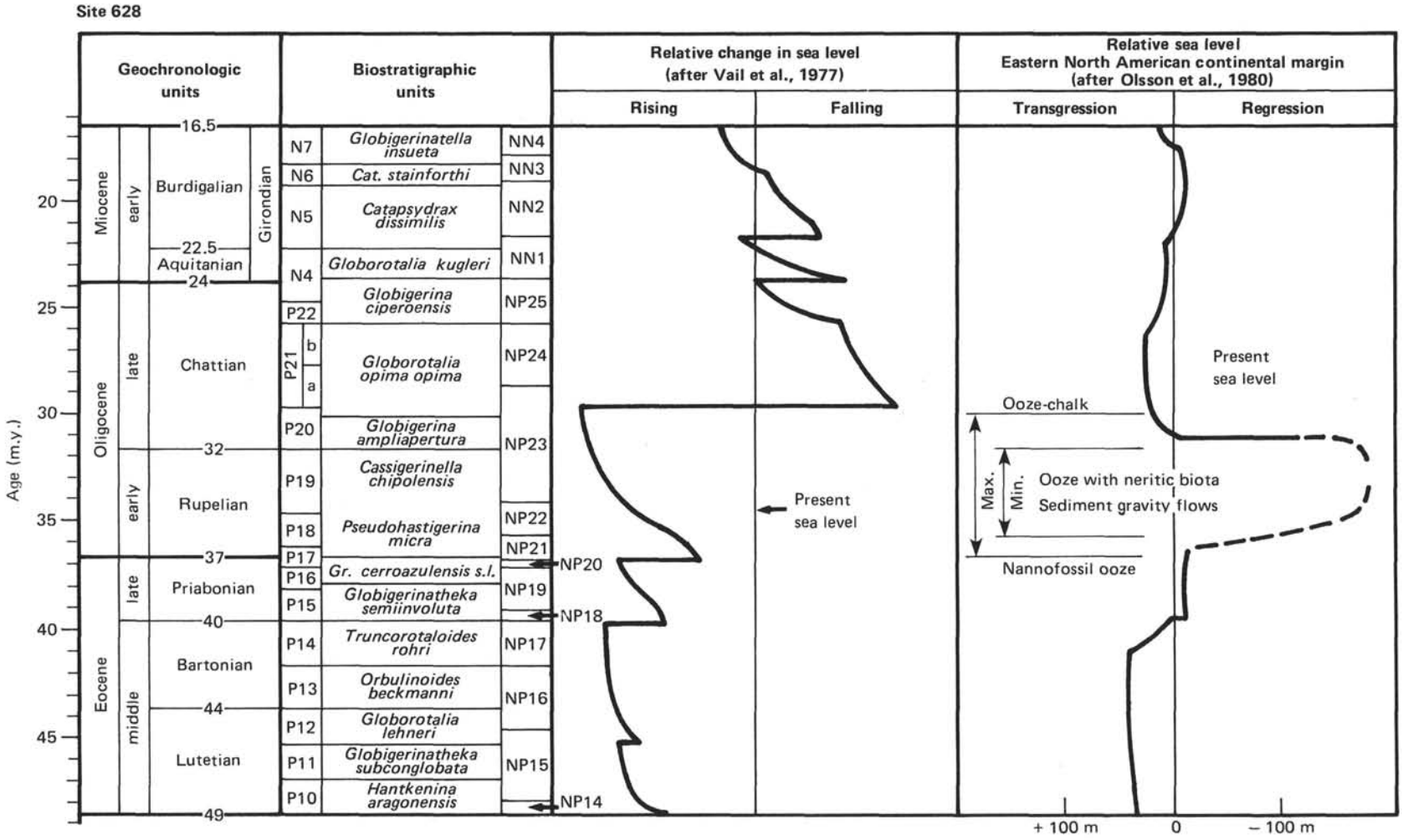

Figure 25. Possible Oligocene sea-level lowstand documented at Site 628.

SITE 628 HOLE A CORE 1H CORED INTERVAL 963.5-967.1 mbsl; 0-3.6 mbsf

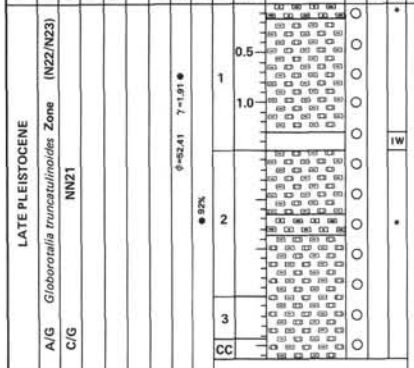

LITHOLOGIC DESCRIPTION

UNLITHIFIED FLOATSTONE and UNLITHIFIED PACKSTONE

UNLITHIFIED FLOATSTONE, white (10YR 8/1), throughout core, interbedded with UNLITHIFIED PACKSTONE. Contains clasts of skeletal foraminiferal LITHIFIED PACKSTONE, rounded to subrounded, up to 6 cm diameter; matrix consists of planktonic foraminiferal UNLITHIFIED PACKSTONE.

UNLITHIFIED PACKSTONE, light gray (10YR 7/1) to very pale brown (10YR 7/3), occurs as discrete beds in Section 1, 0-13 cm, and Section 2, 64-84 cm. Consists predominantly of planktonic foraminifers; pteropods, echinoid spines and shell fragments up to 4 cm diameter are also present.

SMEAR SLIDE SUMMARY (%):

	1,8 M	2,75 D
COMPOSITION:		
Clay	10	—
Micrite	70	30
Foraminifers	—	5
Nannofossils	5	45
Pteropods	—	Tr
Skeletal Fragments	15	20

SITE 628 HOLE A CORE 2H CORED INTERVAL 967.1-976.7 mbsl; 3.6-13.2 mbsf

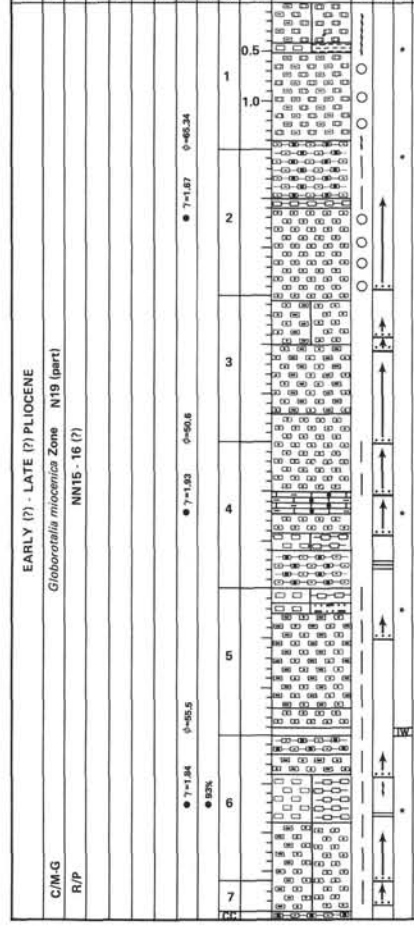

LITHOLOGIC DESCRIPTION

UNLITHIFIED to PARTIALLY LITHIFIED PACKSTONE and UNLITHIFIED GRAINSTONE, with minor UNLITHIFIED FLOATSTONE to UNLITHIFIED RUDSTONE, CALCAREOUS OOZE and CHALK, LITHIFIED PACKSTONE and MARLY OOZE

UNLITHIFIED to PARTIALLY LITHIFIED PACKSTONE and UNLITHIFIED GRAINSTONE, various shades of white (10YR 8/1, 5Y 8/2, 2.5Y 8/2, 5Y 8/1), occur throughout core interbedded with minor lithologies. PACKSTONE and GRAINSTONE units contain numerous grain aggregates pteropods, and planktonic foraminifers; grain size is medium to fine sand; subtle grading is present.

UNLITHIFIED FLOATSTONE to UNLITHIFIED RUDSTONE, white (10YR 8/1), occurs in Section 1, 0-139 cm. Contains subangular clasts of foraminiferal PACKSTONE/GRAINSTONE, up to 6 cm diameter; matrix consists of planktonic foraminifers and grain aggregates. May be drilling breccia in part.

CALCAREOUS OOZE and CHALK, white (10YR 8/1 to 2.5Y 8/0), occurs in Section 2, 52-59 cm, Section 4, 93-110 cm, Section 5, 0-15 cm, and Section 6, 42-92 cm.

LITHIFIED PACKSTONE, white (2.5Y 8/0), occurs in Section 4, 57-72 cm.

MARLY OOZE, light gray (5Y 7/1 to 2.5Y 7/2), occurs in Section 1, 46-51 cm, and in Section 5, 15-25 cm.

SMEAR SLIDE SUMMARY (%):

	1,48 M	2,10 D	4,70 D	5,21 M	6,75 D
COMPOSITION:					
Clay	10	—	—	10	—
Dolomite	Tr	—	—	5	—
Accessory Minerals:					
Micrite	80	10	30	25	35
Foraminifers	—	20	5	10	10
Nannofossils	5	10	40	30	20
Sponge Spicules	—	Tr	—	—	—
Pteropods	—	20	—	—	5
Ostracods	—	5	—	—	—
Skeletal Fragments	5	30	20	20	30
Clasts	—	5	5	—	—

SITE 628 HOLE A CORE 3H CORED INTERVAL 976.7-986.4 mbsl; 13.2-22.9 mbsf

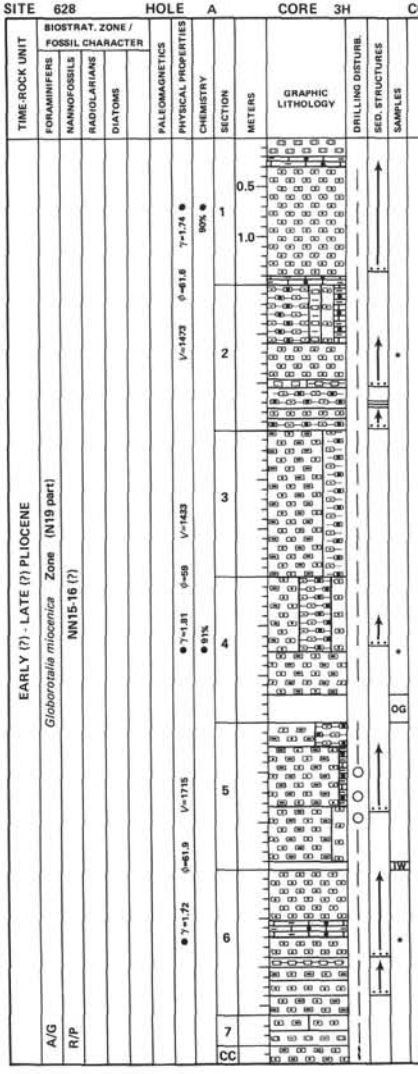

LITHOLOGIC DESCRIPTION

UNLITHIFIED to PARTIALLY LITHIFIED to LITHIFIED PACKSTONE and UNLITHIFIED GRAINSTONE, with minor CALCAREOUS OOZE and CHALK, UNLITHIFIED FLOATSTONE and UNLITHIFIED RUDSTONE (may be drilling breccia)

UNLITHIFIED to PARTIALLY LITHIFIED to LITHIFIED PACKSTONE and GRAINSTONE, various shades of white (2.5Y 8/2, 5Y 8/2, 7.5Y 8/2, 10YR 8/1), throughout core, interbedded with minor lithologies. Grading is present in many intervals. Grain size in PACKSTONE and GRAINSTONE is medium to fine sand; grain types include grain aggregates, planktonic foraminifers and pteropods.

CALCAREOUS OOZE and CHALK, white (10YR 8/2), in Section 2, 98-105 cm, Section 6, 96-100 cm.

UNLITHIFIED RUDSTONE, white (10YR 8/1), in Section 1, 0-20 cm, contains numerous gravel-sized clasts of CHALK and PACKSTONE. May be drilling breccia.

UNLITHIFIED FLOATSTONE, white (10YR 8/1), in Section 7, 10-28 cm, contains small rounded clasts and shell fragments (up to 0.3-0.4 cm diameter).

SMEAR SLIDE SUMMARY (%):

	2,75 D	4,75 D	6,75 D
COMPOSITION:			
Foraminifers	5	15	20
Nannofossils	15	25	25
Pellets	4	5	5
Micrite	25	20	20
Echinoid	1	–	–
Pteropods	20	–	–
Skeletal Fragments	30	20	20
Clasts	–	5	–

SITE 628 HOLE A CORE 4H CORED INTERVAL 986.4-996.1 mbsl; 22.9-32.6 mbsf

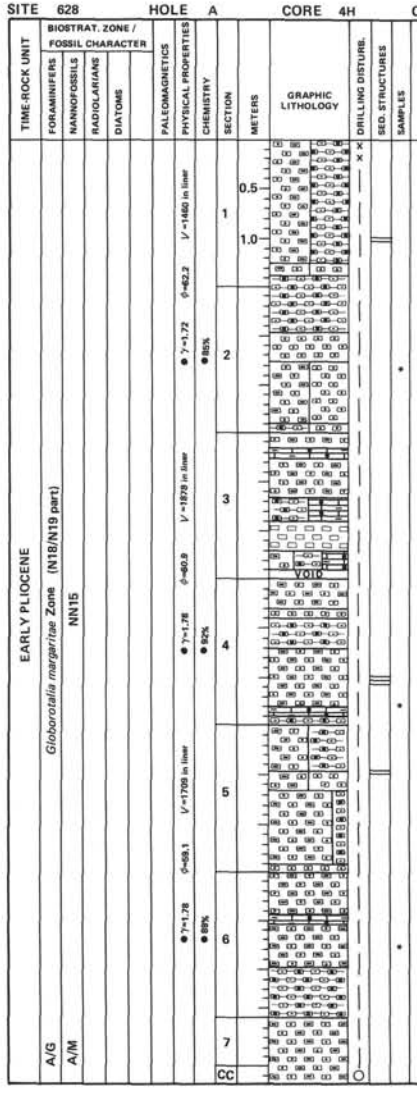

LITHOLOGIC DESCRIPTION

UNLITHIFIED to PARTIALLY LITHIFIED PACKSTONE and UNLITHIFIED to PARTIALLY LITHIFIED GRAINSTONES, with minor CALCAREOUS OOZE

UNLITHIFIED to PARTIALLY LITHIFIED PACKSTONE and UNLITHIFIED GRAINSTONE, various shades of white (10YR 8/1, 5Y 8/1, 7.5YR 8/0), throughout core, interbedded with minor lithologies. Grain size is medium sand; grain types include planktonic foraminifers and grain aggregates. Some skeletal fragments (up to 0.3 cm diameter) occur in Section 5, 48-65 cm.

LITHIFIED PACKSTONE, white (10YR 8/1), occurs in Section 3, 15-25 and 65-70 cm, Section 4, 130-136 cm, and Section 6, 48-52 cm.

CALCAREOUS OOZE, white (7.5YR 8/0), occurs in Section 3, 90-118 cm.

SMEAR SLIDE SUMMARY (%):

	2,84 D	2,74 D	4,80 D	6,75 D
COMPOSITION:				
Foraminifers	20	85	25	20
Nannofossils	50	–	20	30
Micrite	20	10	34	25
Pteropods	–	5	–	–
Echinoid	–	–	1	–
Skeletal Fragments	10	–	20	20
Clasts	–	–	–	5

SITE 628 HOLE A CORE 5H CORED INTERVAL 996.1-1005.4 mbsl; 32.6-41.9 mbsf

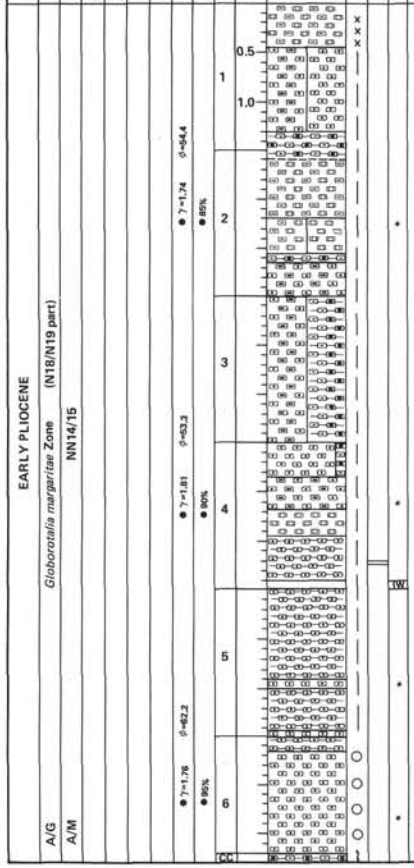

LITHOLOGIC DESCRIPTION

UNLITHIFIED to PARTIALLY LITHIFIED PACKSTONES and UNLITHIFIED to PARTIALLY LITHIFIED GRAINSTONES, with minor UNLITHIFIED RUDSTONE to UNLITHIFIED FLOATSTONE and UNLITHIFIED FLOATSTONE (may be drilling breccia)

UNLITHIFIED to PARTIALLY LITHIFIED PACKSTONES and UNLITHIFIED to PARTIALLY LITHIFIED GRAINSTONES, various shades of white (2.5Y 8/2, 5Y 8/1, 2.5Y 8/0, and 7.5Y 8/0), occur throughout core interbedded with minor lithologies. Medium to coarse grained, contain grain aggregates, planktonic foraminifers and lithified clasts up to 0.8 cm diameter.

UNLITHIFIED RUDSTONE to UNLITHIFIED FLOATSTONE, white (10YR 8/1), in Section 1, 0-47 cm (may be drilling breccia), contains bored stained clasts (up to 3 cm diameter); also in Section 2, 79-106 cm, contains PACKSTONE clasts of up to 5 cm diameter in a matrix of grain aggregates and planktonic foraminifers.

UNLITHIFIED FLOATSTONE, white (10YR 8/1), occurs in Section 2, 10-72 cm, coarse grained with clasts up to 5 cm diameter.

SMEAR SLIDE SUMMARY (%):

	2,75 D	4,65 D	6,80 D	5,95 D
COMPOSITION:				
Foraminifers	15	25	35	50
Nannofossils	35	35	25	–
Pellets	5	–	–	–
Micrite	20	25	25	10
Echinoids	–	–	–	5
Skeletal Fragments	20	15	15	25
Clasts	–	–	–	15

SITE 628 HOLE A CORE 6H CORED INTERVAL 1005.4-1015.0 mbsl; 41.9-51.5 mbsf

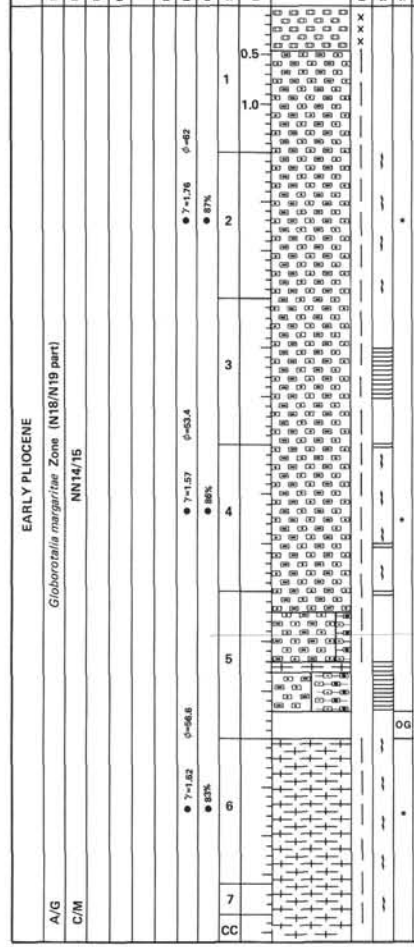

LITHOLOGIC DESCRIPTION

UNLITHIFIED PACKSTONE and FORAM-NANNOFOSSIL OOZE, with minor UNLITHIFIED to PARTIALLY LITHIFIED PACKSTONE and UNLITHIFIED RUDSTONE (probably drilling breccia)

UNLITHIFIED PACKSTONE, various shades of white (7.5YR 8/0, 2.5Y 7/0, 2.5Y 8/0, 5Y 8/0, and 10YR 8/1) in Section 1, 41 cm, through Section 5, 18 cm. Less cemented, finer grained and more homogeneous than PACKSTONE in overlying cores.

FORAM-NANNOFOSSIL OOZE, white (7.5Y 8/0), occurs in Section 5, 74-78 cm, and in Section 6, 0 cm, through the base of the core; bioturbated, contains some grains and mudstone clasts (up to 2 cm diameter).

UNLITHIFIED to PARTIALLY LITHIFIED PACKSTONE, white (whiter than 5Y 8/1), occurs in Section 5, 18-74 cm (minor partial lithification) and 78-120 cm (about 50% partial lithification); traces of horizontal bedding present in lower interval.

UNLITHIFIED RUDSTONE, white (7.5YR 8/0), in Section 1, 0-41 cm; contains pebble-sized chalk clasts, possibly drilling breccia.

SMEAR SLIDE SUMMARY (%):

	2,75 D	4,75 D	6,75 D
COMPOSITION:			
Dolomite	–	Tr	–
Foraminifers	15	20	15
Nannofossils	25	55	70
Sponge Spicules	–	Tr	–
Pellets	5	–	–
Micrite	20	15	10
Pteropods	Tr	–	–
Skeletal Fragments	25	10	5

SITE 628 HOLE A CORE 7H CORED INTERVAL 1015.0-1024.4mbsl; 51.5-60.9 mbsf

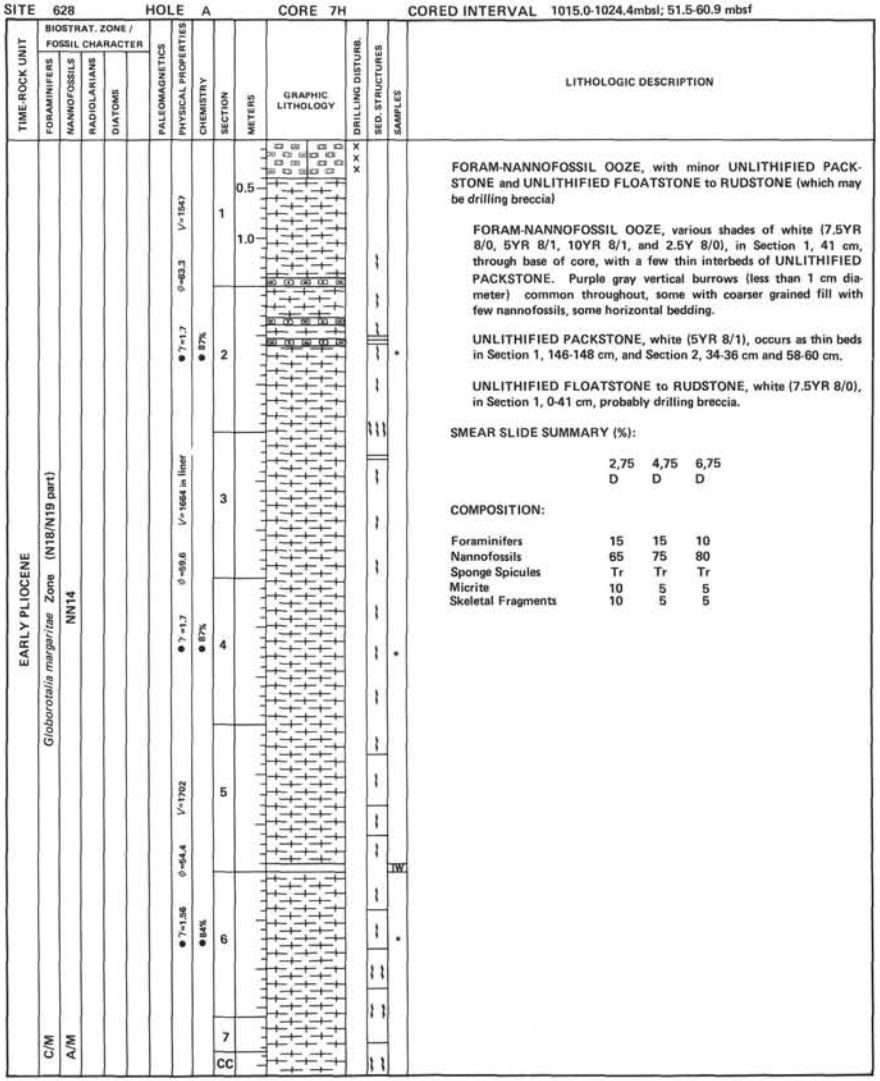

LITHOLOGIC DESCRIPTION

FORAM-NANNOFOSSIL OOZE, with minor UNLITHIFIED PACKSTONE and UNLITHIFIED FLOATSTONE to RUDSTONE (which may be drilling breccia)

FORAM-NANNOFOSSIL OOZE, various shades of white (7.5YR 8/0, 5YR 8/1, 10YR 8/1, and 2.5Y 8/0), in Section 1, 41 cm, through base of core, with a few thin interbeds of UNLITHIFIED PACKSTONE. Purple gray vertical burrows (less than 1 cm diameter) common throughout, some with coarser grained fill with few nannofossils, some horizontal bedding.

UNLITHIFIED PACKSTONE, white (5YR 8/1), occurs as thin beds in Section 1, 146-148 cm, and Section 2, 34-36 cm and 58-60 cm.

UNLITHIFIED FLOATSTONE to RUDSTONE, white (7.5YR 8/0), in Section 1, 0-41 cm, probably drilling breccia.

SMEAR SLIDE SUMMARY (%):

	2,75 D	4,75 D	6,75 D
COMPOSITION:			
Foraminifers	15	15	10
Nannofossils	65	75	80
Sponge Spicules	Tr	Tr	Tr
Micrite	10	5	5
Skeletal Fragments	10	5	5

SITE 628 HOLE A CORE 8H CORED INTERVAL 1024.4-1034.1 mbsl, 60.9-70.6 mbsf

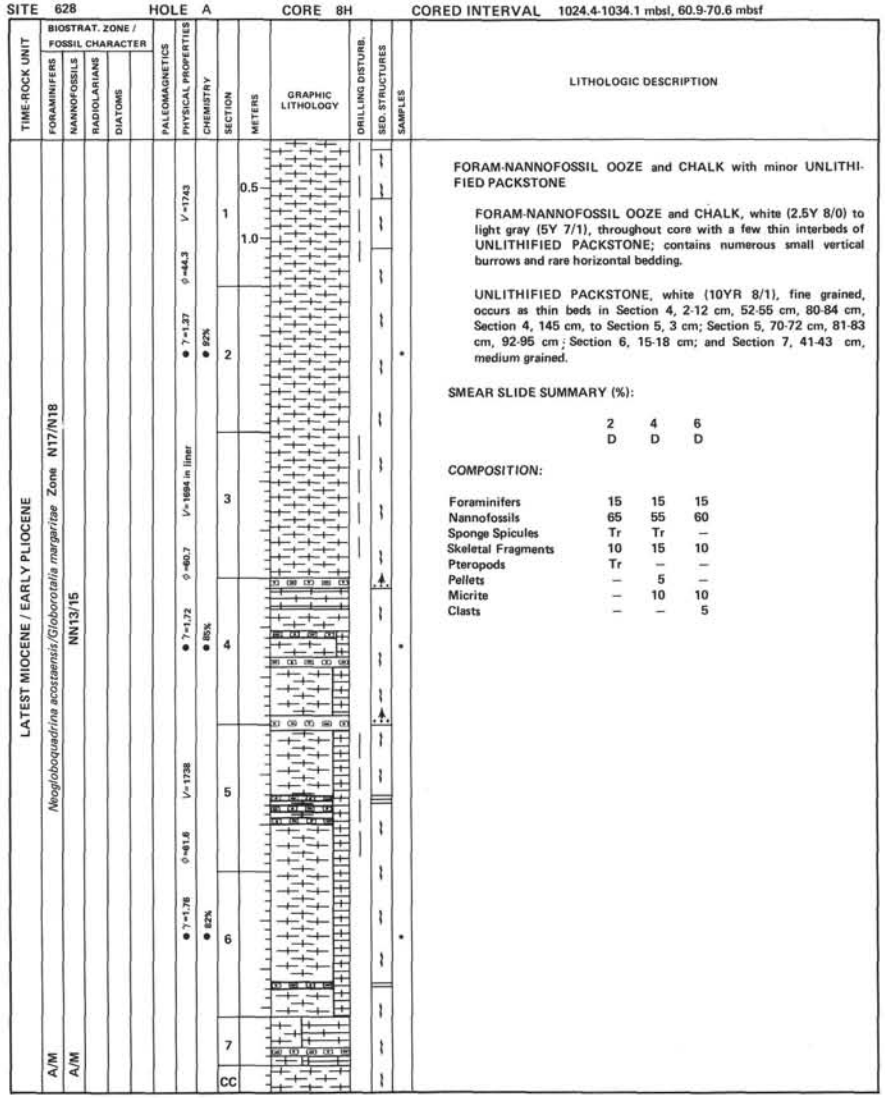

LITHOLOGIC DESCRIPTION

FORAM-NANNOFOSSIL OOZE and CHALK with minor UNLITHIFIED PACKSTONE

FORAM-NANNOFOSSIL OOZE and CHALK, white (2.5Y 8/0) to light gray (5Y 7/1), throughout core with a few thin interbeds of UNLITHIFIED PACKSTONE; contains numerous small vertical burrows and rare horizontal bedding.

UNLITHIFIED PACKSTONE, white (10YR 8/1), fine grained, occurs as thin beds in Section 4, 2-12 cm, 52-55 cm, 80-84 cm, Section 4, 145 cm, to Section 5, 3 cm; Section 5, 70-72 cm, 81-83 cm, 92-95 cm; Section 6, 15-18 cm; and Section 7, 41-43 cm, medium grained.

SMEAR SLIDE SUMMARY (%):

	2 D	4 D	6 D
COMPOSITION:			
Foraminifers	15	15	15
Nannofossils	65	55	60
Sponge Spicules	Tr	Tr	—
Skeletal Fragments	10	15	10
Pteropods	Tr	—	—
Pellets	—	5	—
Micrite	—	10	10
Clasts	—	—	5

SITE 628 HOLE A CORE 9H CORED INTERVAL 1034.1-1043.2 mbsl; 70.6-79.7 mbsf

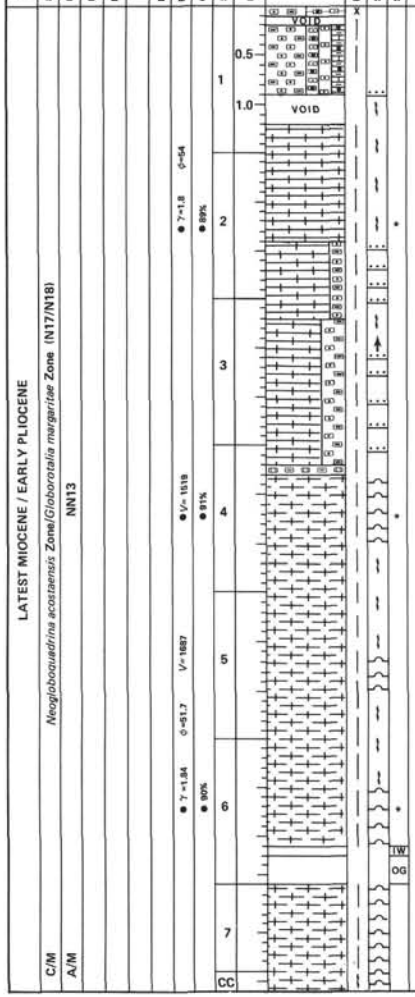

LITHOLOGIC DESCRIPTION

FORAM-NANNOFOSSIL OOZE and CHALK, with minor UNLITHIFIED PACKSTONE, PARTIALLY LITHIFIED PACKSTONE, LITHIFIED PACKSTONE, UNLITHIFIED GRAINSTONE and UNLITHIFIED FLOATSTONE

FORAM-NANNOFOSSIL OOZE, white (5Y 8/1 to 5Y 8/1), in Section 4, 28 cm, through base of core. Contains slumps and bioturbated intervals.

FORAM-NANNOFOSSIL CHALK, white (2.5Y 8/0 to 5Y 8/1), in Section 1, 120 cm, through Section 4, 27 cm, with thin interbeds of UNLITHIFIED PACKSTONE. Minor bioturbation and pyrite specks present throughout.

UNLITHIFIED PACKSTONE, white (2.5Y 8/2) to light gray (8Y 7/2) and gray (2.5Y 7/0). Occurs as thin interbeds in CHALK, between Section 2, 96 cm, and Section 3, 137 cm, and interbedded with PARTIALLY LITHIFIED PACKSTONE, LITHIFIED PACKSTONE, and UNLITHIFIED GRAINSTONE in Section 1, 0-95 cm. The interval from Section 1, 1-10 cm, is probably drilling breccia.

UNLITHIFIED FLOATSTONE, white (2.5Y 8/2), in Section 4, 19-27 cm. Contains clasts to 2 cm diameter.

SMEAR SLIDE SUMMARY (%):

	2,75 D	4,75 D	6,75 D
COMPOSITION:			
Dolomite	–	Tr	–
Foraminifers	15	30	15
Nannofossils	55	40	69
Sponge Spicules	Tr	–	–
Pteropods	–	–	1
Skeletal Fragments	10	15	5
Micrite	10	15	10
Clasts	10	–	–

SITE 628 HOLE A CORE 10H CORED INTERVAL 1043.2-1052.6 mbsl; 79.7-89.1 mbsf

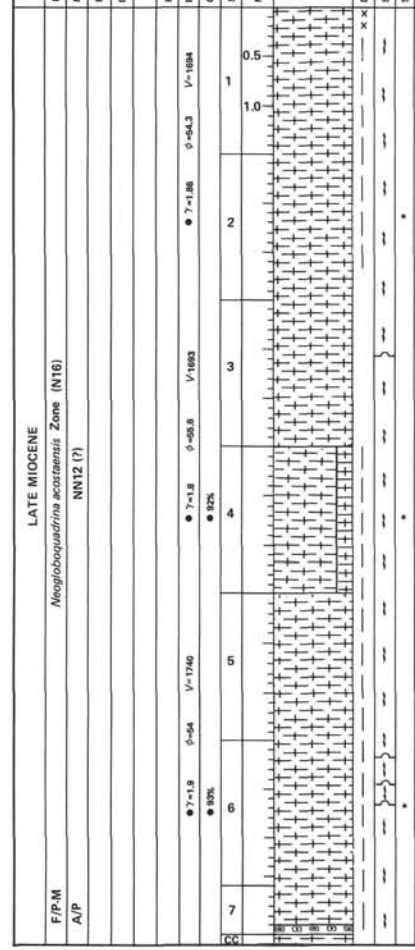

LITHOLOGIC DESCRIPTION

FORAM-NANNOFOSSIL OOZE with minor CHALK and UNLITHIFIED PACKSTONE

FORAM-NANNOFOSSIL OOZE, white (5Y 8/1 to 10YR 8/1), in Section 1, 0 cm, through base of core, with minor lithologies interbedded. An interval of drilling breccia is present in Section 1, 0-30 cm. OOZE is bioturbated, with burrow fills variably gray (pyritic, 5Y 7/1), brown (10YR 8/2), greenish, or whiter than matrix.

FORAM-NANNOFOSSIL CHALK, white (5Y 8/1), occurs in Section 4, 0-150 cm, with FORAM-NANNOFOSSIL OOZE.

UNLITHIFIED PACKSTONE, white (2.5Y 8/0), in Section 7, 40-64 cm. Medium-grained sand; contains pyrite specks and foraminifers.

SMEAR SLIDE SUMMARY (%):

	2,75 D	4,75 D	6,75 D
COMPOSITION:			
Foraminifers	10	15	10
Nannofossils	60	60	70
Pellets	1	1	1
Pteropods	–	Tr	–
Skeletal Fragments	5	10	5
Micrite	20	10	14
Clasts	4	4	–

SITE 628 HOLE A CORE 11H CORED INTERVAL 1052.6-1062.0 mbsl; 89.1-98.5 mbsf

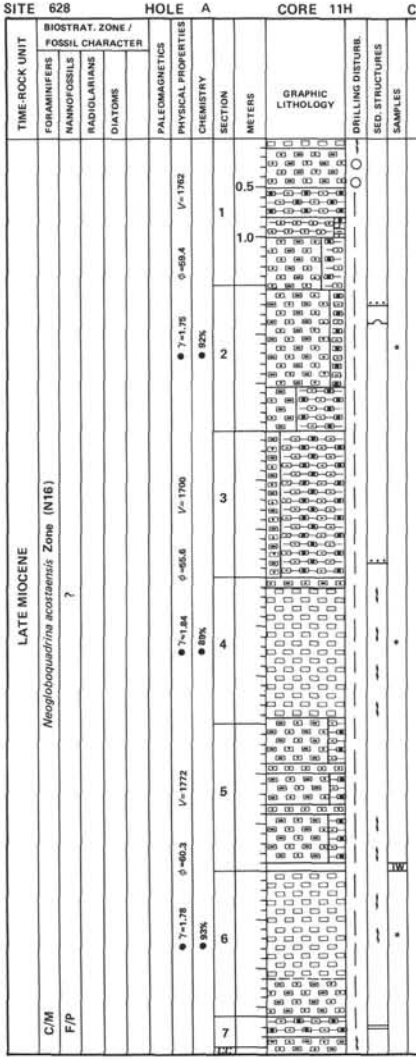

LITHOLOGIC DESCRIPTION

UNLITHIFIED PACKSTONE, PARTIALLY LITHIFIED PACKSTONE and CALCAREOUS OOZE, with minor UNLITHIFIED GRAINSTONE, PARTIALLY LITHIFIED GRAINSTONE and LITHIFIED PACKSTONE

UNLITHIFIED PACKSTONE, various shades of white (2.5Y 8/0, 5Y 8/1, 10YR 8/1), interbedded with PARTIALLY LITHIFIED PACKSTONE *in Section 1, 12-77 cm, and Section 6, 115 cm, through* the base of the core; grades to PARTIALLY LITHIFIED PACKSTONE in Section 1, 109 cm, through Section 3, 150 cm, and Section 4, 146 cm, through Section 5, 140 cm. PACKSTONES are medium to coarse grained, contain pyrite grains, foraminifers, some burrows and horizontal bedding.

CALCAREOUS OOZE, white (10YR 8/1), in Section 4, 10-146 cm, and Section 6, 0-110 cm; contains gray layers and burrows.

UNLITHIFIED GRAINSTONE, white (10YR 8/1), occurs as thin beds in Section 5, 45-48 cm and 87-90 cm.

PARTIALLY LITHIFIED GRAINSTONE, light gray (2.5Y 7/0), occurs in Section 1, 77-100 cm, with LITHIFIED PACKSTONE (clast?) interbedded 92-95 cm. GRAINSTONE is coarse to very coarse, and contains skeletal fragments to 0.4 cm diameter.

SMEAR SLIDE SUMMARY (%):

	2,75 D	4,75 D	6,75 D
COMPOSITION:			
Foraminifers	30	30	25
Nannofossils	30	30	40
Sponge Spicules	Tr	–	–
Skeletal Fragments	20	20	10
Micrite	15	15	20
Clasts	5	5	5

SITE 628 HOLE A CORE 12H CORED INTERVAL 1062.0-1071.4 mbsl, 98.5-107.9 mbsf

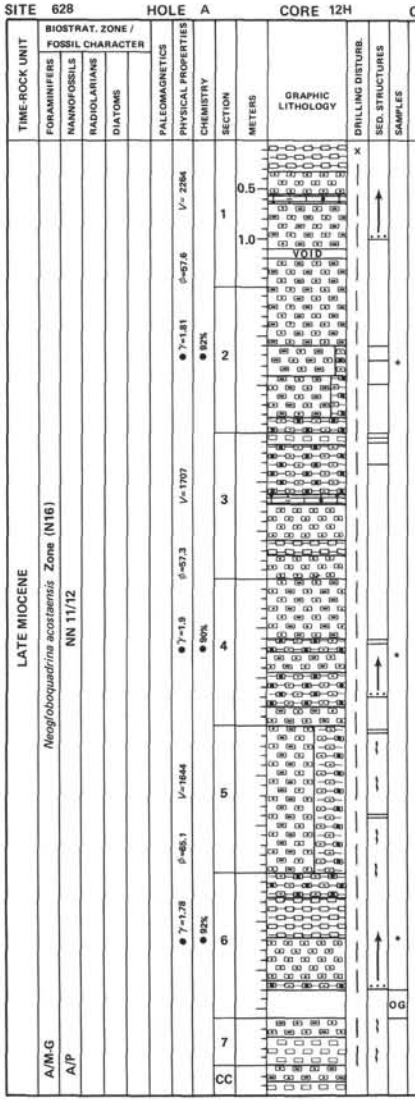

LITHOLOGIC DESCRIPTION

UNLITHIFIED PACKSTONE and PARTIALLY LITHIFIED PACKSTONE, with minor CALCAREOUS OOZE and CHALK, UNLITHIFIED GRAINSTONE, and LITHIFIED PACKSTONE

UNLITHIFIED PACKSTONE and PARTIALLY LITHIFIED PACKSTONE, various shades of white (10YR 8/1, 2.5Y 8/0, 2.5Y 8/1, 2.5Y 8/2, 5Y 8/1) to gray (2.5Y 7/0, 7.5YR 7/0). Occur throughout *core, both interbedded and intergrading; alternate with minor* lithologies. Medium to coarse grain size, some vertical burrows (1 cm diameter).

CALCAREOUS OOZE, white (10YR 8/1), occurs in Section 3, 0-15 cm, Section 7, 15-59 cm, and in the CC, 16-28 cm. Contains thin vertical burrows 9.5 cm in diameter.

CHALK, white (10YR 8/1), occurs in Section 1, 0-33 cm (0-11 cm may be drilling breccia), Section 3, 112-125 cm, and Section 6, 24-68 cm.

UNLITHIFIED GRAINSTONE, white (10YR 8/1, 2.5Y 8/2), occurs in Section 1, 33-52 cm; Section 3, 71-112 cm and 125-150 cm; and Section 6, 68-112 cm, the latter interval grading from coarse to medium grained at the base to medium grained at the top.

SMEAR SLIDE SUMMARY (%):

	2,75 D	4,75 D	6,75 D
COMPOSITION:			
Foraminifers	20	25	35
Nannofossils	40	30	17
Sponge Spicules	Tr	Tr	–
Pteropods	–	–	2
Skeletal Fragments	10	10	20
Clasts	25	30	20
Micrite	25	30	20
Biotite	–	Tr	–
Pellets	–	–	2

SITE 628 HOLE A CORE 13H CORED INTERVAL 1071.4-1080.9 mbsl; 107.9-117.4 mbsf

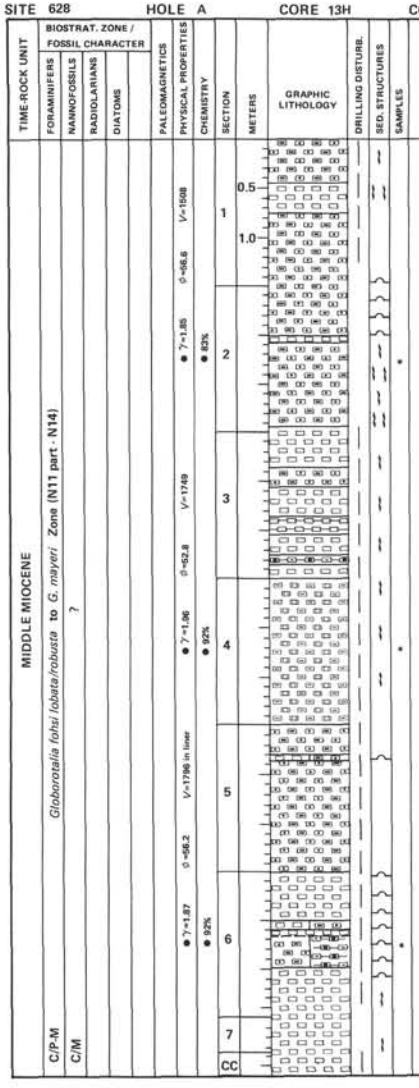

LITHOLOGIC DESCRIPTION

UNLITHIFIED PACKSTONE and CALCAREOUS OOZE, with minor UNLITHIFIED FLOATSTONE, CHALK, and PARTIALLY LITHIFIED PACKSTONE

UNLITHIFIED PACKSTONE, white (5Y 8/1), in Section 1, 0 cm, through Section 3, 55 cm, with interbedded CALCAREOUS OOZE; in Section 5, 0 cm, through Section 6, 99 cm, interbedded and intergraded with CALCAREOUS OOZE and PARTIALLY LITHIFIED PACKSTONE. PACKSTONE contains foraminifers and skeletal debris in a matrix containing nannofossils. Slumps are present in several intervals.

CALCAREOUS OOZE, various shades of white (5Y 8/1, 2.5Y 8/0, 10YR 8/1, 10YR 8/2), occurs interbedded and intergraded with other lithologies as described above. Some intervals are slumped; others contain burrows up to 1.5 cm diameter.

UNLITHIFIED FLOATSTONE, white (10YR 8/1), in Section 4, 0-150 cm, contains mostly small (1-2 cm diameter) clasts, although some reach 10 cm diameter, most rounded to subrounded. Matrix is muddy medium to fine sand containing foraminifers.

CHALK, white (7.5YR 8/0), in Section 3, 85-105 cm.

PARTIALLY LITHIFIED PACKSTONE, white (7.5YR 8/0), occurs in Section 3, 125-136 cm, and in Section 6, 65-99 cm (intergrading with UNLITHIFIED PACKSTONE).

SMEAR SLIDE SUMMARY (%):

	2,75	4,75	6,75
	D	D	D
COMPOSITION:			
Foraminifers	20	25	30
Nannofossils	40	35	10
Pellets	5	5	5
Skeletal Fragments	10	10	20
Micrite	20	20	30
Clasts	5	5	5

SITE 628 HOLE A CORE 14H CORED INTERVAL 1080.9-1090.5 mbsl; 117.4-127.0 mbsf

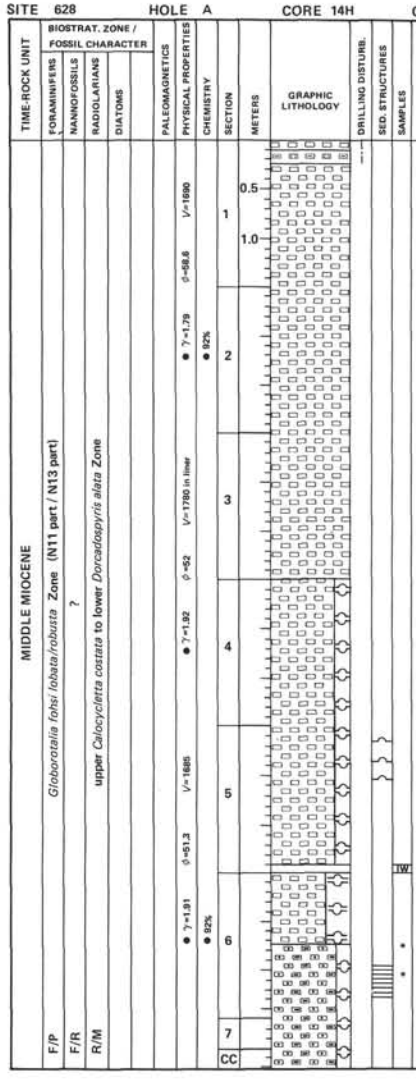

LITHOLOGIC DESCRIPTION

SILICEOUS SPONGE SPICULE-RICH CALCAREOUS OOZE and UNLITHIFIED PACKSTONE, with minor UNLITHIFIED FLOATSTONE

SILICEOUS SPONGE SPICULE-RICH CALCAREOUS OOZE, white (10YR 8/1 and 2.5Y 8/2), in Section 1, 0 cm, through Section 6, 73 cm, with a thin interbed of UNLITHIFIED FLOATSTONE in Section 1. Siliceous sponge spicule content ranges from trace amounts to 20%. An apparent slump structure occurs in Section 5. Coarse grains occur in some intervals of Section 6. Contact with underlying UNLITHIFIED PACKSTONE is gradational.

UNLITHIFIED PACKSTONE, white (5Y 8/2) to pale yellow (5Y 7/3), in Section 6, 73 cm, through base of core, contains planktminifers.

UNLITHIFIED FLOATSTONE, white (10YR 8/1), in Section 1, 11-23 cm, contains chalky clasts up to 2 cm diameter. May be drilling breccia.

SMEAR SLIDE SUMMARY (%):

	2,75	4,75	6,75	6,106
COMPOSITION:				
Foraminifers	5	10	30	30
Nannofossils	15	20	10	–
Sponge Spicules (siliceous)	Tr	20	25	15
Pellets	40	20	10	–
Skeletal Fragments	Tr	10	–	–
Micrite	40	20	25	25
Clasts	–	–	–	30

SITE 628 HOLE A CORE 15H CORED INTERVAL 1090.5-1100.1 mbsl; 127.0-136.6 mbsf

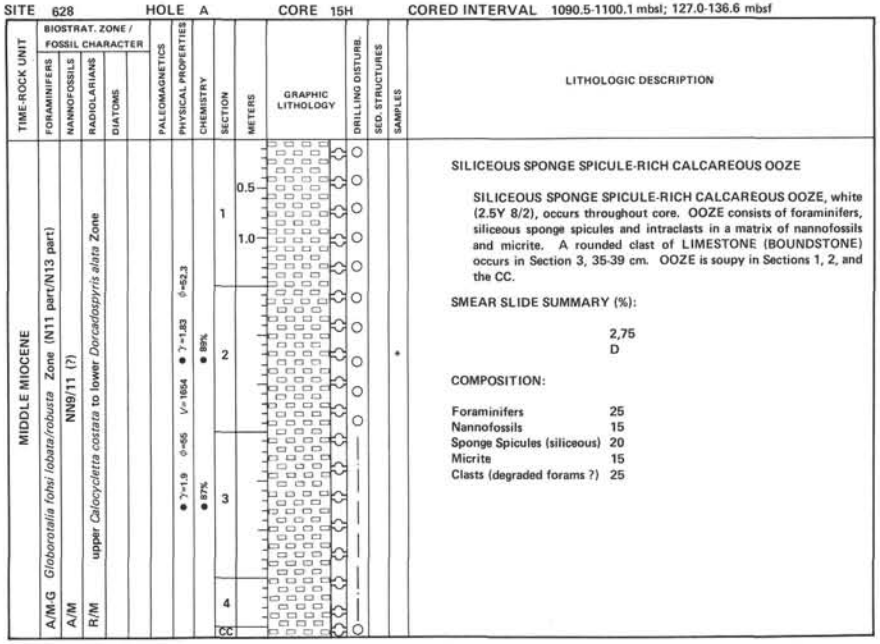

LITHOLOGIC DESCRIPTION

SILICEOUS SPONGE SPICULE-RICH CALCAREOUS OOZE

SILICEOUS SPONGE SPICULE-RICH CALCAREOUS OOZE, white (2.5Y 8/2), occurs throughout core. OOZE consists of foraminifers, siliceous sponge spicules and intraclasts in a matrix of nannofossils and micrite. A rounded clast of LIMESTONE (BOUNDSTONE) occurs in Section 3, 35-39 cm. OOZE is soupy in Sections 1, 2, and the CC.

SMEAR SLIDE SUMMARY (%):

	2,75
	D
Foraminifers	25
Nannofossils	15
Sponge Spicules (siliceous)	20
Micrite	15
Clasts (degraded forams ?)	25

SITE 628 HOLE A CORE 16H CORED INTERVAL 1100.1-1109.6 mbsl; 136.6-146.1 mbsf

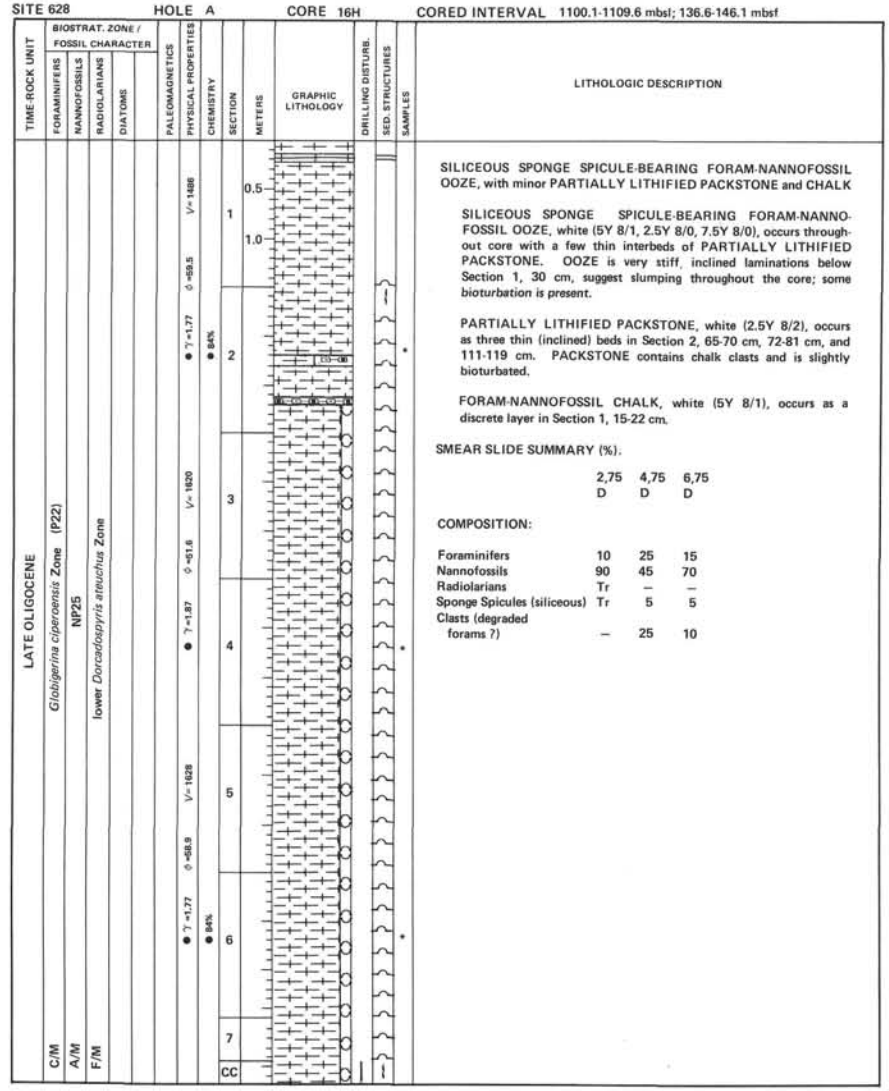

LITHOLOGIC DESCRIPTION

SILICEOUS SPONGE SPICULE-BEARING FORAM-NANNOFOSSIL OOZE, with minor PARTIALLY LITHIFIED PACKSTONE and CHALK

SILICEOUS SPONGE SPICULE-BEARING FORAM-NANNOFOSSIL OOZE, white (5Y 8/1, 2.5Y 8/0, 7.5Y 8/0), occurs throughout core with a few thin interbeds of PARTIALLY LITHIFIED PACKSTONE. OOZE is very stiff, inclined laminations below Section 1, 30 cm, suggest slumping throughout the core; some *bioturbation is present.*

PARTIALLY LITHIFIED PACKSTONE, white (2.5Y 8/2), occurs as three thin (inclined) beds in Section 2, 65-70 cm, 72-81 cm, and 111-119 cm. PACKSTONE contains chalk clasts and is slightly bioturbated.

FORAM-NANNOFOSSIL CHALK, white (5Y 8/1), occurs as a discrete layer in Section 1, 15-22 cm.

SMEAR SLIDE SUMMARY (%).

	2,75	4,75	6,75
	D	D	D
Foraminifers	10	25	15
Nannofossils	90	45	70
Radiolarians	Tr	–	–
Sponge Spicules (siliceous)	Tr	5	5
Clasts (degraded forams ?)	–	25	10

SITE 628 HOLE A CORE 17H CORED INTERVAL 1109.6-1119.2 mbsl; 146.1-155.7 mbsf

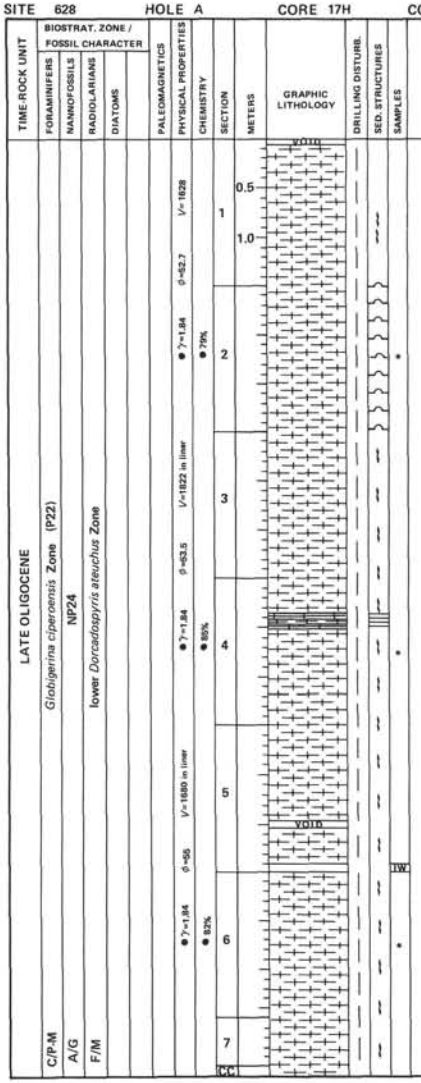

LITHOLOGIC DESCRIPTION

SILICEOUS SPONGE SPICULE-BEARING FORAM-NANNOFOSSIL OOZE and minor CHALK

SILICEOUS SPONGE SPICULE-BEARING FORAM-NANNOFOSSIL OOZE, white (5Y 8/1), occurs throughout core with two intervals of CHALK in Section 4, 36-40 cm and 45-48 cm. OOZE is stiff, bioturbated throughout, with pyrite concentrated in burrows. Inclined burrows in Section 2 may indicate slumping.

SMEAR SLIDE SUMMARY (%):

	2,75 D	4,75 D	6,75 D
TEXTURE:			
Sand	10	10	15
Silt	15	15	5
Clay	75	75	80
COMPOSITION:			
Foraminifers	15	15	15
Nannofossils	70	70	75
Radiolarians	–	Tr	–
Sponge Spicules	5	5	5
Micrite Needles	5	5	5
Clasts	5	5	Tr

SITE 628 HOLE A CORE 18H CORED INTERVAL 1119.2-1128.7 mbsl; 155.7-165.2 mbsf

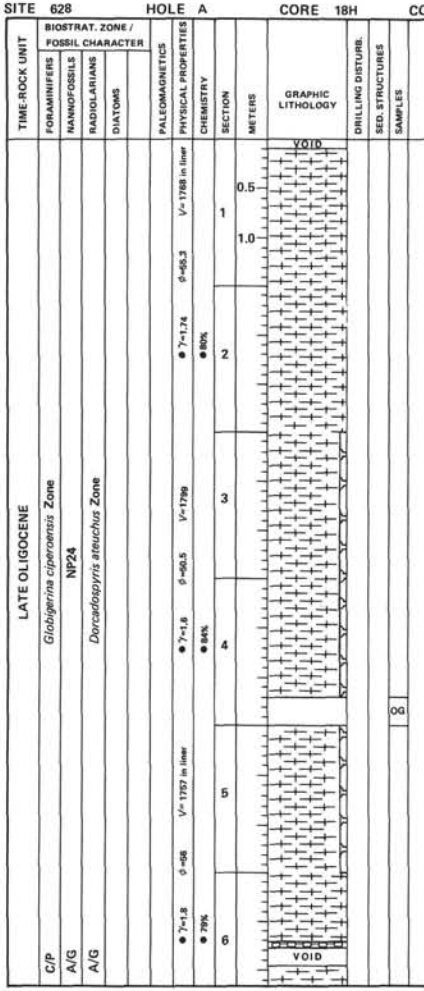

LITHOLOGIC DESCRIPTION

SILICEOUS SPONGE SPICULE-BEARING FORAM-NANNOFOSSIL OOZE and minor CHALK

SILICEOUS SPONGE SPICULE-BEARING FORAM-NANNOFOSSIL OOZE, white (5Y 8/1), occurs throughout core. OOZE is stiff from the top of the core to Section 5, 110 cm; below this it becomes less firm. Pyrite flecks, laminations, and burrows are present (a pyritized burrow occurs in Section 3, 60 cm). A layer of CHALK occurs in Section 6, 75 cm. During core splitting, the presence of this poorly indurated layer evidently led to the creation of the underlying void.

SMEAR SLIDE SUMMARY (%).

	2,75 D	4,75 D	6,75 D
COMPOSITION:			
Foraminifers	10	20	20
Nannofossils	75	60	70
Sponge Spicules	5	10	3
Pellets	5	5	4
Micrite	3	2	–
Needles	2	3	3

SITE 628 HOLE A CORE 19H COREDINTERVAL 1128.7-1137.7 mbsl; 165.2-174.2 mbsf

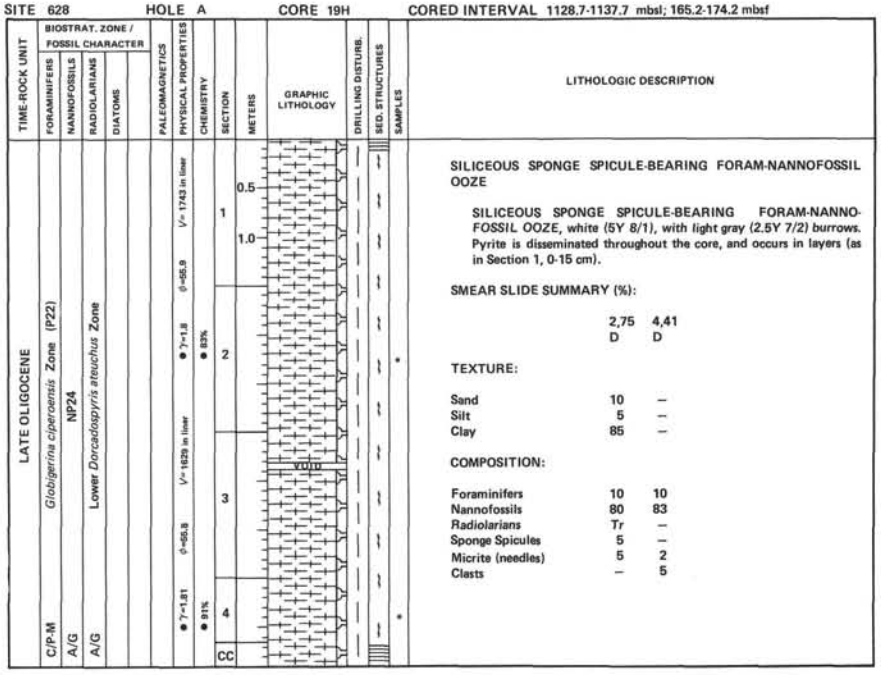

SILICEOUS SPONGE SPICULE-BEARING FORAM-NANNOFOSSIL OOZE

SILICEOUS SPONGE SPICULE-BEARING FORAM-NANNOFOSSIL OOZE, white (5Y 8/1), with light gray (2.5Y 7/2) burrows. Pyrite is disseminated throughout the core, and occurs in layers (as in Section 1, 0-15 cm).

SMEAR SLIDE SUMMARY (%):

	2,75 D	4,41 D
TEXTURE:		
Sand	10	–
Silt	5	–
Clay	85	–
COMPOSITION:		
Foraminifers	10	10
Nannofossils	80	83
Radiolarians	Tr	–
Sponge Spicules	5	–
Micrite (needles)	5	2
Clasts	–	5

SITE 628 HOLE A CORE 20H COREDINTERVAL 1137.7-1146.7 mbsl; 174.2-183.2 mbsf

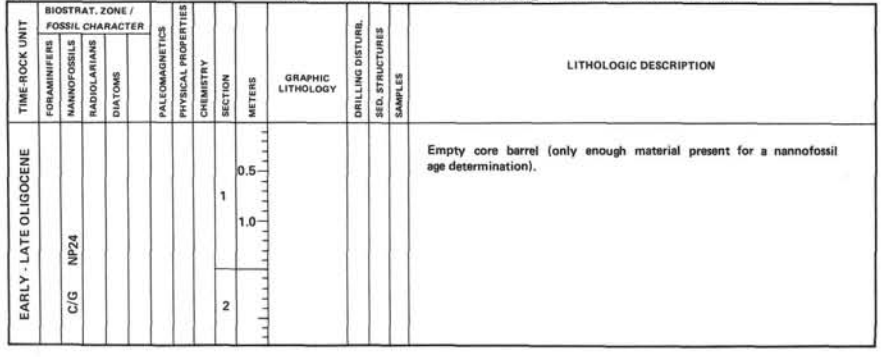

Empty core barrel (only enough material present for a nannofossil age determination).

SITE 628 HOLE A CORE 21H COREDINTERVAL 1146.7-1156.2 mbsl; 183.2-192.7 mbsf

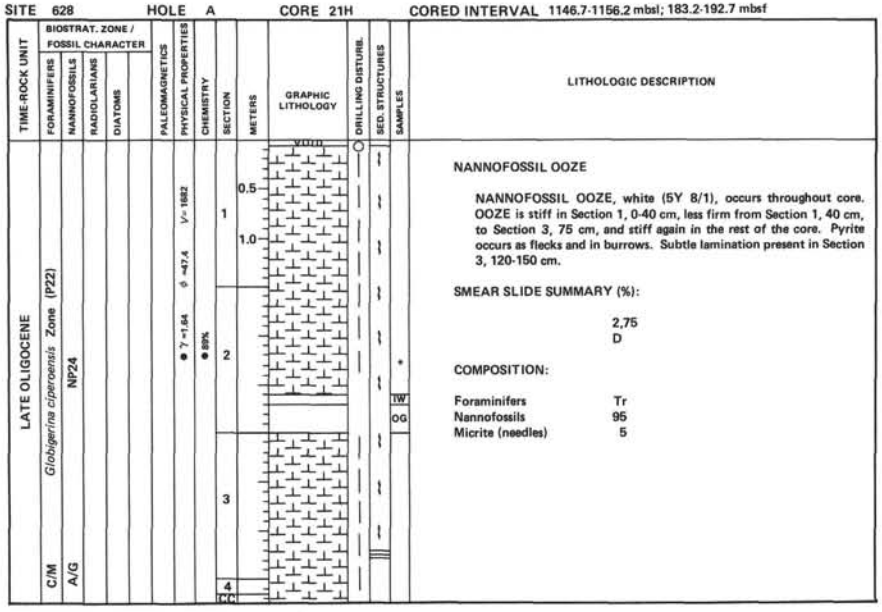

NANNOFOSSIL OOZE

NANNOFOSSIL OOZE, white (5Y 8/1), occurs throughout core. OOZE is stiff in Section 1, 0-40 cm, less firm from Section 1, 40 cm, to Section 3, 75 cm, and stiff again in the rest of the core. Pyrite occurs as flecks and in burrows. Subtle lamination present in Section 3, 120-150 cm.

SMEAR SLIDE SUMMARY (%):

	2,75 D
COMPOSITION:	
Foraminifers	Tr
Nannofossils	95
Micrite (needles)	5

SITE 628 HOLE A CORE 22X CORED INTERVAL 1156.2-1165.8 mbsl; 192.7-202.3 mbsf

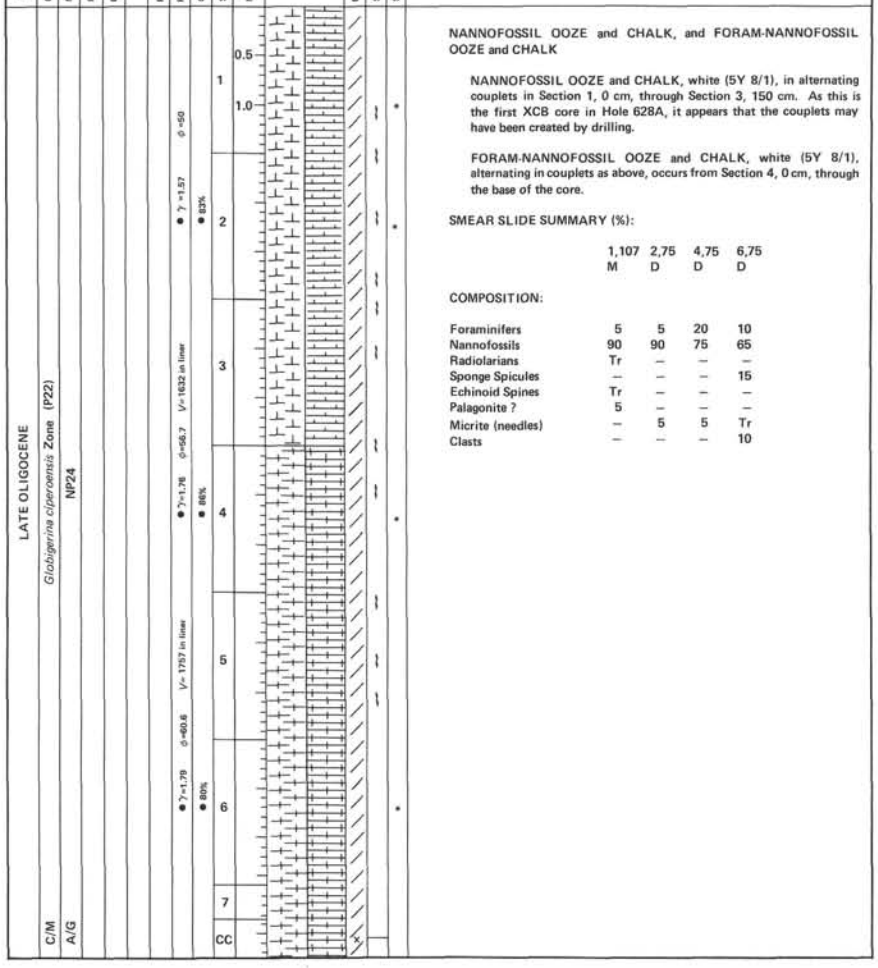

LITHOLOGIC DESCRIPTION

NANNOFOSSIL OOZE and CHALK, and FORAM-NANNOFOSSIL OOZE and CHALK

NANNOFOSSIL OOZE and CHALK, white (5Y 8/1), in alternating couplets in Section 1, 0 cm, through Section 3, 150 cm. As this is the first XCB core in Hole 628A, it appears that the couplets may have been created by drilling.

FORAM-NANNOFOSSIL OOZE and CHALK, white (5Y 8/1), alternating in couplets as above, occurs from Section 4, 0 cm, through the base of the core.

SMEAR SLIDE SUMMARY (%):

	1,107 M	2,75 D	4,75 D	6,75 D
COMPOSITION:				
Foraminifers	5	5	20	10
Nannofossils	90	90	75	65
Radiolarians	Tr	–	–	–
Sponge Spicules	–	–	–	15
Echinoid Spines	Tr	–	–	–
Palagonite ?	5	–	–	–
Micrite (needles)	–	5	5	Tr
Clasts	–	–	–	10

SITE 628 HOLE A CORE 23X CORED INTERVAL 1165.8-1175.4 mbsl; 202.3-211.9 mbsf

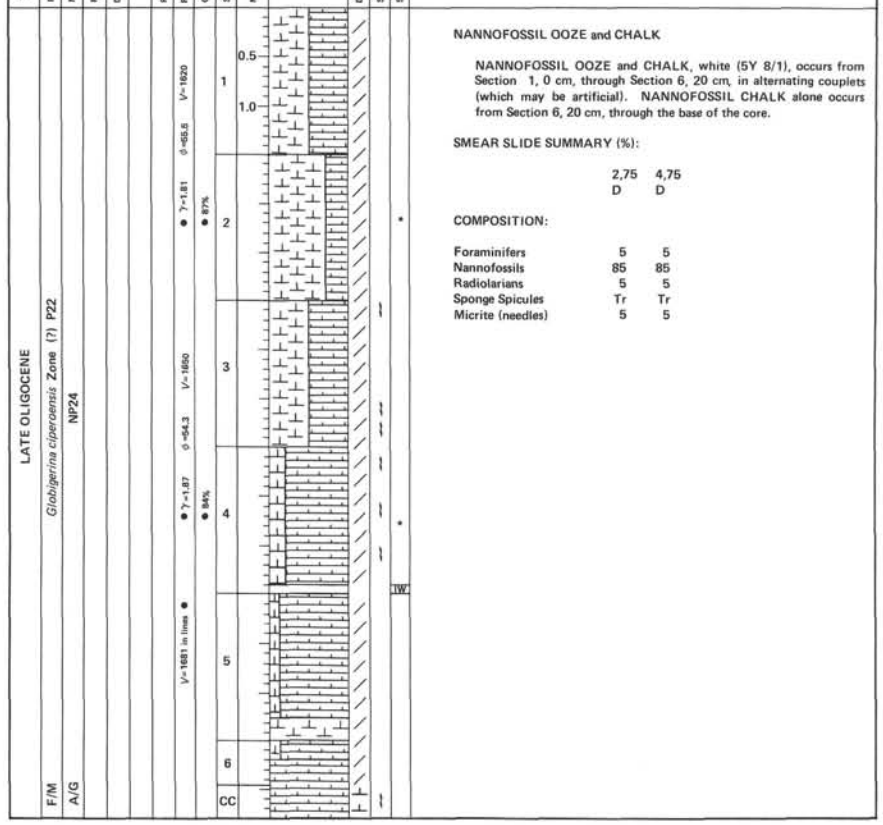

LITHOLOGIC DESCRIPTION

NANNOFOSSIL OOZE and CHALK

NANNOFOSSIL OOZE and CHALK, white (5Y 8/1), occurs from Section 1, 0 cm, through Section 6, 20 cm, in alternating couplets (which may be artificial). NANNOFOSSIL CHALK alone occurs from Section 6, 20 cm, through the base of the core.

SMEAR SLIDE SUMMARY (%):

	2,75 D	4,75 D
COMPOSITION:		
Foraminifers	5	5
Nannofossils	85	85
Radiolarians	5	5
Sponge Spicules	Tr	Tr
Micrite (needles)	5	5

SITE 628 HOLE A CORE 24X CORED INTERVAL 1175.4-1185.0 mbsl; 211.9-221.5 mbsf

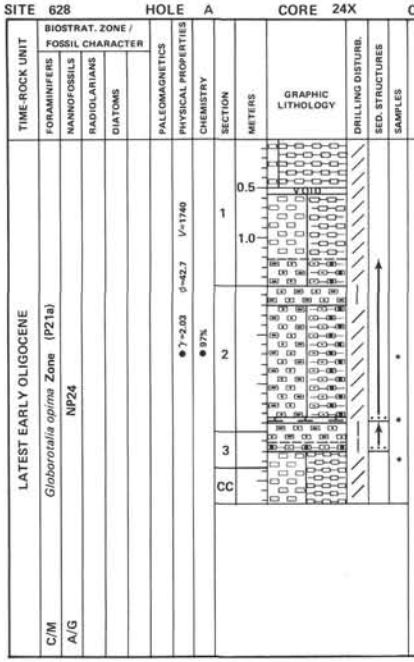

LITHOLOGIC DESCRIPTION

CALCAREOUS OOZE and CHALK, UNLITHIFIED PACKSTONE, PARTIALLY LITHIFIED PACKSTONE, and minor NANNOFOSSIL OOZE

CALCAREOUS OOZE and CHALK, white (5Y 8/1), occurs as alternating couplets (which may be artificial) in Section 1, 0-125 cm; in Section 3, 20-35 cm; and in the CC.

UNLITHIFIED PACKSTONE and PARTIALLY LITHIFIED PACKSTONE, white (10YR 8/1), occurs interbedded and intergraded. Grains vary from medium to coarse sand, consisting of foraminifers, skeletal fragments, and lithoclasts.

NANNOFOSSIL OOZE, white (5Y 8/1), occurs in Section 2, 135-140 cm.

SMEAR SLIDE SUMMARY (%):

	2,75 D	2,138 M	3,30 D
COMPOSITION:			
Foraminifers	5	5	Tr
Nannofossils	20	20	50
Radiolarians	–	5	–
Sponge Spicules	Tr	Tr	Tr
Pellets	40	–	10
Skeletal Fragments	Tr	–	–
Micrite (needles)	35	10	5
Clasts	–	–	35

SITE 628 HOLE A CORE 25X CORED INTERVAL 1185.0-1194.9 mbsl; 221.5-231.4 mbsf

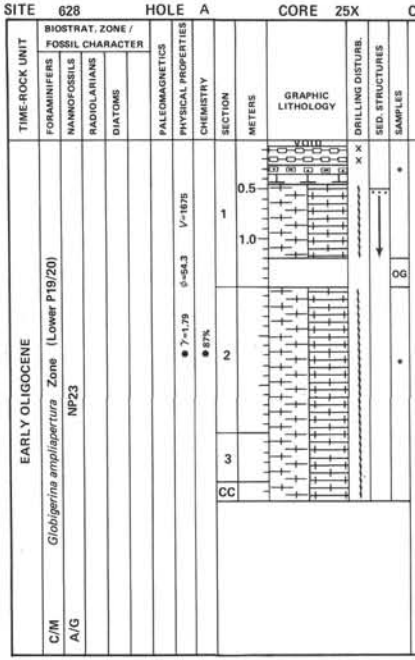

LITHOLOGIC DESCRIPTION

FORAM-NANNOFOSSIL OOZE and CHALK, with minor CALCAREOUS OOZE, NANNOFOSSIL OOZE and UNLITHIFIED PACKSTONE

FORAM-NANNOFOSSIL OOZE and CHALK, white (5Y 8/1), occurs from Section 1, 45 cm, through the base of the core in alternating couplets (which may be artificial). OOZE is slightly finer grained toward the base of the core. Echinoderm spines, shell fragments and some chert fragments occur.

CHALK, white (5Y 8/1), occurs in Section 1, 5-24 cm; contains some coarse grains.

NANNOFOSSIL OOZE, white (5Y 8/1), occurs in Section 1, 33-45 cm.

UNLITHIFIED PACKSTONE, white (10YR 8/1), occurs in Section 1, 24-33 cm. Contains skeletal fragments, glauconite and foraminifers.

SMEAR SLIDE SUMMARY (%):

	1,37 D	2,75 D
COMPOSITION:		
Foraminifers	Tr	10
Nannofossils	80	75
Skeletal Fragments	15	10
Micrite (needles)	5	5

SITE 628 HOLE A CORE 26X CORED INTERVAL 1194.9-1204.5 mbsl; 231.4-241.0 mbsf

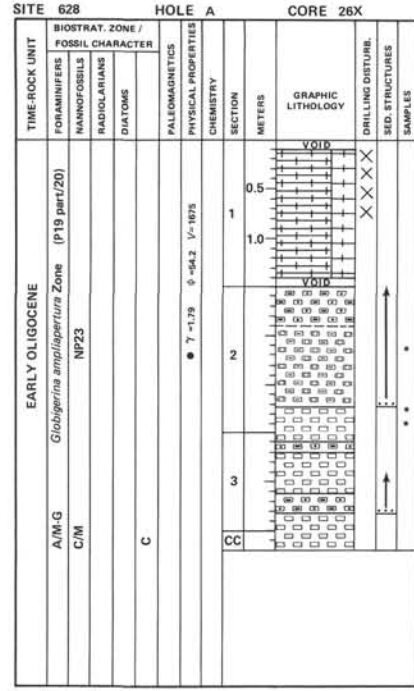

LITHOLOGIC DESCRIPTION

FORAM-NANNOFOSSIL OOZE and CHALK, CALCAREOUS OOZE, UNLITHIFIED PACKSTONE, and UNLITHIFIED FLOATSTONE

FORAM-NANNOFOSSIL OOZE and CHALK, white (5Y 8/1), occurs in Section 1, 10-95 cm; highly fragmented 10-55 cm; occurs as alternating OOZE/CHALK couplets (may be artificial) 55-95 cm.

CALCAREOUS OOZE, white (2.5Y 8/0[N 8/0], whiter than 5Y 8/1), occurs from Section 2, 123 cm, through the base of the core, with two interbeds of UNLITHIFIED PACKSTONE.

UNLITHIFIED PACKSTONE, white (5Y 8/1), occurs as interbeds with CALCAREOUS OOZE in Section 3, 10-15 cm and 65-85 cm; also overlying UNLITHIFIED FLOATSTONE in an apparent fining-upwards sequence, in Section 2, 0-39 cm. Grain types include large benthic foraminifers.

UNLITHIFIED FLOATSTONE, white (5Y 8/1), occurs in Section 2.

SMEAR SLIDE SUMMARY (%):

	2,75 D	2,139 D	2,143 M
COMPOSITION:			
Foraminifers	10	10	20
Nannofossils	35	45	10
Radiolarians	–	–	5
Skeletal Fragments	10	4	Tr
Micrite	35	40	50
Clasts	10	–	15

SITE 628 HOLE A CORE 27X CORED INTERVAL 1204.5-1214.1 mbsl; 241.0-250.6 mbsf

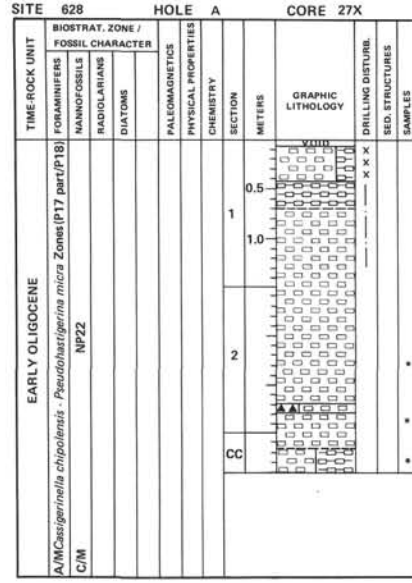

LITHOLOGIC DESCRIPTION

CALCAREOUS OOZE and CHALK

CALCAREOUS OOZE and CHALK, white (5Y 8/1), occurs in alternating couplets (which may be artificial) in Section 1, 0-43 cm, and in the CC, 16 cm; OOZE alone occurs from Section 1, 70 cm, through the CC, 16 cm; CHALK alone occurs in Section 1, 43-70 cm. Micrite is generally more abundant than nannofossils in matrix; benthic and planktonic foraminifers are present. CHERT fragments in Section 2, 118-125 cm.

SMEAR SLIDE SUMMARY (%):

	2,75 D	2,140 D	CC,26
COMPOSITION:			
Accessory Minerals:			
Glauconite	–	–	Tr
Foraminifers	5	20	5
Nannofossils	45	Tr	–
Radiolarians	–	Tr	–
Sponge Spicules	Tr	Tr	–
Echinoid Fragments	–	10	–
Skeletal Fragments	–	–	20
Clasts	5	10	10
Micrite	45	60	65

SITE 628 HOLE A CORE 28X CORED INTERVAL 1214.1-1223.7 mbsl; 250.6-260.2 mbsf

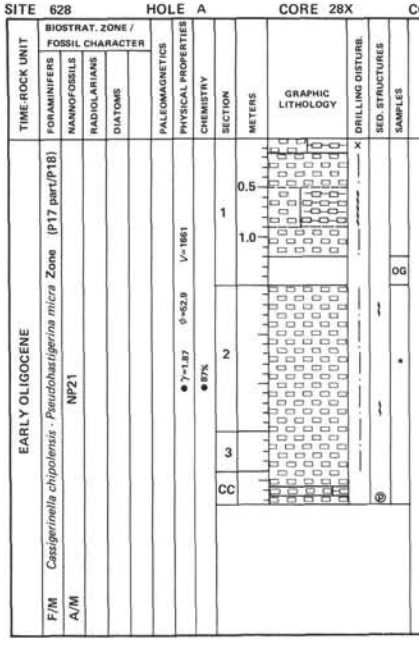

LITHOLOGIC DESCRIPTION

CALCAREOUS OOZE and CHALK

CALCAREOUS OOZE and CHALK, white (2.5Y 8/0); OOZE alone occurs throughout core, with OOZE/CHALK alternating couplets (which may be artificial) in Section 1, 0-12 cm and 50-93 cm. CHALK occurs alone as a thin layer in the CC, 18-21 cm. Streaks and specks of pyrite occur throughout, as do burrows. Micrite is abundant; nannofossils are much more abundant than foraminifers.

SMEAR SLIDE SUMMARY (%):

	2,75
	M
COMPOSITION:	
Foraminifers	5
Nannofossils	45
Sponge Spicules	Tr
Clasts	5
Micrite	45

SITE 628 HOLE A CORE 29X CORED INTERVAL 1223.7-1233.4 mbsl; 260.2-269.9 mbsf

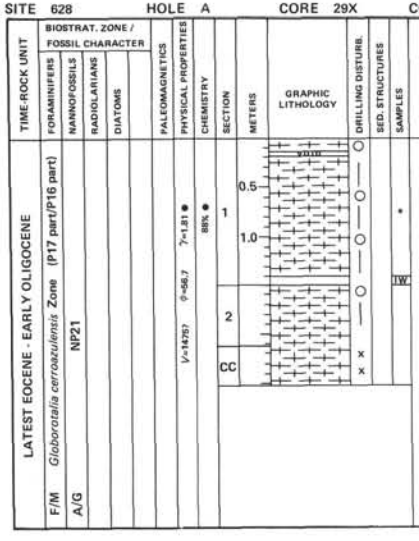

LITHOLOGIC DESCRIPTION

NANNOFOSSIL OOZE

NANNOFOSSIL OOZE, white (2.5Y 8/0), occurs throughout core. OOZE is bioturbated, with some burrows 1 cm in diameter. Very little micrite is present.

SMEAR SLIDE SUMMARY (%):

	1,75
	D
COMPOSITION:	
Foraminifers	1
Nannofossils	90
Sponge Spicules	Tr
Micrite	4
Calcispheres	5

SITE 628 HOLE A CORE 30X CORED INTERVAL 1233.4-1242.7 mbsl; 269.9-279.2 mbsf

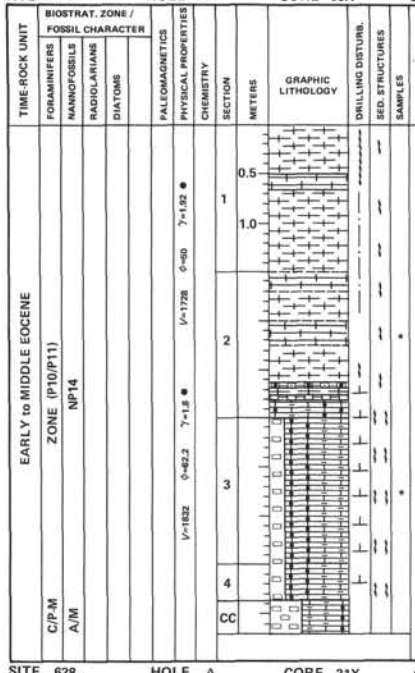

LITHOLOGIC DESCRIPTION

NANNOFOSSIL OOZE and CHALK, LITHIFIED PACKSTONE and CALCAREOUS OOZE (probably drilling slurry), with minor PARTIALLY LITHIFIED PACKSTONE

NANNOFOSSIL OOZE and CHALK, white (10YR 8/1), occurs from Section 1, 0 cm, through Section 2, 134 cm. Some OOZE/CHALK alternating couplets (may be artificial) are present.

LITHIFIED PACKSTONE, white (10YR 8/1), occurs from Section 2, 134 cm, through the base of core; PACKSTONE fragments alternate with CALCAREOUS OOZE, which is probably drilling slurry. PACKSTONE is highly bioturbated; contains primarily planktonic foraminifers.

PARTIALLY LITHIFIED PACKSTONE, white (10YR 8/2), occurs in Section 2, 116-118 cm, as a thin bed within NANNOFOSSIL OOZE.

SMEAR SLIDE SUMMARY (%):

	2,75	3,75
	D	D
COMPOSITION:		
Foraminifers	2	20
Nannofossils	80	60
Sponge Spicules	—	Tr
Skeletal Fragments	1	3
Micrite	15	15
Calcispheres	1	1
Clasts	1	—

SITE 628 HOLE A CORE 31X CORED INTERVAL 1242.7-1252.3 mbsl; 279.2-288.8 mbsf

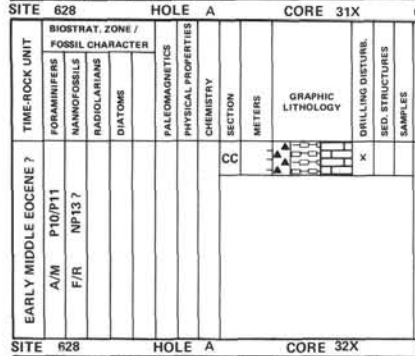

LITHOLOGIC DESCRIPTION

Empty core barrel. CC contains clasts of CHALK and small fragments of CHERT and green LIMESTONE.

SITE 628 HOLE A CORE 32X CORED INTERVAL 1252.3-1261.9 mbsl; 288.8-298.4 mbsf

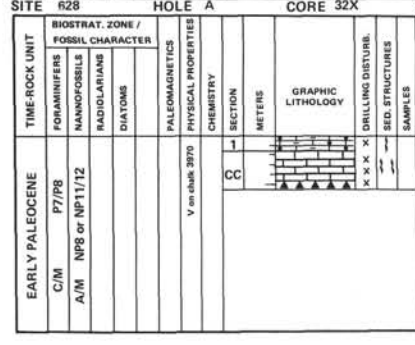

LITHOLOGIC DESCRIPTION

LITHIFIED PACKSTONE, LIMESTONE, and CHERT

LITHIFIED PACKSTONE, white (10YR 8/1), occurs as broken fragments in Section 1, 0-15 cm.

LIMESTONE, green (5GY 7/2), possibly siliceous or dolomitic, occurs as broken fragments in CC.

CHERT, brown (10YR 5/1), occurs as a single fragment (4 cm diameter) at base of core.

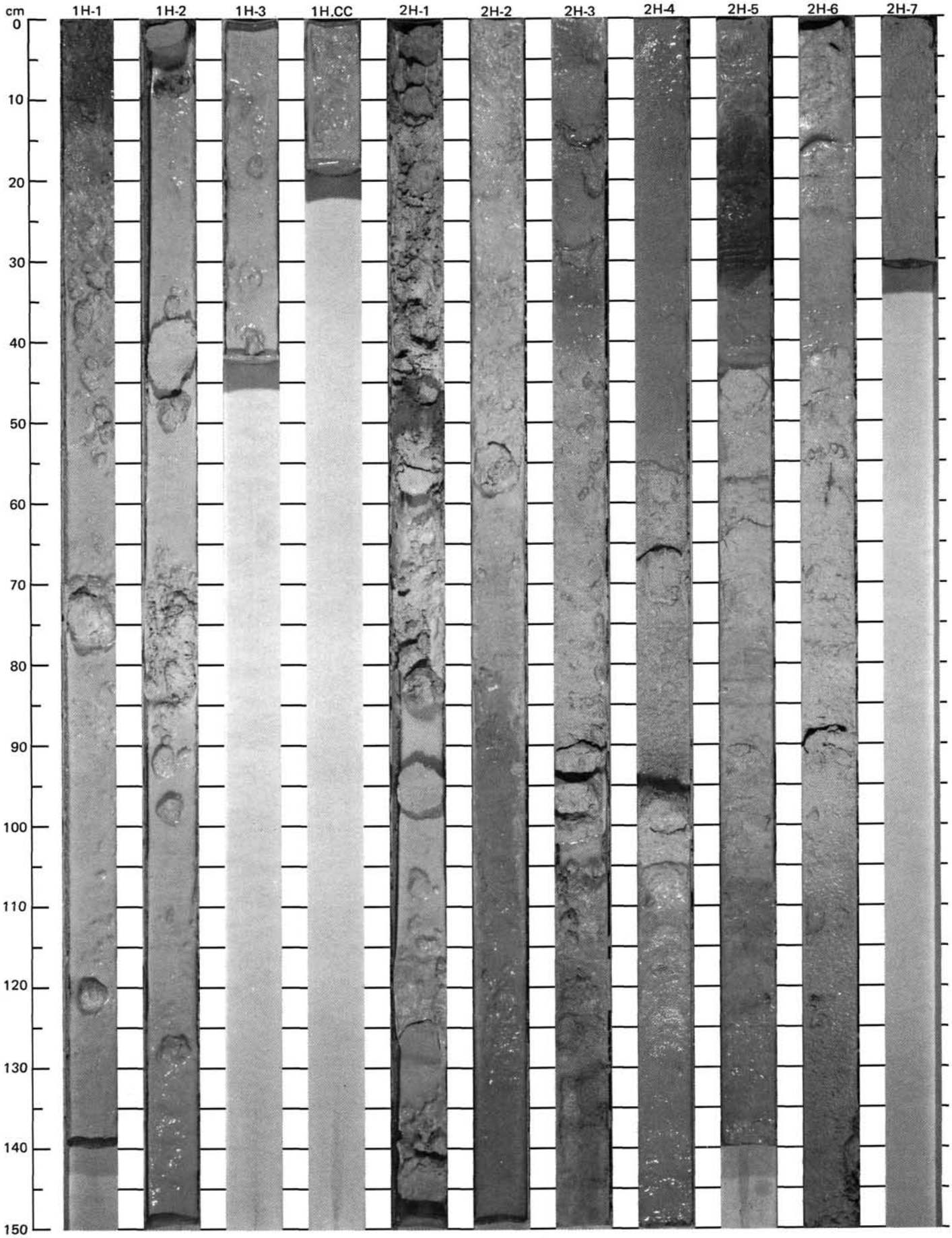
cm
1H-1
1H-2
1H-3
1H.CC
2H-1
2H-2
2H-3
2H-4
2H-5
2H-6
2H-7
0
10
20
30
40
50
60
70
80
90
100
110
120
130
140
150

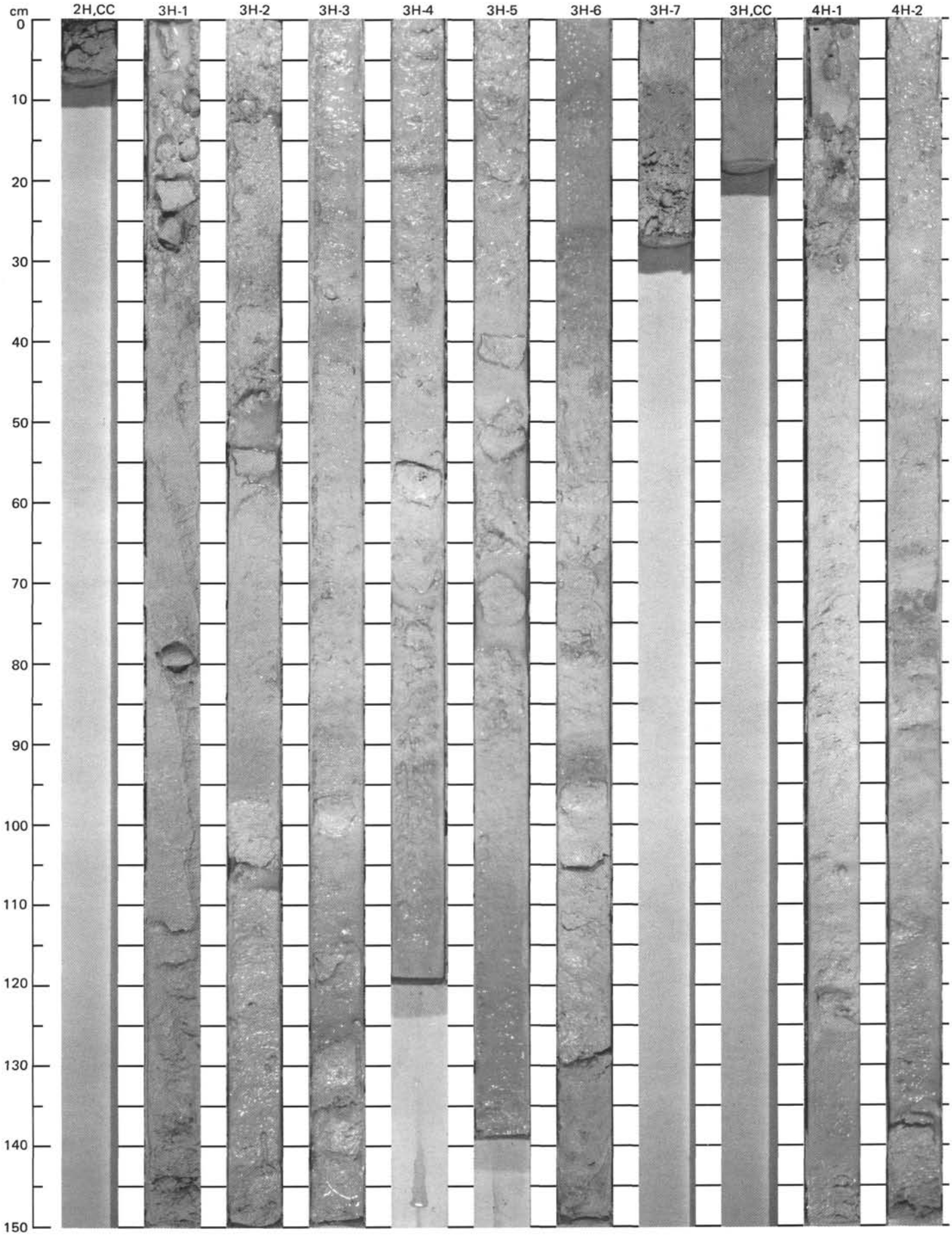
cm
2H,CC
3H-1
3H-2
3H-3
3H-4
3H-5
3H-6
3H-7
3H,CC
4H-1
4H-2
0
10
20
30
40
50
60
70
80
90
100
110
120
130
140
150

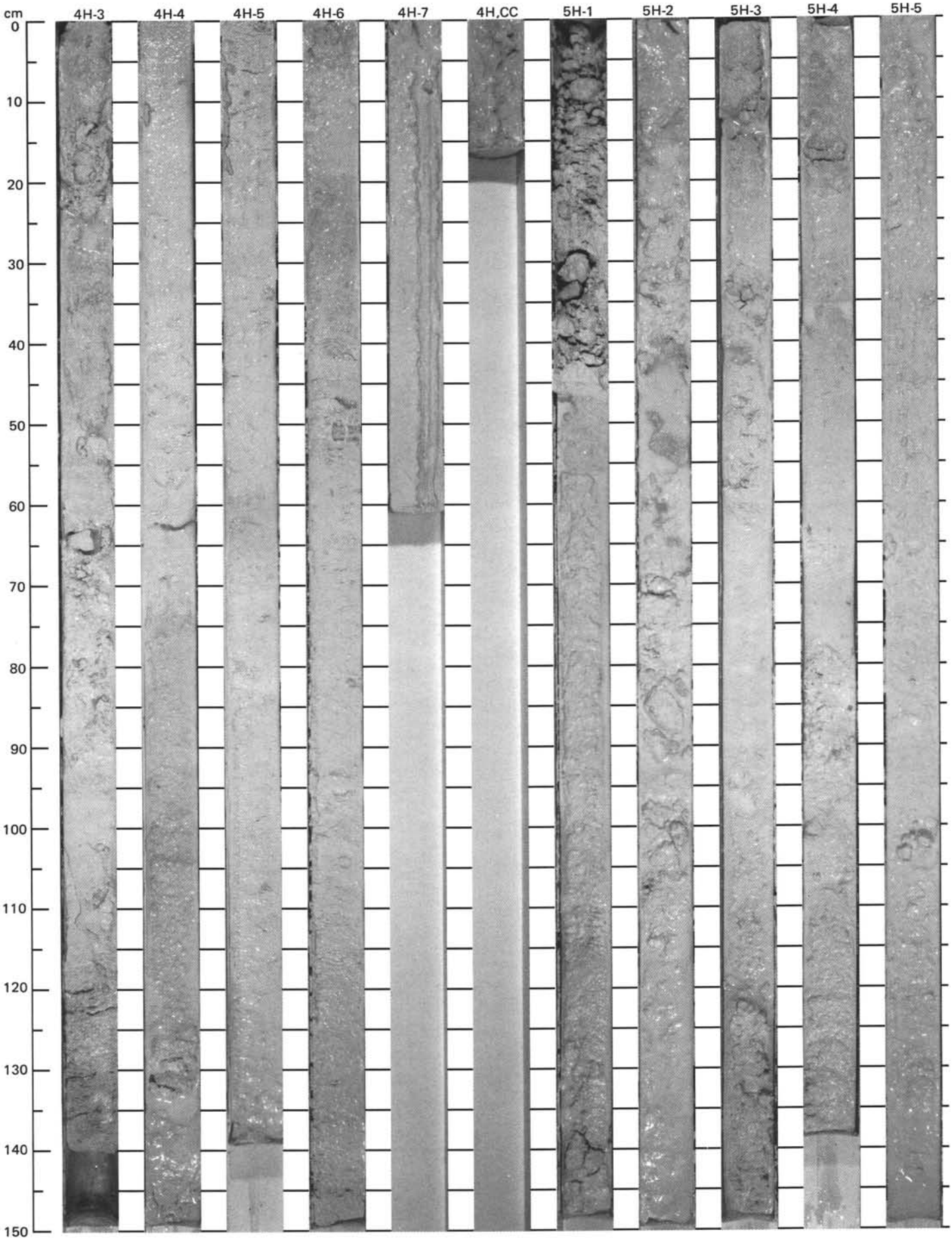
cm
4H-3
4H-4
4H-5
4H-6
4H-7
4H,CC
5H-1
5H-2
5H-3
5H-4
5H-5
0
10
20
30
40
50
60
70
80
90
100
110
120
130
140
150

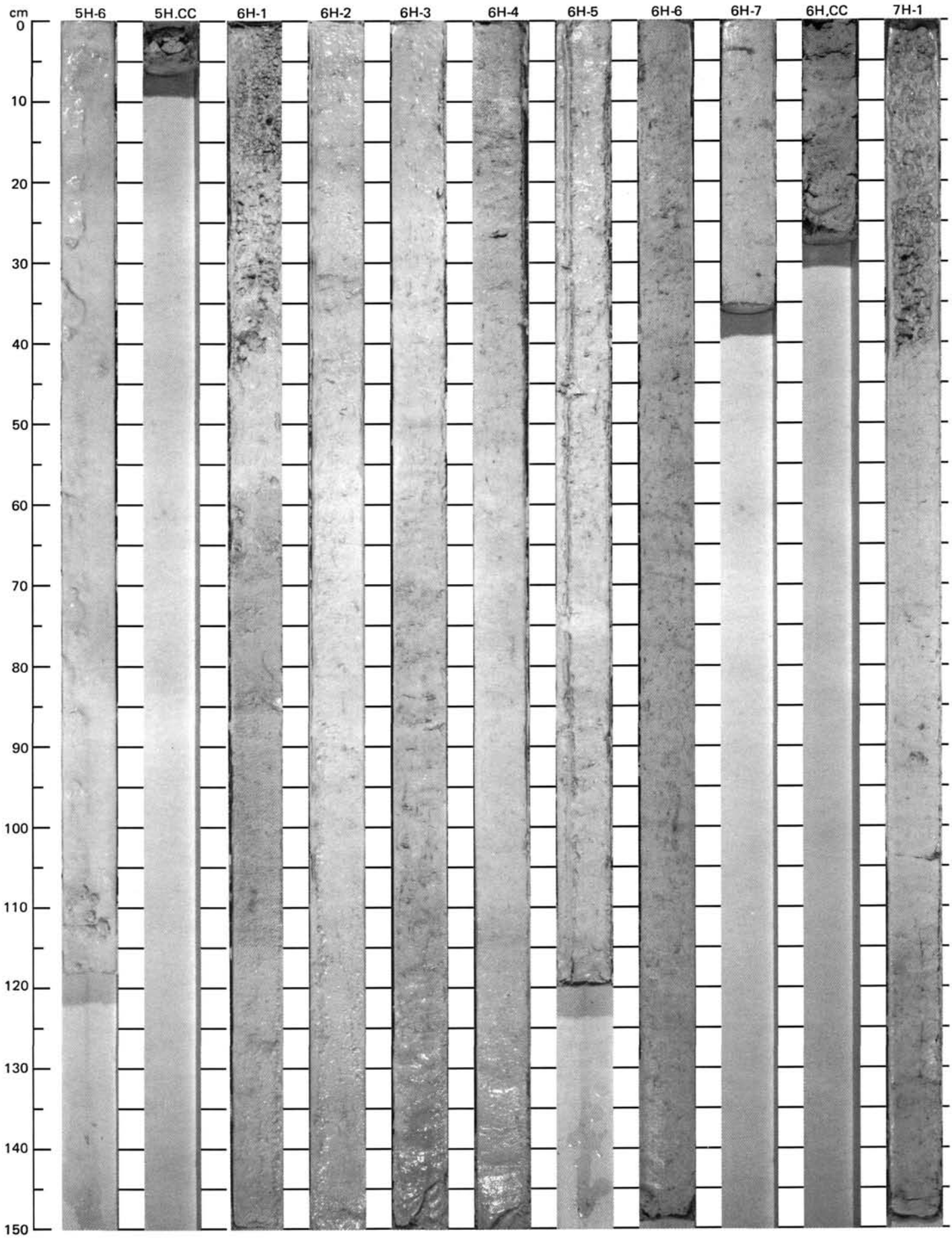
cm
5H-6
5H,CC
6H-1
6H-2
6H-3
6H-4
6H-5
6H-6
6H-7
6H,CC
7H-1
0
10
20
30
40
50
60
70
80
90
100
110
120
130
140
150

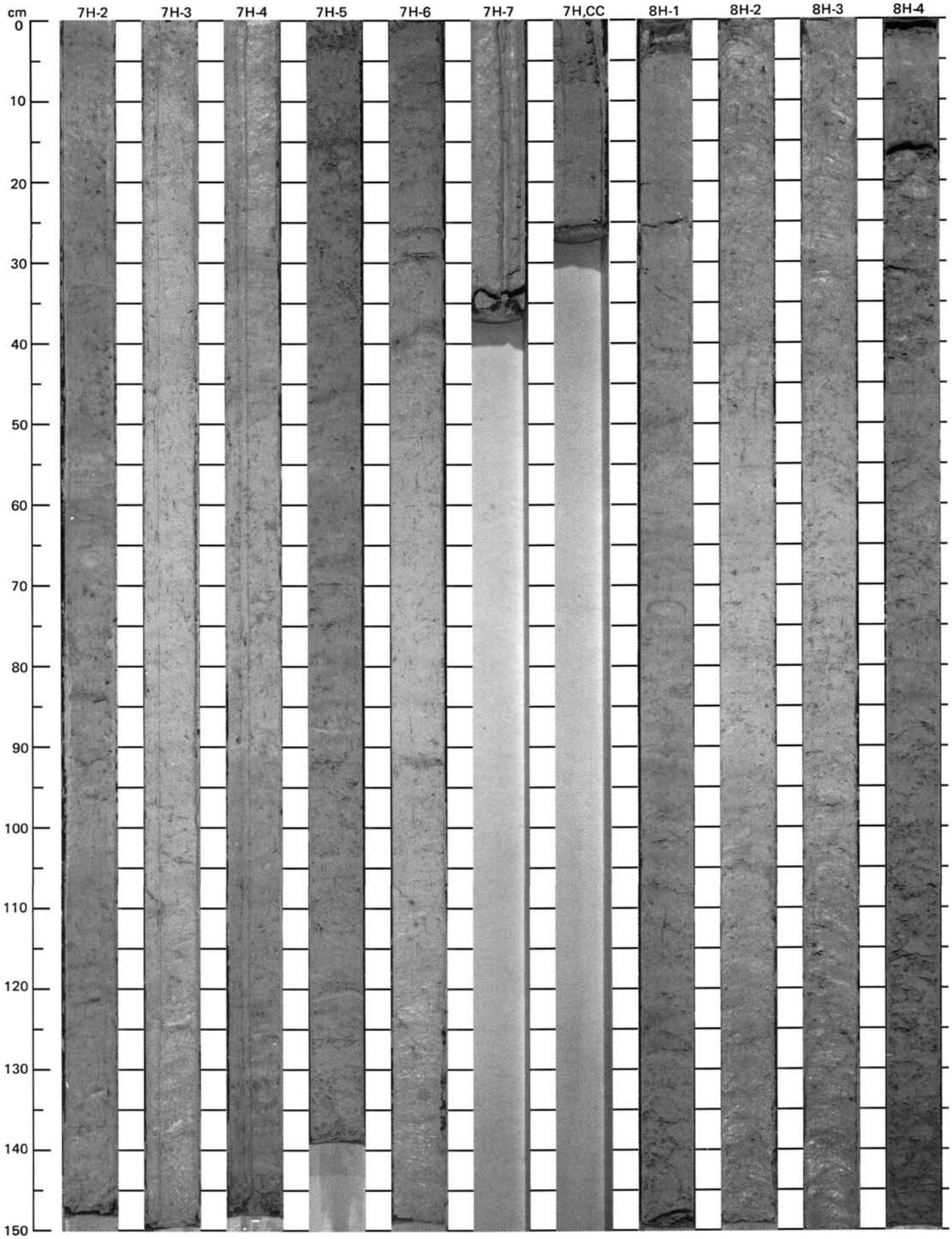
cm
7H-2
7H-3
7H-4
7H-5
7H-6
7H-7
7H,CC
8H-1
8H-2
8H-3
8H-4
0
10
20
30
40
50
60
70
80
90
100
110
120
130
140
150

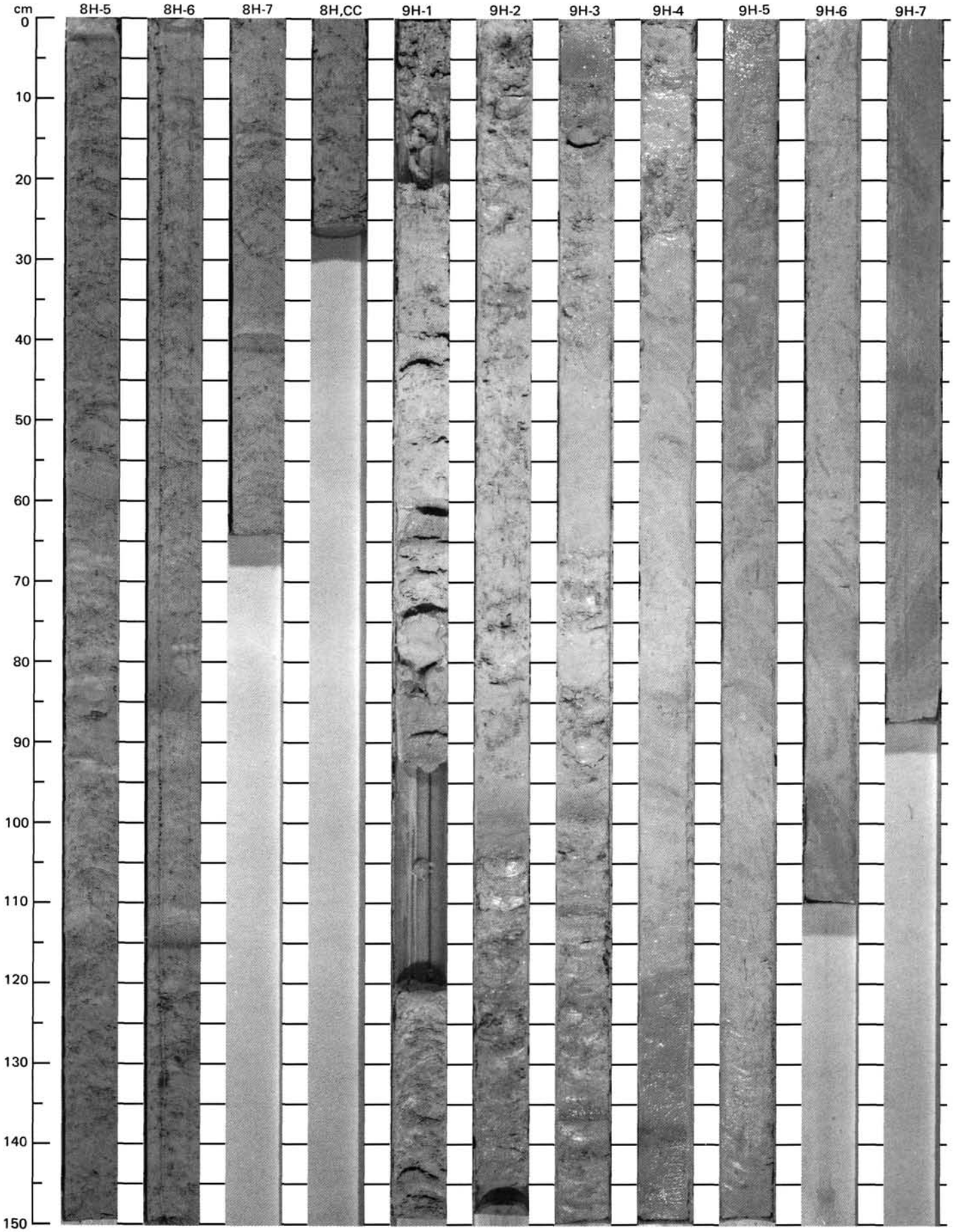
cm
8H-5
8H-6
8H-7
8H,CC
9H-1
9H-2
9H-3
9H-4
9H-5
9H-6
9H-7
0
10
20
30
40
50
60
70
80
90
100
110
120
130
140
150

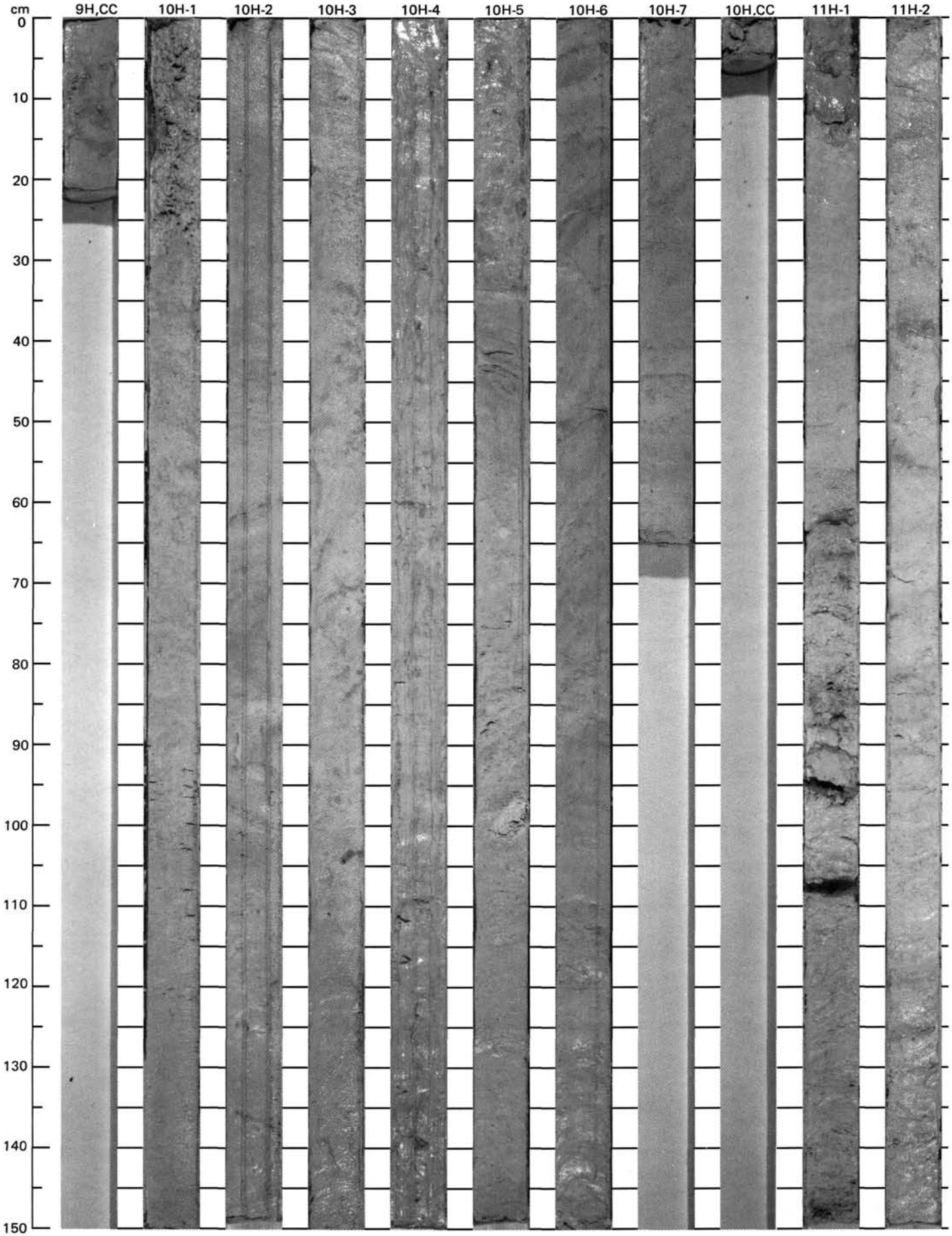
cm
9H,CC
10H-1
10H-2
10H-3
10H-4
10H-5
10H-6
10H-7
10H,CC
11H-1
11H-2
0
10
20
30
40
50
60
70
80
90
100
110
120
130
140
150

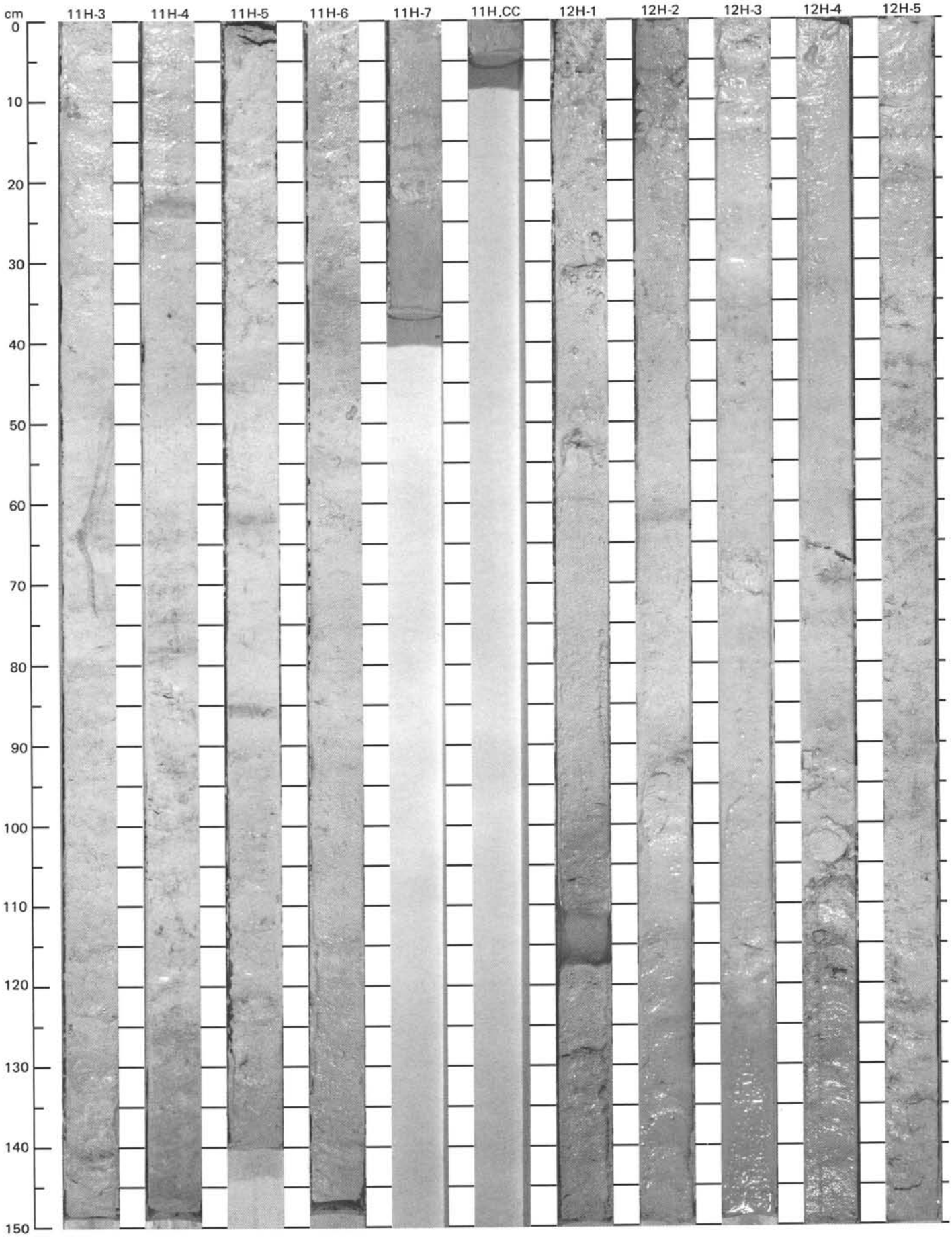
cm
11H-3
11H-4
11H-5
11H-6
11H-7
11H,CC
12H-1
12H-2
12H-3
12H-4
12H-5
0
10
20
30
40
50
60
70
80
90
100
110
120
130
140
150

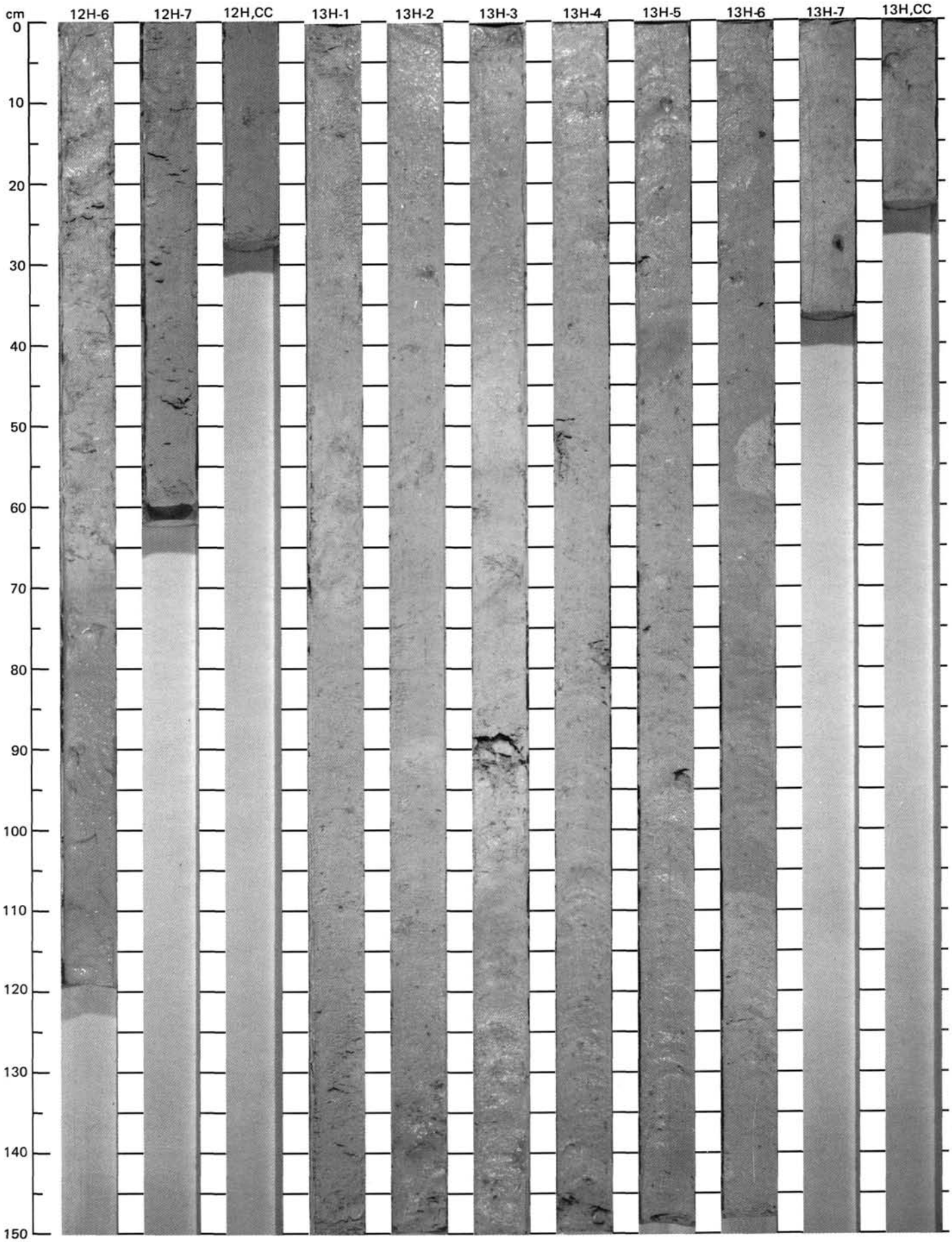
cm
12H-6
12H-7
12H,CC
13H-1
13H-2
13H-3
13H-4
13H-5
13H-6
13H-7
13H,CC
0
10
20
30
40
50
60
70
80
90
100
110
120
130
140
150

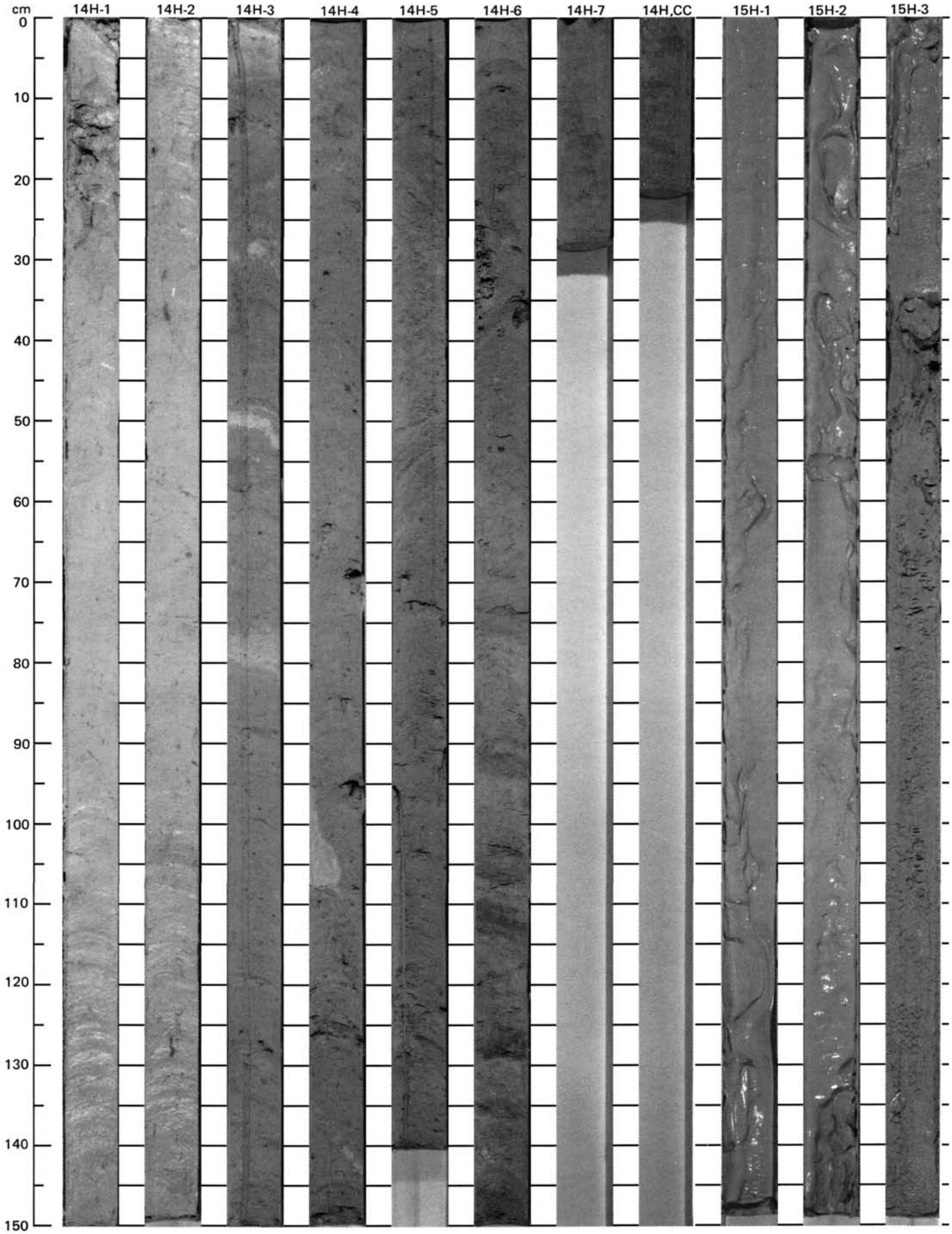
cm
14H-1
14H-2
14H-3
14H-4
14H-5
14H-6
14H-7
14H,CC
15H-1
15H-2
15H-3
0
10
20
30
40
50
60
70
80
90
100
110
120
130
140
150

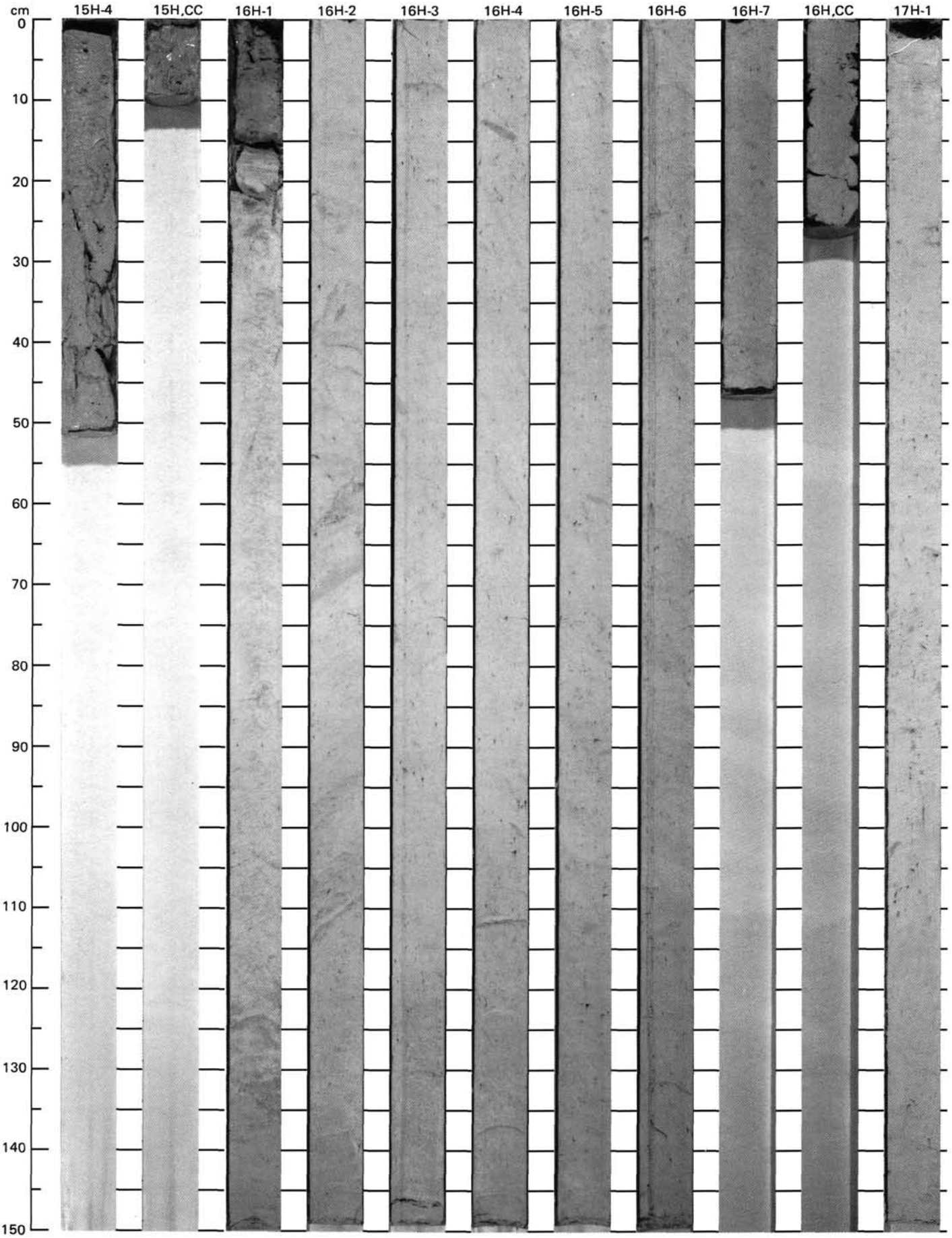
cm
15H-4
15H,CC
16H-1
16H-2
16H-3
16H-4
16H-5
16H-6
16H-7
16H,CC
17H-1
0
10
20
30
40
50
60
70
80
90
100
110
120
130
140
150

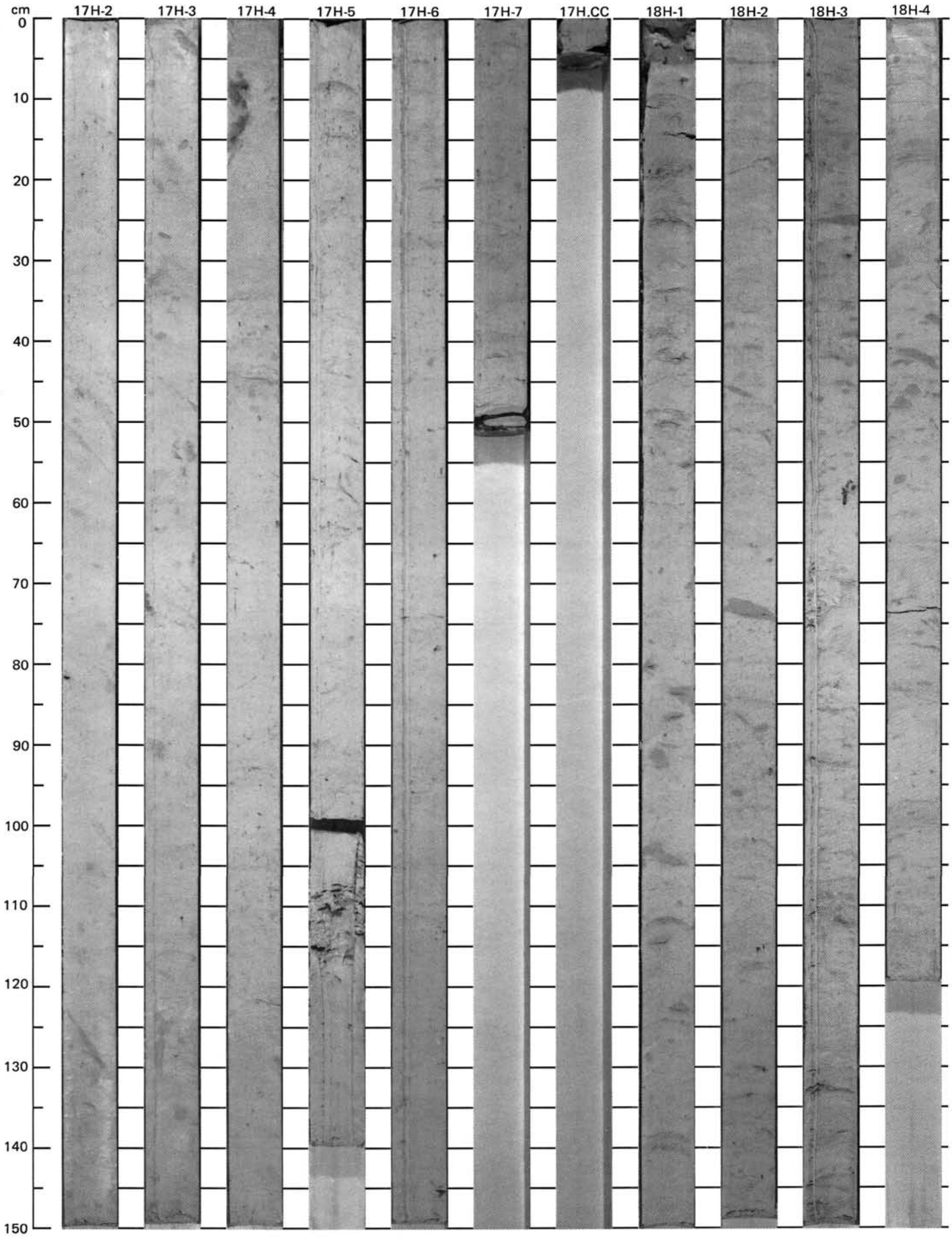
cm
17H-2
17H-3
17H-4
17H-5
17H-6
17H-7
17H.CC
18H-1
18H-2
18H-3
18H-4
0
10
20
30
40
50
60
70
80
90
100
110
120
130
140
150

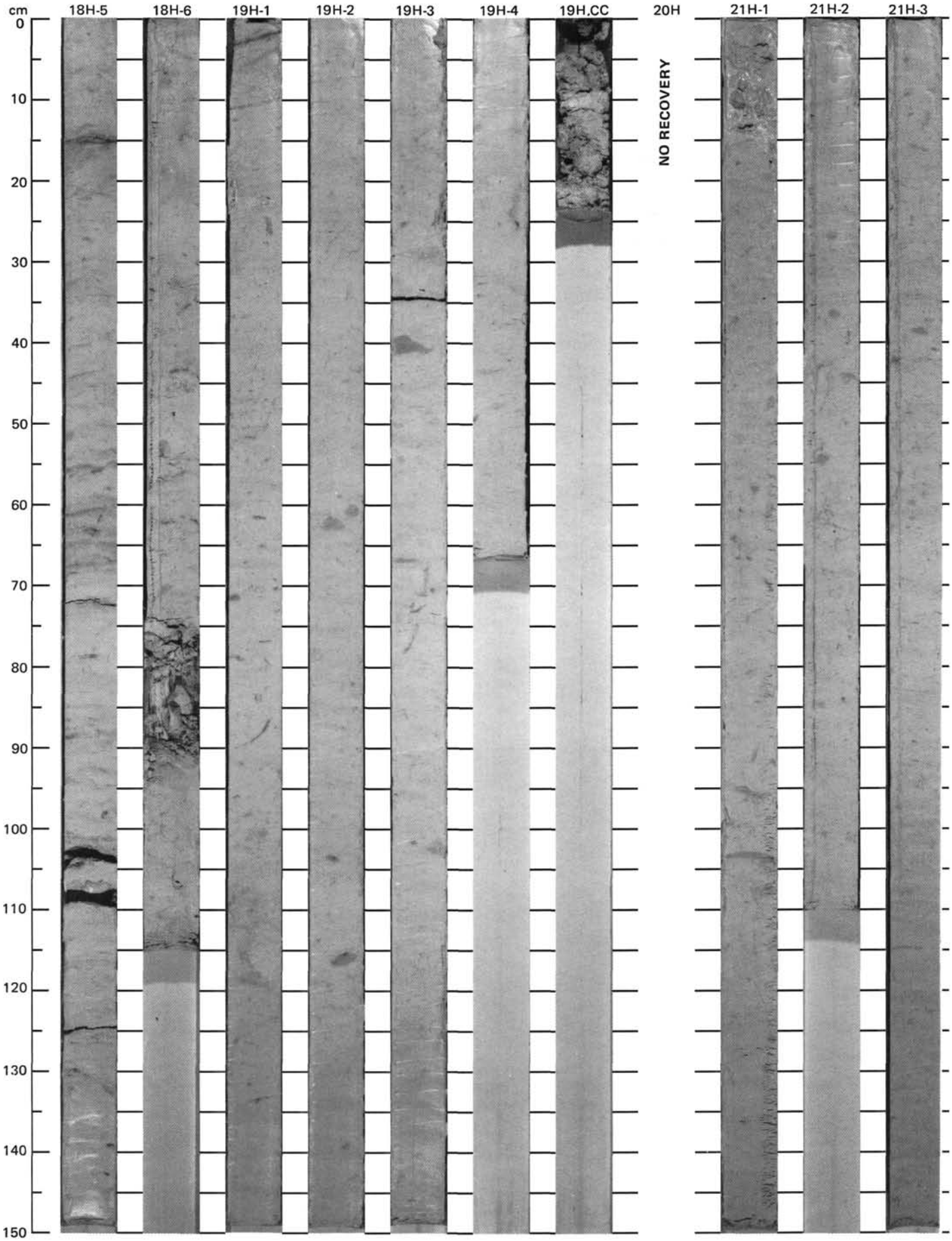
cm
18H-5
18H-6
19H-1
19H-2
19H-3
19H-4
19H,CC
20H
NO RECOVERY
21H-1
21H-2
21H-3
0
10
20
30
40
50
60
70
80
90
100
110
120
130
140
150

SITE 628 (HOLE A)

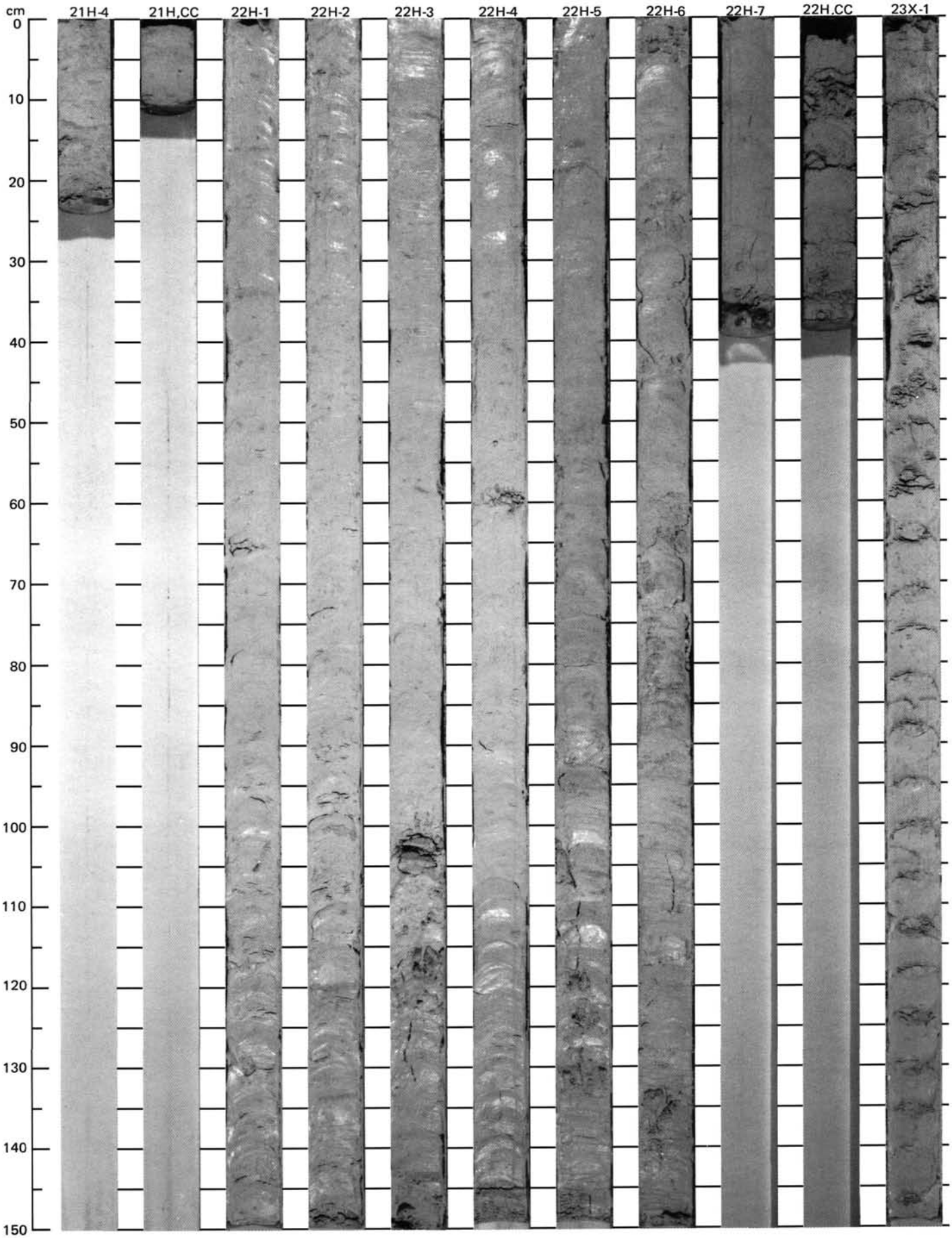

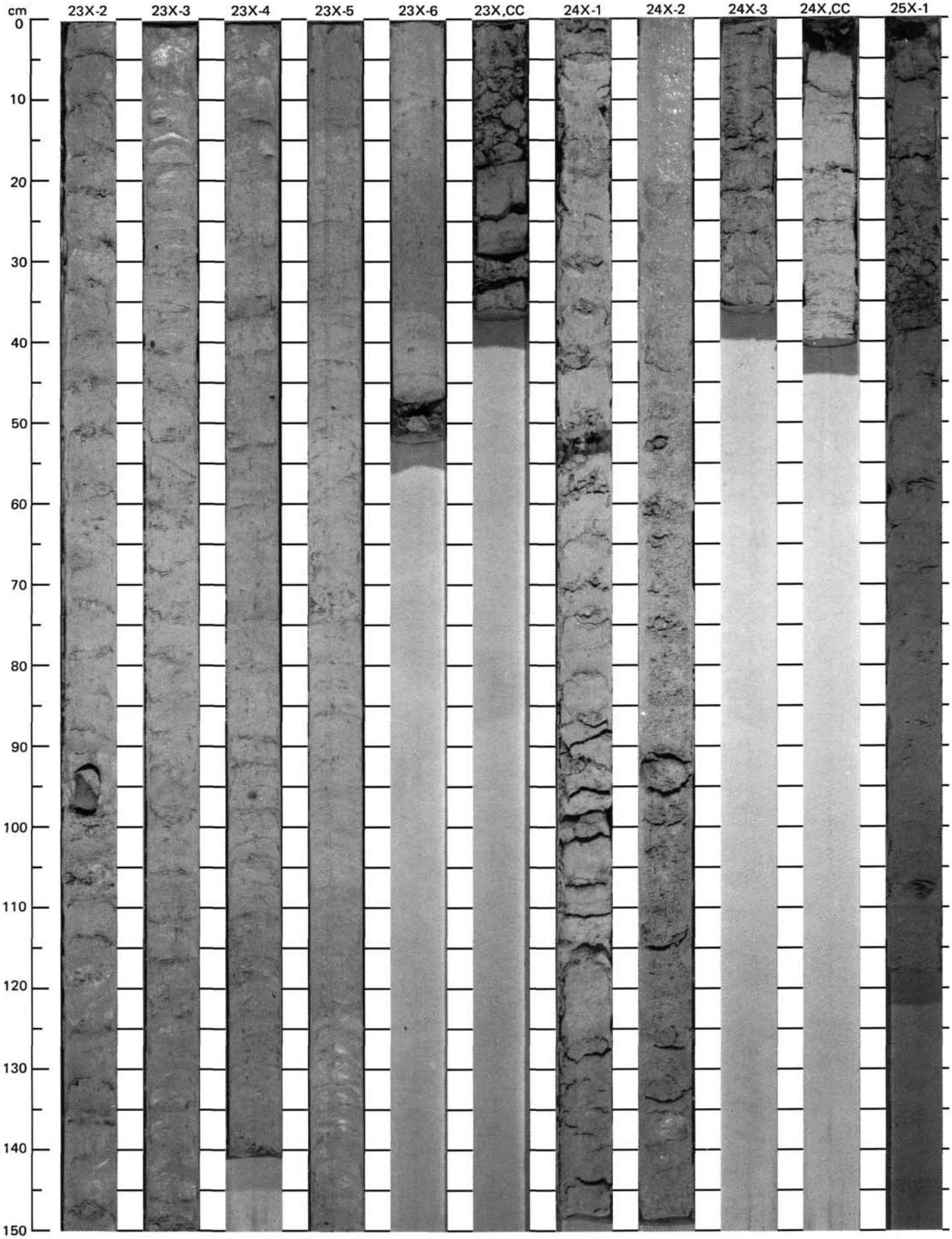
cm
23X-2
23X-3
23X-4
23X-5
23X-6
23X,CC
24X-1
24X-2
24X-3
24X,CC
25X-1
0
10
20
30
40
50
60
70
80
90
100
110
120
130
140
150

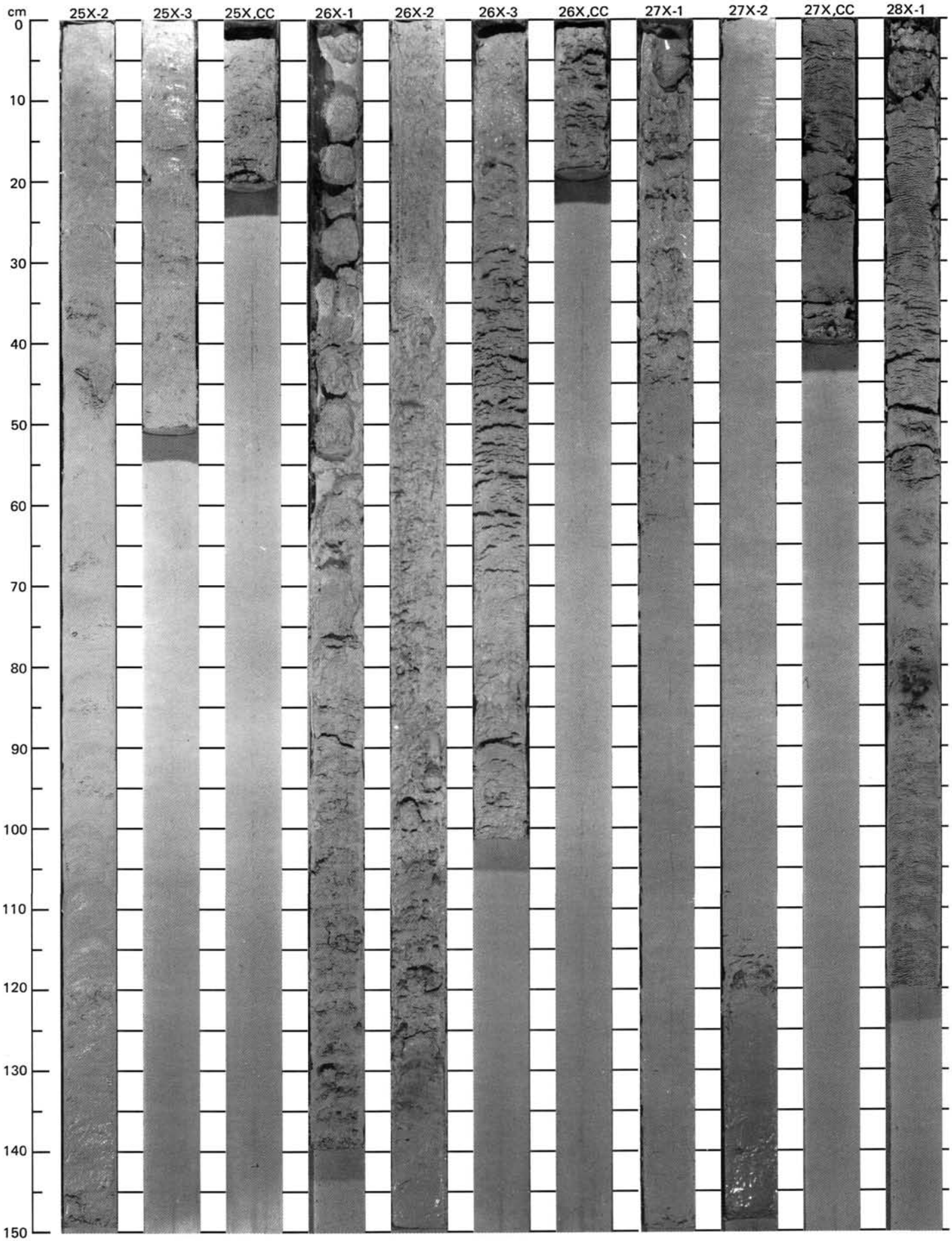
cm
25X-2
25X-3
25X,CC
26X-1
26X-2
26X-3
26X,CC
27X-1
27X-2
27X,CC
28X-1
0
10
20
30
40
50
60
70
80
90
100
110
120
130
140
150

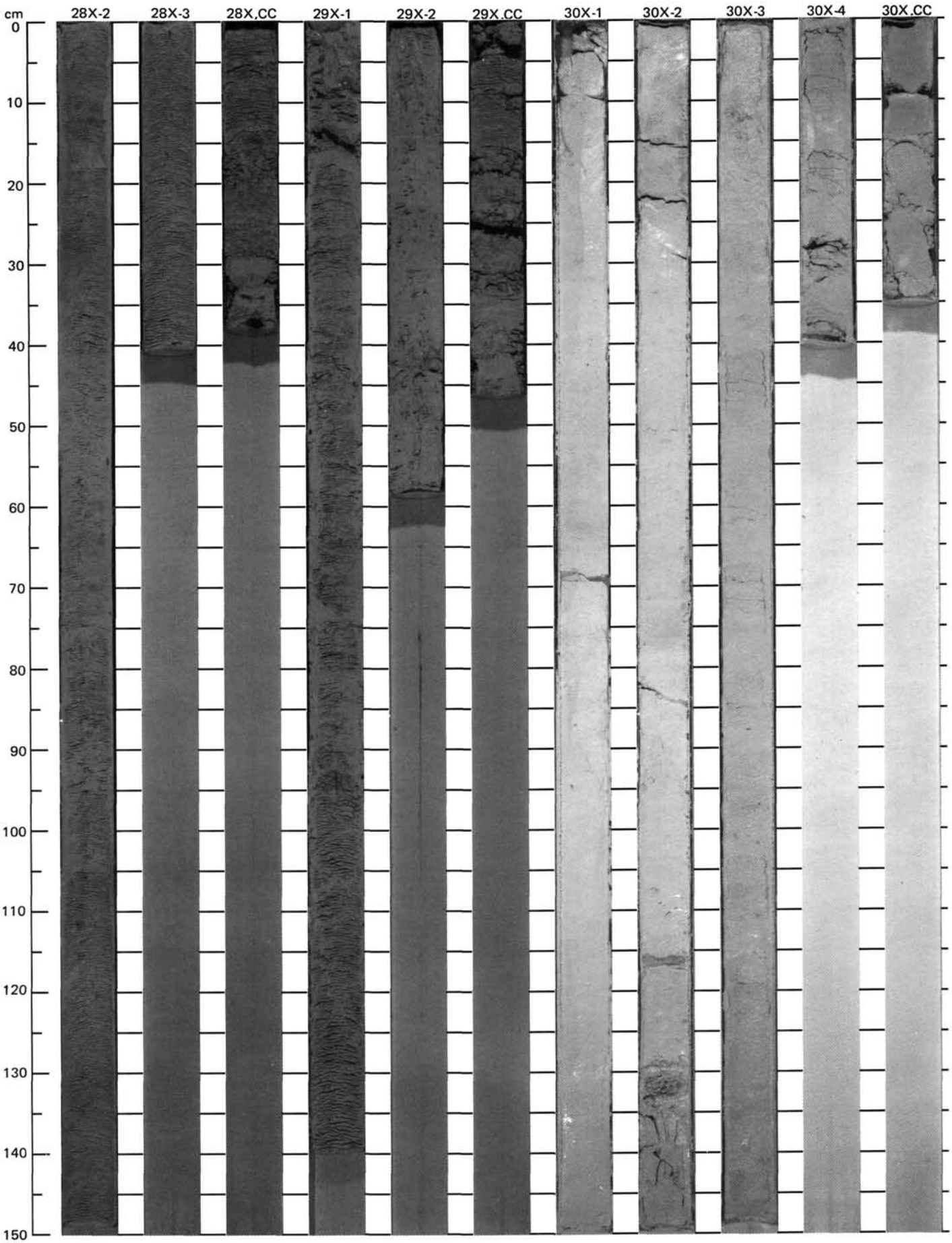
cm
28X-2
28X-3
28X,CC
29X-1
29X-2
29X,CC
30X-1
30X-2
30X-3
30X-4
30X,CC
0
10
20
30
40
50
60
70
80
90
100
110
120
130
140
150
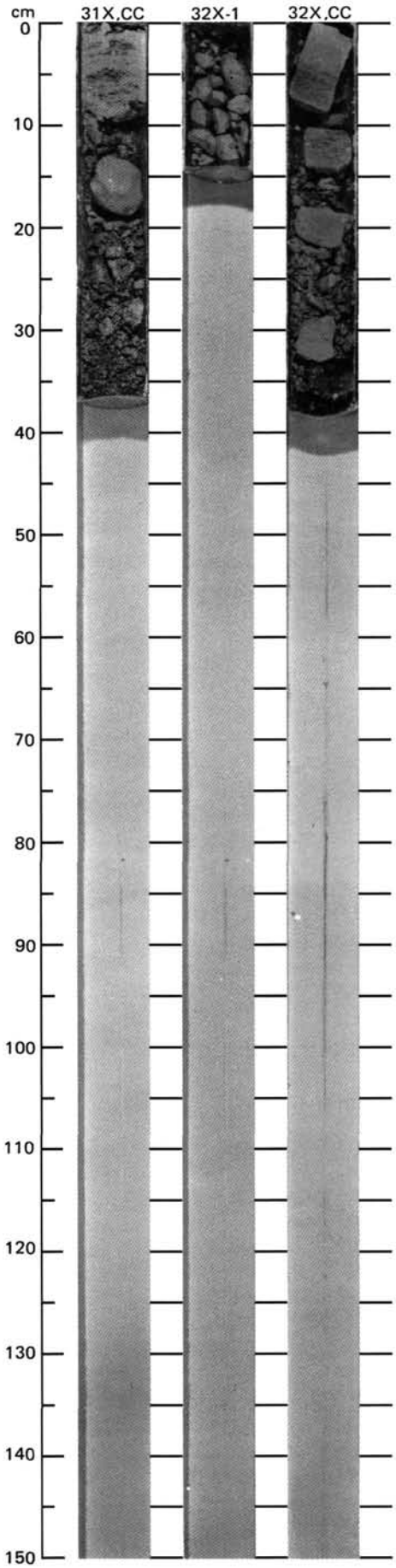
SITE 628 (HOLE A)